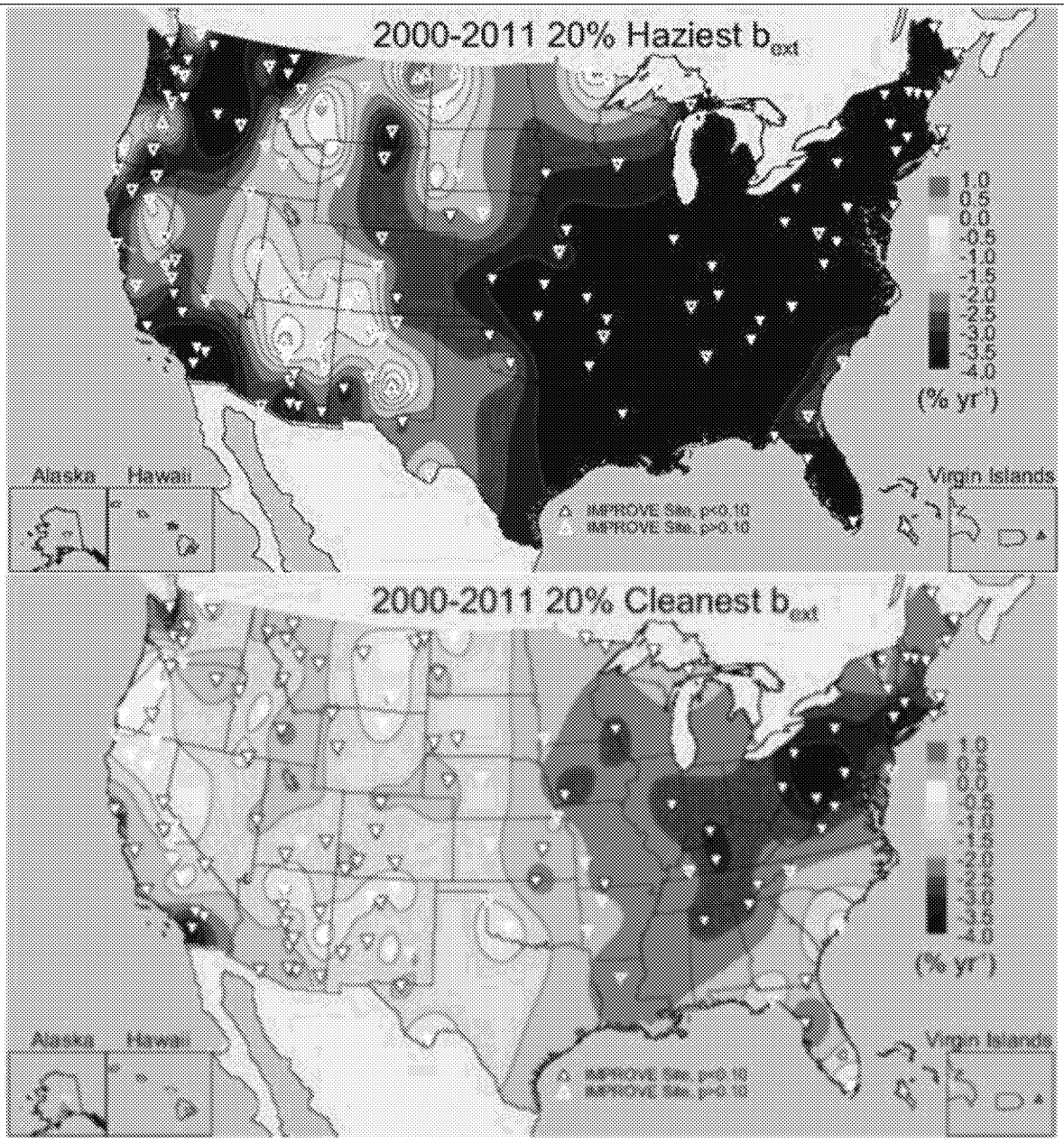

Note: Triangles correspond to IMPROVE sites; upward-pointing triangles correspond to increased b_{ext} and downward-pointing triangles correspond to decreased b_{ext}.

Source: Permission pending, Hand et al. (2011).

Figure 13-15 IMPROVE 2000–2011 trends (% yr^{-1}) in the reconstructed mean 20% haziest (top) and clearest (bottom) ambient light extinction coefficient (b_{ext} at 550 nm).

ED_002220_00002287-01791

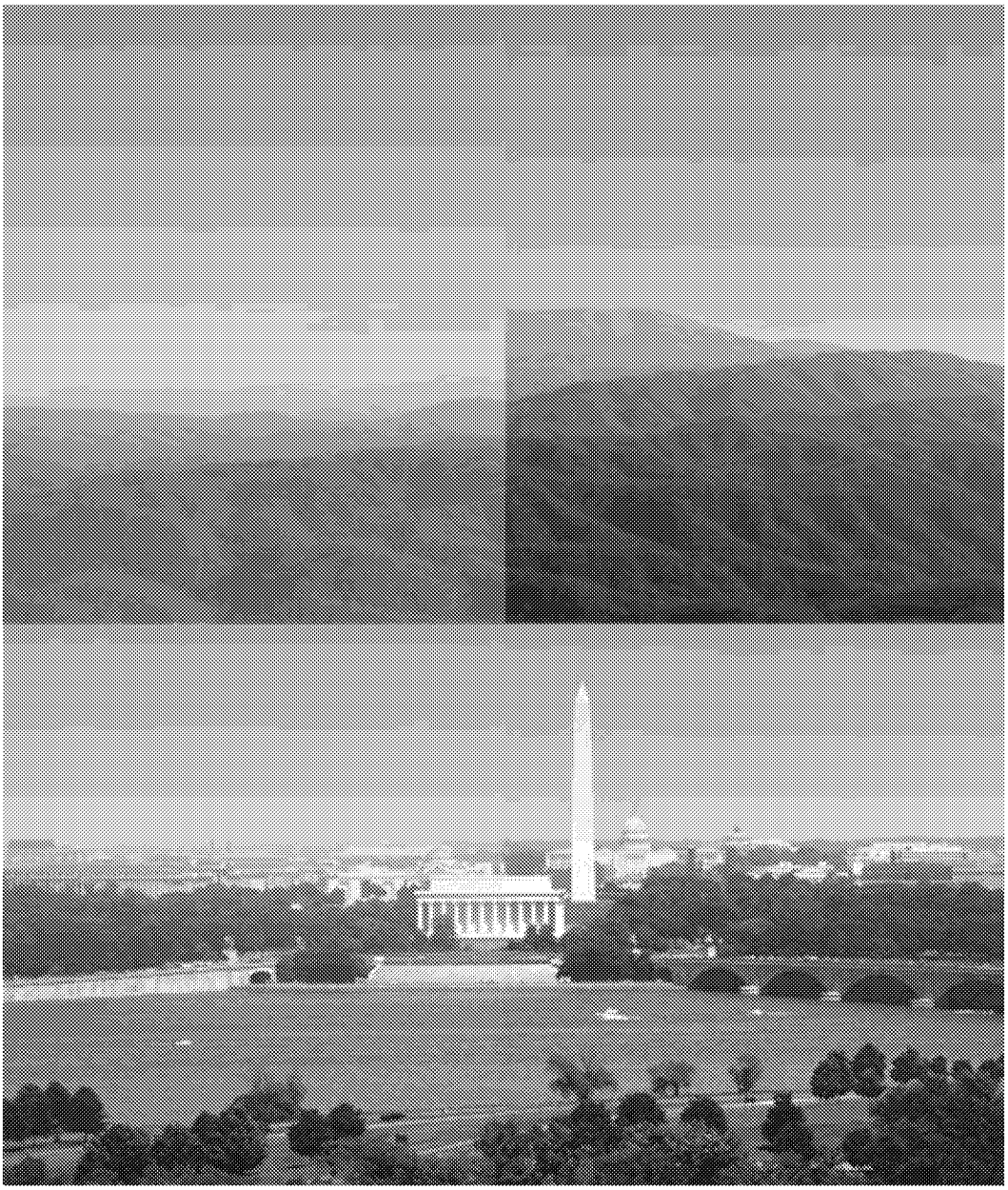

Source: Permission pending, Hand et al. (2014a).

Figure 13-16 Simulations of the view at Great Smoky Mountains National Park, TN (top), and Washington, DC (bottom), corresponding to the mean 20% haziest b_{ext} in 1990 (left side of image) and 2012 (right side of image). Contributions from Rayleigh scattering are included.

ED_002220_00002287-01792

13.2.4.3 Characteristic Fine Particulate Mass Light Scattering Efficiencies

The effective $PM_{2.5}$ mass extinction efficiencies, i.e., b_{ext} to $PM_{2.5}$ concentrations vary depending on the $PM_{2.5}$ composition and relative humidity. Based on Equation 13-7 and Section 13.2.3, the PM components can be divided into three groups: 1) soil and coarse mass (low scattering efficiency); 2) organic mass and sea salt and associated water (mid scattering efficiency); and 3) ammonium sulfate nitrate and associated water, and EC (high extinction efficiency).

As discussed in Section 2.5 and Section 13.2.4.2, these PM components vary regionally and seasonally, as well as by urban versus rural settings. The ratio of the sum of PM component concentrations to light extinction by season averaged over the years 2011–2013 is presented in Figure 13-17. These values were calculated using the same procedures as in Hand et al. (2012a); Hand et al. (2011) listed in Table 13-3 and Equation 13-7. In general, regardless of season $PM_{2.5}$ b_{ext} is largest in the eastern half of the U.S. including the Northeast, Southeast, and Midwest, and lowest in the Southwest and interior portions of the Western U.S. A relatively high b_{ext} in urban areas, such as in the Northwest, and in those urban centers near the higher elevation rural sites in the Appalachian Mountains, is evident.

The average annual $PM_{2.5}$ extinction efficiency and standard deviation across all sites is 5.1 ± 1.1 m^2/g and a factor of 2.8 between the lowest and highest values. There is some variation in the $PM_{2.5}$ extinction efficiencies seasonally but the overall average and standard deviation across the seasons are similar to the annual values at 5.2 ± 1.3 m^2/g. These values are somewhat higher than reported in the literature and summarized in Table 13-1 possibly because of RH effects.

ED_002220_00002287-01793

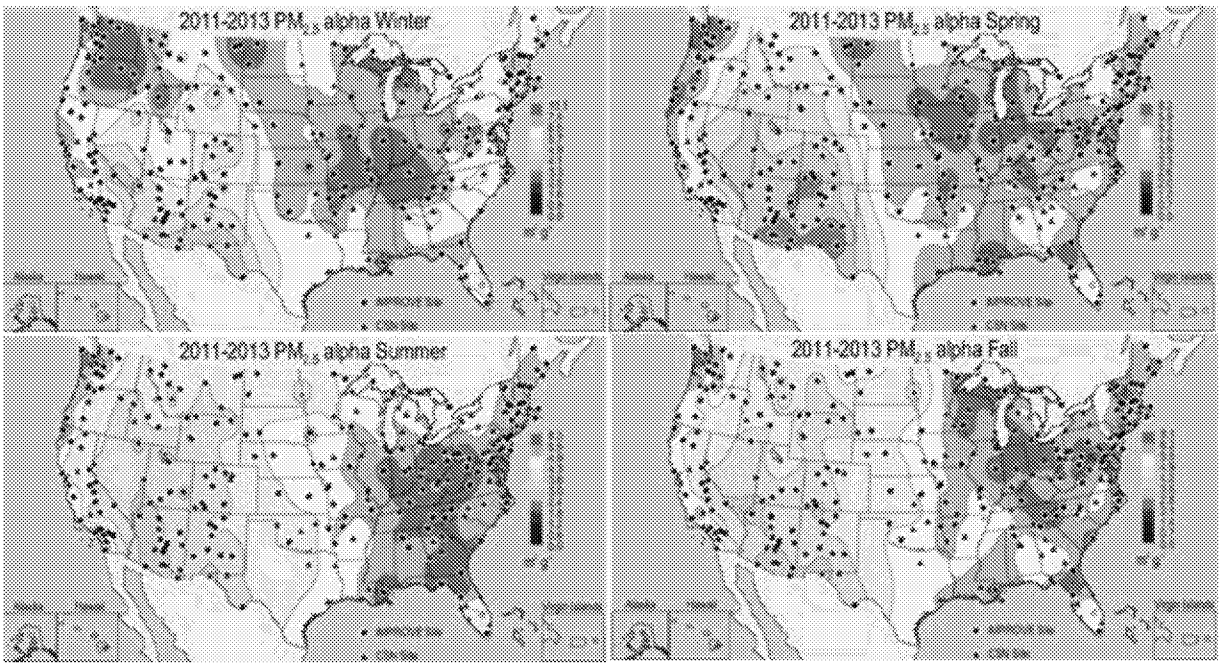

Source: Permission pending, http://vista.cira.colostate.edu/IMPROVE/

Figure 13-17 The effective $PM_{2.5}$ light extinction efficiency calculated as the ratio of the annual average reconstructed $PM_{2.5}$ b_{ext} and $PM_{2.5}$ concentrations.

13.2.5 Human Perception of Haze and Landscape Features

The 2009 PM ISA (U.S. EPA, 2009) provided a detailed review of urban visibility preference studies from which haze and acceptability response curves were derived. Results indicated a wide range in the responses for a given deciview (dv) haze index (see Section 13.2.2.1) between urban areas, depending on their setting. Since then, no new visibility preference studies have been conducted in the U.S. Outside of the U.S., a visibility preference study was carried out in Beijing, China (Fajardo et al., 2013), but will not be further discussed because the high $PM_{2.5}$ concentrations in Beijing outside the range typically observed in the U.S.

As reported in the 2009 PM ISA (U.S. EPA, 2009), four North American urban visibility studies were conducted in Phoenix, Arizona (AZ-DEQ, 2003), two cities in British Columbia, Canada (Pryor, 1996), Denver, Colorado (Ely et al., 1991), and Washington, D.C. (Abt, 2001). The studies estimated the visibility preference, or level of visibility impairment judged acceptable, by respondents using a focus-group method with photographs of a single scene. A broad downtown area and hills or mountains making up the scene's backdrop were in each photograph. As described in U.S. EPA (2009), there was a large variance in the mean dv value for a preference of 50%, with 19 dv at Denver and 28 dv at Washington, D.C. The most distant landscape feature varied from 150 km away for the Denver scene to only 8 km away for the Washington, D.C., scene. The closer the landscape features are to the observer,

ED_002220_00002287-01794

the more particulate matter, as represented by dv levels, it takes to cause the same level of perceived haziness. The deciview corresponding to 50% preference levels for each location is shown in Figure 13-18.

Figure 13-18 shows that considerably more haze was required to cause the Washington, D.C. scene to be judged unacceptable than the Denver scene. Between Washington, D.C. scene and the Denver scene there was a 9.2 dv difference in the amount of haze required for an unacceptable judgment at the 50% level, corresponding to about 30 μg/m^3 of particulate matter, assuming the particles are not hygroscopic. Consequently, it takes about 250% more particulate mass or b_{ext} to reach an unacceptable level of haze in the Washington, D.C. scene than in the Denver setting. In other scenes, the amount of haze required to be judged unacceptable was in between the amounts in Washington, D.C. and Denver.

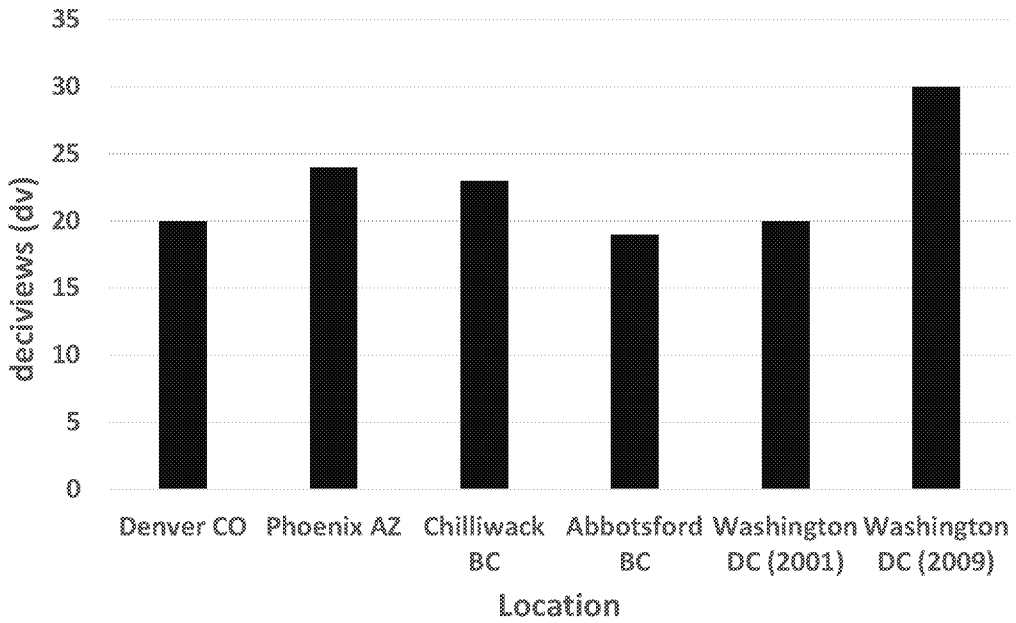

Source: Permission pending, adapted from 2009 PM ISA U.S. EPA (2009).

Figure 13-18 Mean deciview (dv) values of 50% acceptability in 5 visibility preference studies (CO, AZ, BC, DC 2001, DC 2009).

ED_002220_00002287-01795

These results clearly demonstrate a large range in dv or any transform of b_{ext} at a given level of acceptability, indicating these metrics are not universal indicators of visibility preference levels. For context, the 50% preference deciview range between 19 and 30 dv corresponds to a b_{ext} range of approximately 60 to 180 mM^{-1}, which can be compared to b_{ext} estimates by season and region in Figure 13-9, Figure 13-10, Figure 13-11, Figure 13-12, Note: The letters on the x-axis correspond to the month and "A" corresponds to "annual" mean. Ammonium sulfate (AS) in yellow, ammonium nitrate (AN) in red, particulate organic matter (POM) in green, light absorbing carbon (LAC) in black, soil in brown, and sea salt in blue. The shaded area corresponds to the regions that comprise the sites used in the analysis, shown as dots. Extinction coefficients were determined from Equation 13-7 (see text). Wavelength corresponds to 550 nm.

Source: Permission pending, Hand et al. (2011).

Figure 13-13, and Figure 13-14 in Section 13.2.4.3. Roughly half of the CSN regions evaluated in Section 13.2.4.3 had at least one monthly average b_{ext} estimate within that range in 2011–2014.

There is little new published information regarding preference levels in the U.S. The single new study by Smith (2013) was an investigation of "framing bias" in preference studies that can potentially occur because preference levels are chosen in part based on experimental variables such as number of photographs shown or range of the range of dv levels participants are shown when asked to state a preference about whether scenes in photographs are acceptable.

13.2.6 Summary and Causality Determination

Overall, visibility in most regions of the U.S. has improved since the 2009 PM ISA, as indicated by lower estimates of $PM_{2.5}$ mass extinction. The greatest improvements have occurred in the eastern half of the U.S., in regions with the poorest visibility. This has likely occurred because of a reduction in SO_2 emissions resulting in lower ammonium sulfate concentrations, because ammonium sulfate has historically accounted for a larger fraction of $PM_{2.5}$ mass than other $PM_{2.5}$ components, and also because ammonium sulfate is more effective than other $PM_{2.5}$ components at scattering light. The resulting decrease in $PM_{2.5}$ in the Eastern U.S. has resulted in better visibility.

Rural visibility impairment is greatest in Eastern U.S. regions, including the Southeast, East Coast, Mid-South, Central Great Plains, and Appalachian regions. In contrast, visibility is better on average in most regions of the Western U.S. Urban visibility is also generally better in the Western U.S. than in the Eastern U.S., with exceptions of urban areas in California and Alaska. In part, this reflects the difference in $PM_{2.5}$ composition between the East and West, with a greater fraction of ammonium sulfate in the Eastern U.S., and particulate organic matter in the Western U.S. The effectiveness of light extinction by $PM_{2.5}$ depends on composition and relative humidity, with low scattering efficiency from $PM_{10-2.5}$, moderate scattering efficiency by organic mass and sea salt, and high extinction efficiency by ammonium sulfate, ammonium nitrate, and light absorbing carbon. However, the difference in extinction

ED_002220_00002287-01796

between the Eastern U.S. and Western U.S. also reflects considerably higher $PM_{2.5}$ concentrations in the Eastern U.S. and California than in the rest of the Western U.S.

Altogether, new results and observations regarding atmospheric visibility provide evidence atmospheric visibility has improved as PM concentrations have decreased, that regional and seasonal differences in atmospheric visibility parallel regional and seasonal PM concentration patterns, and that regional differences in the relationship between PM and visibility are due to differences in PM composition characteristics, rather than any factors beyond PM. These results confirm a well-established relationship between PM and visibility summarized in the 2009 PM ISA and earlier assessments. **Overall the evidence is sufficient to conclude that a causal relationship exists between PM and visibility impairment.**

13.3 Effects on Climate

13.3.1 Introduction

The 2009 PM ISA (U.S. EPA, 2009) concluded that there was sufficient evidence to determine a causal relationship between PM and climate effects—specifically on the radiative forcing of the climate system, and including both direct effects of PM on radiative forcing and indirect effects involving cloud processes. This section examines the role of anthropogenic PM in driving global and regional climate change, with a focus on the U.S. PM in the atmosphere significantly influences global and regional climate through interactions with incoming solar radiation and with clouds. For example, certain PM species reflect solar radiation back to space, leading to cooling at the Earth's surface. On the other hand, PM species that absorb solar radiation can heat the atmosphere and change the vertical temperature profile, with consequences for atmospheric stability, cloud formation, and convective rainfall. By providing cloud condensation or ice nuclei, PM can also influence cloud cover and affect the Earth's radiative balance, with additional impacts on the distribution and intensity of precipitation. Finally, because PM is not distributed evenly across the globe, spatial variation in these radiative and hydrologic impacts can also contribute to shifts in atmospheric circulation patterns over a range of space and time scales.

As the abundance of natural or anthropogenic PM changes over time, the effects on climate may be substantial. A key question for the scientific community is to what extent trends in anthropogenic PM have influenced climate through the 20th and early 21st centuries. Global trends in PM have varied by species. For example, U.S. emissions of SO_2, a precursor to sulfate PM, tripled from 1900 to 1980 (Smith et al., 2011), while black carbon (BC) emissions peaked in the early to mid-20th century (Bond et al., 2007). In more recent decades, as regulatory actions have been put in place to improve air quality, U.S. levels of sulfate and other PM species have declined rapidly (Keene et al., 2014; Murphy et al., 2011).

ED_002220_00002287-01797

The climate impacts of such trends are currently topics of intensive research (Fiore et al., 2015; Mickley et al., 2014; Bond et al., 2013; Boucher, 2013; Myhre, 2013).

Assessing the role of anthropogenic activity in past and future climate change is the mandate of the Intergovernmental Panel on Climate Change (IPCC), an initiative begun in 1988 by the World Meteorological Organization (WMO) and the United Nations Environmental Program. The IPCC supports the work of the Conference of Parties to the United Nations Framework Convention on Climate Change (UNFCCC). New IPCC reports are issued every 5 to 7 years, and the climate discussion in the 2009 PM ISA (U.S. EPA, 2009) relied heavily on the Fourth IPCC Assessment Report (AR4), published in 2007. The Fifth IPCC Assessment Report (AR5) (IPCC, 2013) reports on the key scientific advances in understanding the climate effects of PM since AR4. This section thus accordingly draws substantially upon AR5 in summarizing these effects.

Section 13.3.2 provides an overview of the physics of climate as well as the metrics used to assess climate change (discussion of the models used to simulate climate, atmospheric chemistry, and the behavior of PM in the atmosphere is provided in Chapter 2). Section 13.3.3 describes the mechanisms of PM's influence on the Earth's energy budget. Sections 13.3.4 and Section 13.3.5 report the estimated radiative forcing for total PM and individual PM components, respectively. Section 13.3.6 describes the climate response to changing PM, including the feedbacks of climate onto PM abundance. Section 13.3.7 provides further details on the climate response to PM trends in specific U.S. regions, especially in the eastern half of the country, and Section 13.3.8 summarizes key uncertainties in gauging the role of PM in driving climate. Section 13.3.9 provides the final summary and causality determination. Note that, in the climate science community, PM is encompassed by what is typically referred to as aerosol (though the definitions do not completely overlap), but this section on the climate effects of PM uses the term PM throughout for consistency with the rest of this ISA. Exceptions to this practice include certain acronyms that are widely used by the climate community that include the term aerosol (e.g., aerosol optical depth, or AOD).

13.3.2 Overview of the Physics of Climate Change and Radiative Forcing

The Earth's climate is driven by energy from the sun. Radiant solar energy enters the atmosphere in a range of wavelengths, peaking strongly in the visible part of the spectrum. Approximately 70% of incoming solar energy is absorbed by the earth-atmosphere system, while the rest is reflected back to space, mainly by clouds and by snow- and ice-covered surfaces (Trenberth et al., 2009).

Atmospheric PM also interacts with incoming solar radiation. Many species of PM (e.g., sulfate and nitrate) are efficient scatterers of solar energy. By enhancing reflection of solar energy back to space, scattering PM exerts a cooling effect on the surface below. Certain species of PM such as BC, brown carbon (BrC), or dust can also absorb incoming sunlight. Whether absorbing PM warms or cools the

ED_002220_00002287-01798

underlying surface depends on several factors, including the altitude of the PM layer relative to cloud cover and the albedo of the surface (Ban-Weiss et al., 2014). PM also perturbs incoming solar energy by influencing cloud cover and cloud lifetime. For example, PM provides nuclei upon which water vapor condenses, forming cloud droplets. Finally, absorbing PM deposited on snow and ice can diminish surface albedo and lead to regional warming. More detailed information about these complex and sometimes competing effects of PM on climate is provided in Sections 13.3.3 and Section 13.3.4.

About two-thirds of the solar energy absorbed by the earth-atmosphere system is absorbed by the Earth's surface (Stephens et al., 2012; Trenberth et al., 2009). Much of that energy, in turn, is re-emitted at longer, infrared wavelengths, while some absorbed energy is also transformed into latent or sensible heat (Jung et al., 2011). Polyatomic gases such as water vapor, CO_2, methane, and ozone absorb and re-emit the infrared radiation upwelling from the Earth's surface, reducing the total amount of radiant energy that returns to space, keeping the surface and lower atmosphere substantially warmer than they would be in the absence of these gases. This heat trapping also contributes to further warming by increasing the concentration of water vapor, itself a strongly radiatively active gas, in the atmosphere, through increases in evaporation from the Earth's surface. In general, water vapor acts as an amplifier of the climate effects of other greenhouse gases; this process is one of the most important feedbacks in the climate system.

An important concept, used throughout this section, is "radiative forcing." Radiative forcing provides a simple way of characterizing and quantifying the net change in Earth's radiation budget resulting from a perturbation by one or more radiatively active atmospheric constituents, whether greenhouse gases, clouds, or PM species. Alternative definitions of radiative forcing (and related metrics), useful in different contexts, have been developed. The most relevant of these for the purposes of this ISA are defined below.

13.3.2.1 Observed Recent Climate Change: Detection and Attribution

Since the late 19th century, the global mean surface temperature of the Earth has warmed by ~0.85°C (Hartmann, 2013). The first decade of the 21st century represents the warmest decade in the instrumental record (Melillo et al., 2014), and 2016 was the warmest year globally (NOAA NCEI, 2017). Other indicators of climate change include a shrinking Arctic ice cap and a sharp decline in snow cover over North America, an increase in global-mean sea level by ~0.2 m since 1900, consistent with thermal expansion of ocean waters and diminishing glaciers in a warming climate, and an increase in average precipitation over the mid-latitude land areas of the northern hemisphere (Stocker, 2013). Detecting trends in climatological variables such as temperature, and attributing these trends to a given causal factor, such as increases in greenhouse gases or PM, first requires distinguishing them from natural climate system variability, and then evaluating the relative contributions of relevant causal factors to the trends, with appropriate measures of statistical confidence (Bindoff et al., 2013; Hegerl et al., 2010).

ED_002220_00002287-01799

Sensitivity studies using climate models have shown that the observed global temperature trends can be reproduced only when both natural and anthropogenic emissions of greenhouse gases, PM, and their precursors are taken into account (Jones et al., 2013). The IPCC concluded that, globally, anthropogenic forcings caused more than half of the warming for 1951–2010, with a likely contribution range of 0.6 to 0.7°C (1.1°F to 1.3°F), compared with the observed warming of about 0.65°C (1.2°F) (Bindoff et al., 2013).

In general, detecting and attributing climate change—and projecting future change—is more difficult for regional scales compared to globally, for shorter time periods compared to longer ones, and for certain variables (e.g., precipitation) that are particularly "noisy" in space and time. This is because the natural variability over years and decades inherent in the climate system is relatively more important at these scales, compared to the forced signal of climate change, especially for some variables (Northrop and Chandler, 2014; Deser et al., 2012; Hawkins and Sutton, 2009). Nevertheless, it is possible to make some robust detection and attribution statements for North America and/or the U.S. For example, as with the globe as a whole, surface temperatures in the U.S. have also warmed, though with large spatial and temporal variation. Alaska has warmed most rapidly, by ~1.2°C since 1900 (Melillo et al., 2014). The continental U.S. warmed by about 0.9°C over this period, with most of the increase occurring after 1980 (Vose et al., 2012; Lawrimore et al., 2011). Over the time period 1930–1990, however, much of the Southeast experienced a net cooling of ~1°C, a trend that some studies have linked to changes in the concentration of anthropogenic PM (Yu et al., 2014; Leibensperger et al., 2012a, b), though others have suggested that internal climate system variability (Knutson et al., 2013; Meehl et al., 2012) or land-use change (Xu et al., 2015; Goldstein et al., 2009) was responsible. This cooling trend in the Southeast, which will be discussed in greater detail in Section 13.3.7, has since reversed to warming.

In addition to mean temperatures, heatwave frequency across the U.S. has also increased since the 1970s. For example, Meehl et al. (2009) found that the ratio of daily record high maximum temperatures to record low minimum temperatures in the U.S. is approximately two to one, a result confirmed in a more recent study (Meehl et al., 2016). With respect to precipitation, average annual precipitation over the U.S. has increased by roughly 5% since 1900, though with important regional differences (Melillo et al., 2014). Precipitation trends tend to be positive for the eastern and central states, with increases of as much as 10% since 1900 (McRoberts and Nielsen-Gammon, 2011). The western U.S., on the other hand, has recently experienced its most severe drought since the megadrought of 900–1300 A.D., although the connection to global climate change is uncertain (Griffin and Anchukaitis, 2014; Cook et al., 2010). The heaviest rainfall events, by contrast, have become heavier and more frequent across most of the U.S. For example, since 1991, the amount of rain falling in very heavy precipitation events has been significantly above average, with the greatest increases in the Northeast, Midwest, and upper Great Plains (Melillo et al., 2014).

ED_002220_00002287-01800

13.3.2.2 Metrics of Climate Change, Including Radiative Forcing

Phenomena that perturb the Earth's energy system are known as climate forcing agents. When comparing the efficacy of one climate forcing agent against another it is useful to devise metrics to make such comparisons more systematically. While surface temperature change would seem to be an obvious choice for such a metric, the temperature response to a climate forcing agent is actually the net result of a cascade of feedback effects, both positive and negative, that can either amplify or diminish the initial temperature response to a given forcing (Myhre, 2013). The strengths of such feedbacks are not always well constrained, making it challenging to use surface temperature as a metric of climate forcing agent efficacy, even with the use of climate models.

Four alternative metrics of climate change are identified below: radiative forcing (RF), effective radiative forcing (ERF), global warming potential (GWP), and global temperature potential (GTP). All four metrics are typically calculated with models; RF can also be estimated using a combination of models and satellite data. Of these metrics, RF and ERF provide the most direct descriptions of the radiative effects of PM in the climate system, and are therefore described in the most detail below (and will be focused on throughout the rest of this document). The definitions in this section draw heavily upon, and have been adapted from Myhre (2013) and Fiore et al. (2015).

Radiative forcing (RF) for a given atmospheric constituent is defined as the perturbation in net radiative flux, at the tropopause (or the top of the atmosphere), caused by that constituent, in Wm^{-2}, after allowing for temperatures in the stratosphere to adjust to the perturbation but holding all other climate responses constant, including surface and tropospheric temperatures (Fiore et al., 2015; Myhre, 2013). A positive forcing indicates net energy trapped in the Earth system and suggests warming of the Earth's surface, whereas a negative forcing indicates net loss of energy and suggests cooling. RF is typically classified according to wavelength, either shortwave (solar) or longwave (terrestrial). For PM, surface RF is also commonly reported, since haze events can significantly attenuate incoming solar energy, causing local "dimming."

For IPCC AR5, a new definition of RF was advocated, known as effective radiative forcing (ERF) (Myhre, 2013). ERF takes into account not just the instantaneous forcing but also a set of climate feedbacks, involving atmospheric temperature, cloud cover, and water vapor, that occur naturally in response to the initial radiative perturbation. These variables are allowed to adjust in the calculation of ERF. Climate system adjustments over longer timescales, e.g., involving sea surface temperatures and sea ice cover, are held constant in the calculation of ERF. An advantage of ERF for assessing the radiative forcing of PM is that, since it includes these rapid adjustments, the equilibrium change in global mean surface temperature scales more closely with ERF than with RF, making it more useful for analysis of the climate impacts of PM (Fiore et al., 2015; Myhre, 2013). A limitation of ERF is that quantifying it precisely depends on a robust understanding of all of the fast climate feedback processes. The response of clouds in particular to changing climate is, however, highly uncertain (Zhao et al., 2016; Soden and Vecchi, 2011), as will be discussed in more detail below.

ED_002220_00002287-01801

The global mean values of RF and ERF are important indicators of the climate response to a given perturbation. Figure 13-19 shows the IPCC AR5 estimates of RF and ERF over the 1750–2011 timeframe for a range of anthropogenic climate forcers. For PM and other short-lived species, however, the temporal and spatial variation in such forcings can vary by orders of magnitude. For example, for a severe pollution event over the North China Plain in 2013, Che et al. (2014) reported large RFs from PM of as much as −60 Wm^{-2} at top of atmosphere (TOA) and +200 Wm^{-2} at the surface over several days (in comparison, for example, with the long-term, globally averaged values shown in Figure 13-19).

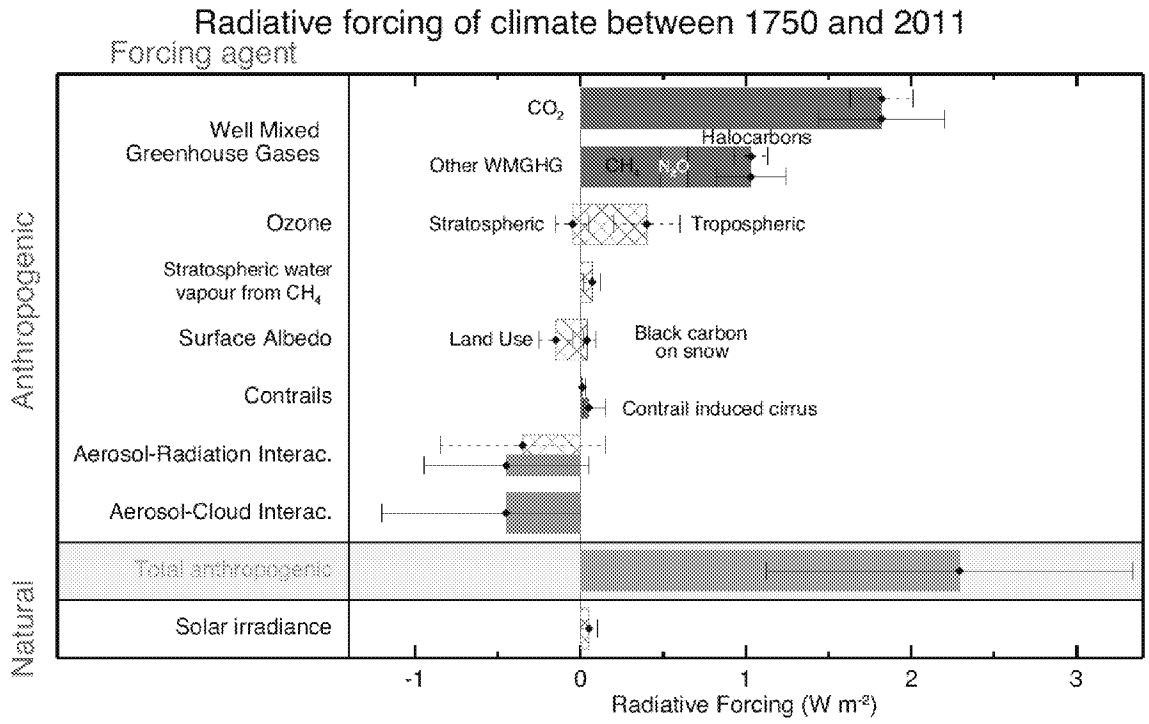

Note: Radiative forcings (RFs) are shown as hatched bars and effective radiative forcings (ERFs) are shown as solid bars. Uncertainties (5% to 95% confidence range) are indicated by dotted lines for RF and solid lines for ERF. Positive forcings denote warming of the Earth's surface, whereas negative forcings denote cooling. WMGHG refers to the well-mixed greenhouse gases, and aerosols refers to PM. The abbreviation "interac." means "interactions."

Source: Permission pending, Myhre (2013).

Figure 13-19 Global mean radiative forcing from anthropogenic activities from 1750 to 2011.

ED_002220_00002287-01802

Two other metrics, GWP and GTP, are also sometimes used. Briefly, GWP is used to compare the climate impacts of a given atmospheric constituent to those of CO_2, taking into account not just the warming (or cooling) effects but also the constituent's atmospheric lifetime. GWP is defined as the integral over a specified time horizon (generally 20, 50, or 100 years) of the global mean RF arising from an emission pulse of a given constituent, normalized by the corresponding integral for an emission pulse of the same mass in CO_2 (Fiore et al., 2015; Myhre, 2013). GTP similarly assesses the effect of a climate forcing agent on surface temperature at a specific time horizon, but based on the surface temperature at the final timestep rather than as an integral. Both GWP and GTP have methodological or computational issues that make them less useful than RF or ERF for estimating the radiative impacts of PM.

The IPCC currently promotes the use of ERF over RF (Myhre, 2013), but not all published papers report ERF. The remainder of this section will therefore focus on RF and, when available, ERF of atmospheric particles. Figure 13-20 diagrams the links between PM sources, atmospheric abundance, radiative forcing, and the resulting climate response. Also illustrated in the figure are feedbacks between PM effects on climate and the ecosystem and PM sources and abundance. The nonuniform spatial and temporal distribution of PM and its constituent species compared to well-mixed greenhouse gases presents significant challenges for designing metrics able to capture the full range of global and regional climate forcing effects of PM. Some research on regional metrics [e.g., (Aamaas et al., 2016; Shindell, 2012)] and responses to regional forcings (Shindell et al., 2012; Shindell and Faluvegi, 2009) has been conducted to date, and additional research is currently ongoing.

ED_002220_00002287-01803

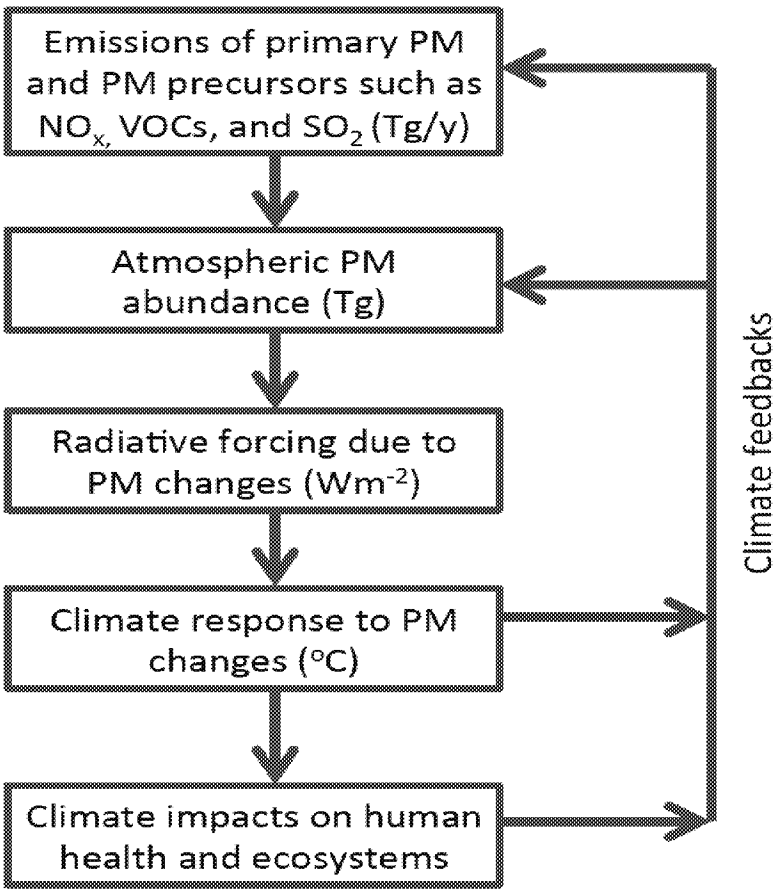

Note: This figure depicts the relationships between PM sources, PM abundance, radiative forcing, climate response, and climate impacts. Units shown are those typical for each quantity illustrated. VOCs stands for volatile organic compounds. Feedbacks from both the climate response and climate impacts on ecosystems can affect both the emissions of PM sources and PM atmospheric abundance through multiple mechanisms.

Figure 13-20 Schematic illustrating the effects of PM on climate.

13.3.3 Effects of PM on Radiative Forcing: Mechanisms

As introduced at the beginning of Section 13.3, PM radiative forcing, both through direct interactions with incoming solar radiation, and through interactions with clouds, affects surface and atmospheric temperatures, with subsequent impacts on precipitation and circulation patterns. This section describes the main mechanisms of PM impact on radiative forcing, including the influence of particle size on these mechanisms. The next two sections summarize quantitative estimates of PM radiative forcing globally for total PM, and by individual PM species, respectively. Later sections discuss the global and regional climate impacts of this PM radiative forcing, climate feedback mechanisms involving PM, and key sources of uncertainty in assessing these radiative and climate effects.

ED_002220_00002287-01804

13.3.3.1 Interactions of PM with Radiation

Atmospheric PM interacts with solar radiation through scattering and absorption. These "aerosol-radiation interactions" (ARI) are also known as the "direct effects" of PM on climate, as opposed to the "indirect effects" that involve PM interactions with clouds (Section 13.3.2.2). The IPCC AR5 devised the acronym RFari to refer to radiative forcing due to ARI (Boucher, 2013). The fate of solar energy intercepted by PM, and thus the magnitude and sign of RFari, depends on the optical properties of the particles. Highly reflective PM such as sulfate scatter the incoming solar energy, with much of that energy returning to space. Highly absorbing PM such as BC convert solar energy to heat. A metric known as the single scattering albedo represents the ratio of the scattering cross section to the sum of scattering and absorbing cross sections for a given PM type and wavelength. The single scattering albedo for sulfate approaches 1.0. The water content and size distribution of PM can significantly also affect the scattering efficacy of PM. Figure 13-21 depicts the mechanisms of RFari, as well as the effective radiative forcing due to ARI (ERFari), which includes the fast meteorological responses to RFari (as described in Section 13.3.2.2 above).

ED_002220_00002287-01805

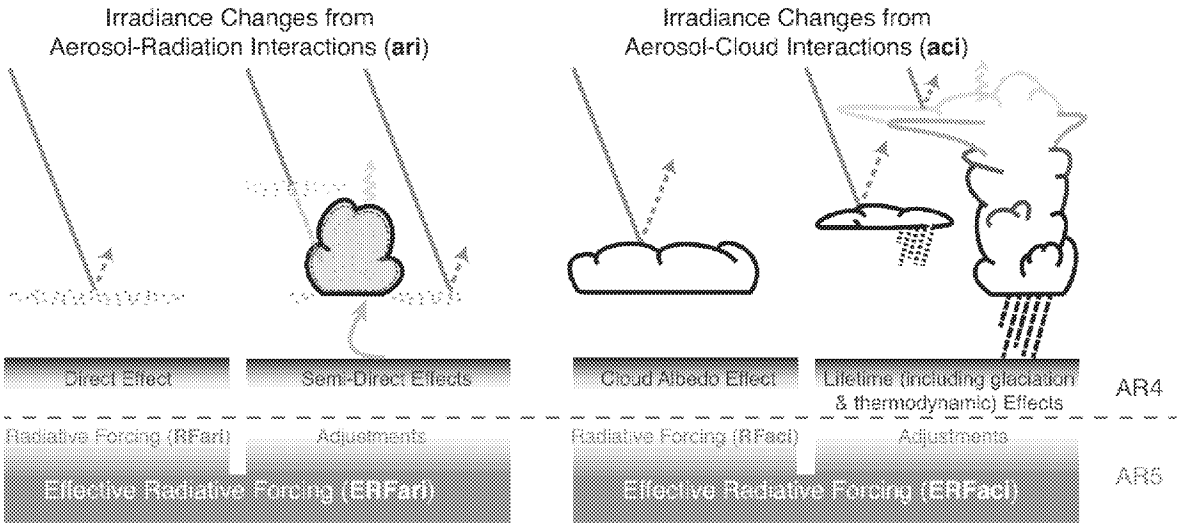

Note: The blue arrows represent solar radiation, the gray arrows represent cloud longwave radiation, and the brown arrow symbolizes the coupling between the surface and the cloud layer that occur on rapid timescales. The left-hand panel depicts aerosol-radiation interactions (ari) and associated forcings: radiative forcing (RFari) for the direct effect and effective radiative forcing (ERFari) for the direct effect plus rapid meteorological adjustments. The right-hand panel shows aerosol-cloud interactions (aci) and associated forcings: radiative forcing (RFaci) for the cloud albedo effect and (ERFaci) for the cloud albedo effect plus rapid meteorological adjustments. Also shown are the equivalent terms for these effects and adjustments in IPCC AR4. See text for further details.

Source: Permission pending, Boucher (2013).

Figure 13-21 Schematic of mechanisms by which PM affects climate and the terminology used in the Intergovernmental Panel on Climate Change (IPCC) Fifth Assessment Report (AR5) to categorize PM radiative forcings.

Reflective PM, by sending a fraction of solar energy back to space, has an overall cooling effect on global climate. In contrast, absorbing PM has an overall warming effect on global climate, and the in situ warmth generated by solar absorption can be transported elsewhere in the atmosphere. Regardless of species type, PM generally cools the underlying surface through attenuation of solar radiation. Absorbing PM can also have complex and sometimes competing effects on regional hydrological cycles, with consequences for the Earth's energy budget. For example, in their model study, Koch and Del Genio (2010) found that BC particles embedded within clouds warm the local atmosphere and reduce cloud cover, while those located above clouds stabilize the atmosphere, enhancing stratocumulus clouds (semidirect effects). When all these effects are considered together, PM has a net cooling effect on global climate (Fiore et al., 2015; Myhre, 2013), as will be discussed in more detail below.

ED_002220_00002287-01806

13.3.3.2 Interactions of PM with Clouds

By providing cloud condensation nuclei, PM increases cloud droplet number and thus cloud droplet surface area and albedo (Twomey, 1977). The climate effects of these perturbations are difficult to quantify but likely enhance the cooling influence of clouds by increasing cloud reflectivity (traditionally called the first indirect effect) and lengthening cloud lifetime (the second indirect effect). Such effects can be difficult to distinguish in the observational record, in part because they likely feed back onto one another (Rosenfeld et al., 2014). The IPCC AR5 defines the first indirect effect as "radiative forcing due to aerosol-cloud interactions" (RFaci), and includes the second indirect effect within "effective radiative forcing due to aerosol-cloud interactions" (ERFaci), which accounts for rapid adjustments in temperature, precipitation, and cloud lifetime. Figure 13-21 depicts the mechanisms of RFaci and ERFaci (Boucher, 2013).

Quantifying RFaci is challenging because it includes the impacts of a complex suite of meteorological and chemical variables (e.g., relative humidity, cloud updraft velocity, and mixing state) on microphysical cloud processes, most of which are not well captured in coarse-grid climate models (Ban-Weiss et al., 2014). Another difficulty involves establishing a baseline for RFaci in the natural atmosphere. For example, Schmidt et al. (2012) showed that the effect of volcanic PM on cloud albedo results in a $-1.0\ Wm^{-2}$ cooling in a pristine environment, but only half that value is achieved in the polluted present-day environment, when more PM are competing for the available water vapor. Still more complex to quantify is ERFaci, which includes the fast meteorological feedbacks to the interactions of PM with clouds. These uncertainties associated with aerosol-cloud interactions and feedbacks (discussed throughout the rest of this chapter section) present to the most significant obstacle to more precisely quantifying the effects of PM on climate.

13.3.3.3 Effects of Absorbing PM on Snow and Ice Albedo

Regions of high albedo, such as snow- and ice-covered surfaces, strongly reflect incoming solar radiation. The transport and subsequent deposition of absorbing PM such as BC to snow- and ice-covered regions can decrease the local surface albedo, leading to surface heating. The absorbed energy, in turn, can melt the snow and ice cover and further depress the albedo, resulting in a positive feedback loop (Bond et al., 2013; U.S. EPA, 2012). This feedback has been invoked to partly explain the rapid increase in temperatures over the Arctic relative to the increase over mid-latitudes [e.g., (Shindell and Faluvegi, 2009)]. BC deposition may also affect surface temperatures over glacial regions. For example, ice core records from the Tibetan plateau indicate at least a doubling in the deposition rates of absorbing species since preindustrial times, with the potential to contribute to increased future melting of the Tibetan glacier (Wang et al., 2015). Recent observations have also shown that dust particle deposition on mountain snowpack strongly controls snowmelt-driven runoff in the Upper Colorado River Basin (Painter et al., 2018).

ED_002220_00002287-01807

13.3.3.4 Effect of Particle Size on the Interactions of PM with Climate

The size of particles influences how they interact with climate. Particles with diameters in the size range of 0.1−1.0 μm efficiently scatter solar radiation because they are within the same size range as the wavelength of solar energy. Thus $PM_{2.5}$, with diameter less than 2.5 μm, is more scattering and leads to greater surface cooling than the larger size fraction of $PM_{10-2.5}$. Most anthropogenic particles (e.g., sulfate and nitrate) fall within the $PM_{2.5}$ classification. Freshly emitted BC, BrC, and dust tend to be larger in size, though the smaller particles of these species have a disproportionately large radiative impact despite the total mass being dominated by the coarse mode (Boucher, 2013). Large particles have a relatively short lifetime and deposit quickly, leaving finer particles to travel further distances and extend their climate impact over a broader region. Large BC particles, however, can coagulate and then collapse into more compact and longer-lived structures (Raes et al., 2000). When exposed to high relative humidity, PM can take up water, deliquesce, and increase in size. As they age and acquire more hydrophilic coatings, even hydrophobic particles such as BC or dust can swell with water. Deliquesced particles tend to scatter more light than solid particles (Freney et al., 2010).

With regard to interactions of PM with clouds, laboratory experiments and model results show that particles with diameters in the range of 0.1−1.0 μm serve as efficient cloud condensation nuclei (Zhang et al., 2002). Thus $PM_{2.5}$ is a key contributor to such interactions. While UFP have traditionally been considered too small to influence cloud formation, they can rapidly grow into the size range required for cloud droplet activation, and so also play an important role in influencing cloud cover (Lee and Adams, 2012). In addition, there is now some evidence that UFP can themselves increase cloud condensation within tropical deep convective cloud systems (Fan et al., 2018). Coarse particles ($PM_{10-2.5}$), on the other hand, make a relatively small contribution to the number concentrations of cloud condensation nuclei, in part because key microphysical processes may occur over longer timescales than the typical residence time of such particles, and in part because $PM_{10-2.5}$ is less abundant (Raes et al., 2000). Mineral dust PM is a particularly important source of ice nuclei (IN) in cold clouds (Atkinson et al., 2013). Models attempting to capture the effects of PM on cloud cover and cloud lifetime often rely on cloud microphysical schemes with size-resolved particles (Pierce and Adams, 2007).

13.3.4 Estimates of Radiative Forcing from Total PM

This section discusses estimates of the forcing due to the sum of all PM species, including trends since the preindustrial era and since 1980. Table 13-4 summarizes this information.

ED_002220_00002287-01808

Table 13-4 Estimates of global mean radiative forcings due to anthropogenic PM.

Reference	Forcing Agent and/or Time Period	Radiative Forcing RF, Wm^{-2}	Effective Radiative Forcing ERF, Wm^{-2}	Data Type
Forcing due to interactions between PM and radiation.				
Bellouin et al. (2011)	Anthropogenic PM	−0.65 Wm^{-2}		Satellite data
Quaas et al. (2008)	Anthropogenic PM	−0.9 ± 0.4Wm^{-2}		Satellite data and models
Koch et al. (2011)	1900−2000	−0.41 Wm^{-2}		GISS ModelE
Myhre et al. (2013)	1850−2000 or 2006 (all models); 1750−2000 (adjusted)	−0.27 (−0.58 to −0.02) Wm^{-2} (all models); −0.35 Wm^{-2} (adjusted)		AeroCom model ensemble
Shindell et al. (2013)	1850−2000	−0.26 (−0.49 to −0.06) Wm^{-2} (all models); −0.42 (−0.50 to −0.33) Wm^{-2} (filtered)		ACCMIP model ensemble
Boucher (2013)	1750−2000	−0.35 ± 0.5 Wm^{-2}	−0.45 ± 0.5 Wm^{-2}	IPCC AR5 best estimate
Forcing due to interactions of PM with clouds				
Quaas et al. (2009)	Anthropogenic PM	−0.7 ± 0.5 Wm^{-2}		Satellite data plus AeroCom
Boucher (2013)	1750−2000		−1.2 to 0 Wm^{-2}	90% confidence range across models.
Total forcing from interactions of PM with both clouds and radiation[a]				
Murphy et al. (2009)	1970−2000		−1.1 ±0.4 Wm^{-2}	Analysis of Earth's energy balance
Wang et al. (2011a)	Anthropogenic PM		−1.05 Wm^{-2}	Multiscale set of models

ED_002220_00002287-01809

Table 13-4 (Continued): Estimates of global mean radiative forcings due to anthropogenic PM.

Reference	Forcing Agent and/or Time Period	Radiative Forcing RF, Wm^{-2}	Effective Radiative Forcing ERF, Wm^{-2}	Data Type
Shindell et al. (2013)	1850–2000 or 1850–2006		−1.17 (−0.71 to −1.44) Wm^{-2}	ACCMIP model ensemble
Boucher (2013)	1750–2000		−0.9 (−1.9 to 0.1) Wm^{-2}	IPCC AR5 best estimate[a]
Forcing due to the effects of absorbing PM on surface albedo				
Flanner et al. (2007)	Fossil fuel and biofuel BC on snow	+0.043 Wm^{-2}		Snow, Ice, and Aerosol Radiative (SNICAR) model
Skeie et al. (2011)	Anthropogenic BC on snow	+0.016 Wm^{-2}		Oslo chemical transport model
Bond et al. (2013)	Anthropogenic BC on snow	+0.034 (+0.007 to +0.074) Wm^{-2}		Best estimate across many model studies
Bond et al. (2013)	Anthropogenic BC on sea ice	+0.010 (+0.006 to +0.015) Wm^{-2}		Best estimate across many model studies
Lee et al. (2013)	1850–2000	+0.014 to +0.019 Wm^{-2}		ACCMIP model ensemble
Boucher (2013)	1750–2000	+0.04 (+0.02 to +0.09) Wm^{-2}		IPCC AR5 best estimate

[a]Excludes the effects of absorbing PM on surface albedo.

13.3.4.1 Forcing Due to Interactions of PM with Radiation

Historically, reflective PM have dominated absorbing PM in terms of forcing, leading to net global cooling and a negative RFari since the preindustrial era (Allen et al., 2013; Myhre, 2013). Koch et al. (2011) calculated a global mean value of −0.41 Wm^{-2} for the change in anthropogenic PM since 1900, while the AeroCom international model intercomparison study reports a value of −0.27 Wm^{-2} for the change since 1850, with values ranging from −0.58 to −0.02 Wm^{-2} across the ensemble of models considered (Myhre et al., 2013). Figure 13-22 shows the range of model estimates for total forcing and for individual species in the AeroCom ensemble. The large uncertainty in the AeroCom RFari arises in part from the neglect in some models of nitrate particles and SOA. Those models that do include SOA

ED_002220_00002287-01810

demonstrate a large range of forcing values for this particle type, and the range of positive forcings from fossil fuel BC is also large (Myhre et al., 2013). Adjustment of the AeroCom average to extend the time horizon and to take into account species missing from some models yields a mean RFari of −0.35 Wm^{-2} over the period since 1750 (Myhre et al., 2013).

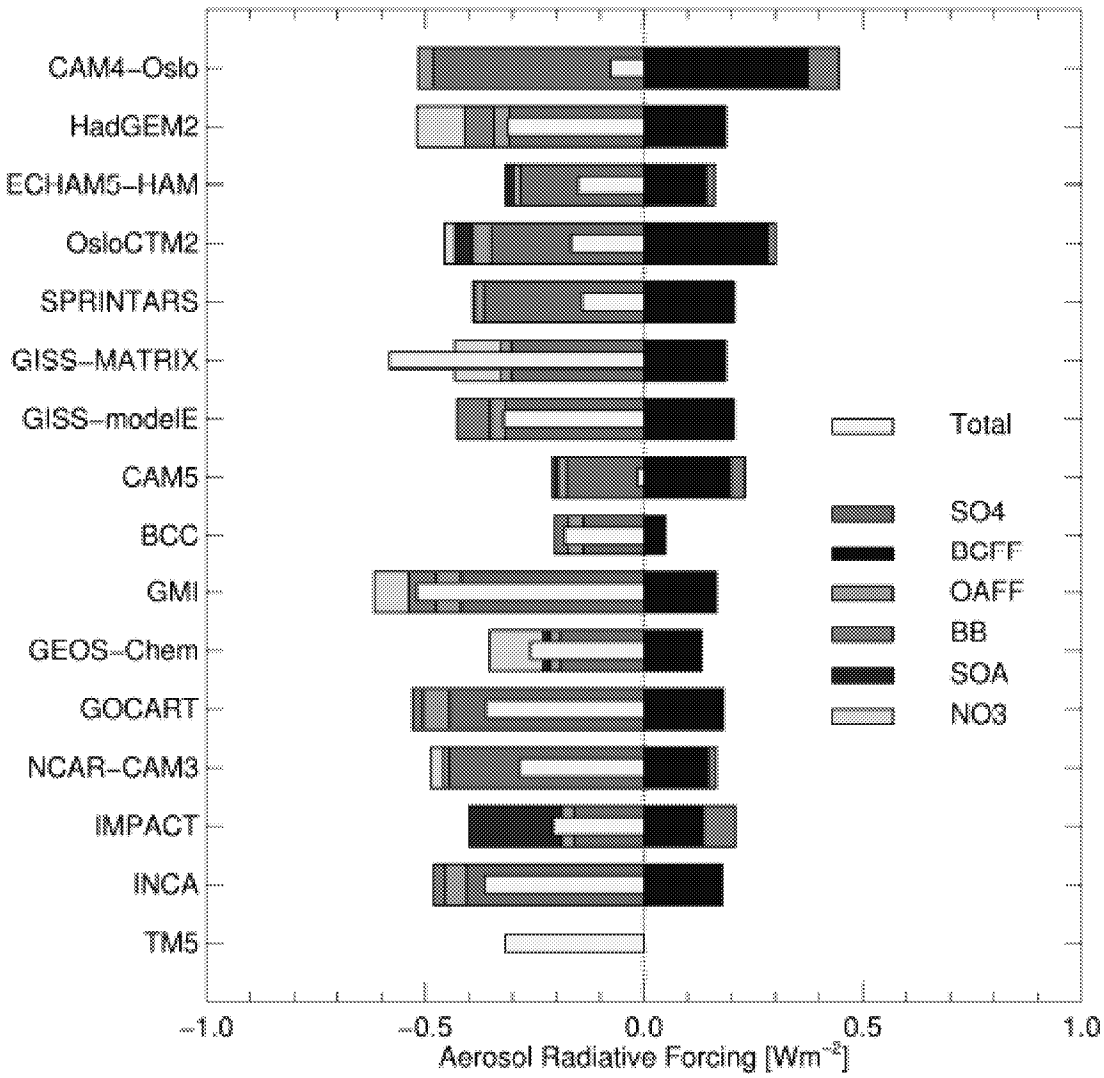

Note: The time period of the forcing is 1850 to 2000 or 2006, depending on the model, and the six components are sulfate (SO_4, blue), BC from fossil fuel (BCFF, black), organic particles from fossil fuel (OAFF, grey), biomass burning particles (BB, green), secondary organic particles (SOA, red), and nitrate (NO_3, brown).

Source: Permission pending, Myhre et al. (2013).

Figure 13-22 Radiative forcing from PM interactions with radiation (RFari) from six PM components in the AeroCom ensemble of models, overlain with total RFari for each model (yellow).

ED_002220_00002287-01811

The ACCMIP model ensemble similarly shows a range of estimates for RFari, −0.26 (−0.06 Wm^{-2} to −0.49) Wm^{-2} (Shindell et al., 2013). Figure 13-23 shows the spatial distribution of the mean and standard deviation of RFari across the ACCMIP models. In general, RFari is greatest over regions of industrial activity—the eastern U.S., Europe, and Asia. As in the AeroCom study, the distribution of standard deviation in Figure 13-23 reveals the large disagreements among models in forcing magnitude.

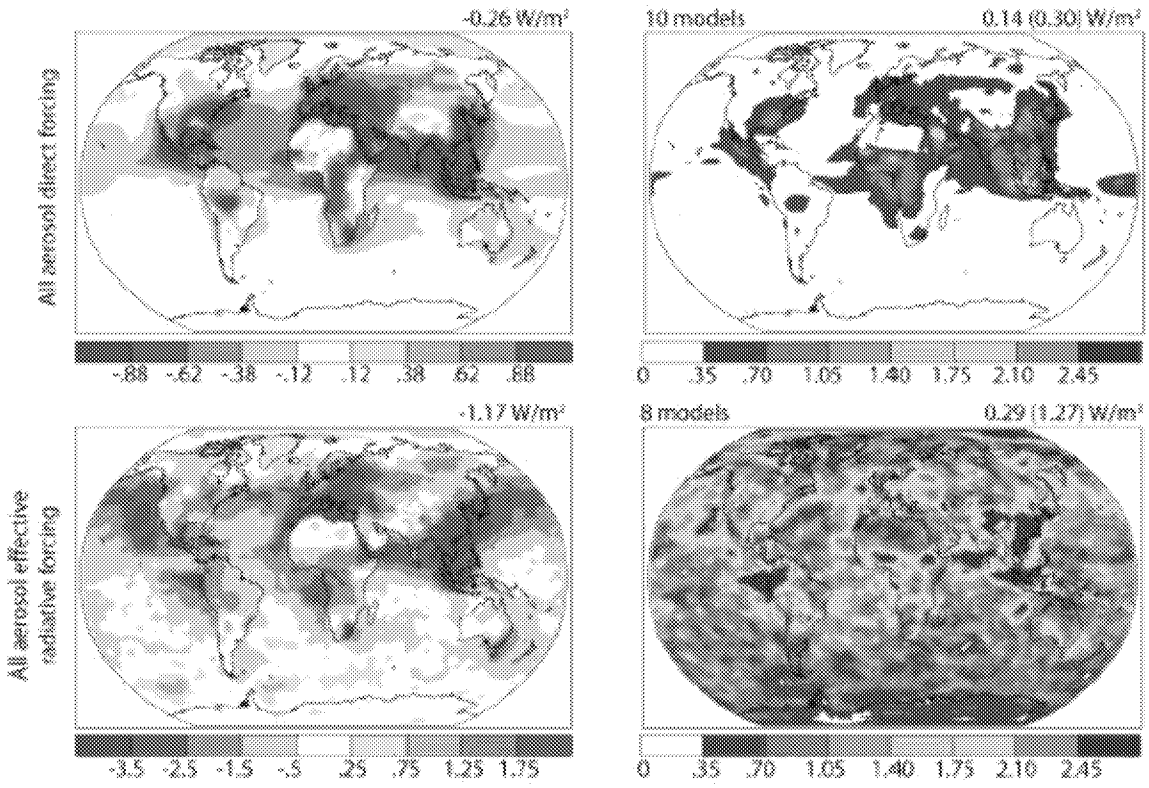

Note: The top panels show the multimodel mean (left) and standard deviation (right) of forcing due to interactions of particles with radiation (RFari), also known as "direct forcing." The bottom panels show the multimodel mean (left) and standard deviation (right) of total effective radiative forcing due to interactions of PM with both radiation and clouds (ERFari+aci). ERF includes fast feedbacks involving clouds, atmospheric temperature, water vapor, and land albedo. Note the difference in color bars for RFari and ERFari+aci.

Source: Permission pending, Shindell et al. (2013).

Figure 13-23 Spatial distributions of radiative forcing due to changing PM from 1850 to 2000 in the Atmospheric Chemistry and Climate Model Intercomparison Project (ACCMIP) model ensemble.

Until recently satellite studies yielded more negative RFari forcings than did models, especially over land, for reasons that were not clear. For example, using remotely sensed data from the Moderate Resolution Imaging Spectroradiometer (MODIS), Bellouin et al. (2008) estimated a present-day RFari

ED_002220_00002287-01812

from anthropogenic PM of −0.65 Wm^{-2}. Quaas et al. (2008) combined satellite data with model simulations to determine an even more negative RFari of −0.9 Wm^{-2}. This discrepancy was largely reconciled in Myhre (2009) by accounting for both direct radiative forcing missing from satellite retrievals and differences in aerosol optical properties between preindustrial and the present-day, bringing both the satellite- and model-based methods into agreement at the less negative values of RFari characteristic of model-based approaches.

Therefore, taking into account both model simulations and satellite observations, the IPCC AR5 reports an RFari from anthropogenic PM of −0.35 ± 0.5 Wm^{-2} (Boucher, 2013), which is slightly reduced in magnitude compared to AR4. Estimates of ERFari, which include the rapid feedback effects of temperature and cloud cover, rely mainly on model simulations, as this forcing is complex and difficult to observe. The IPCC AR5 best estimate for ERFari, −0.45 ± 0.5 Wm^{-2}, reflects this uncertainty (Boucher, 2013). Recall Figure 13-19, which shows the IPCC AR5 estimates of RFari and ERFari over the 1750−2011 timeframe, compared with other anthropogenic forcings.

13.3.4.2 Forcing Due to Interactions of PM with Clouds

Using data from a suite of satellite observations together with the AeroCom ensemble of models, Quaas et al. (2009) estimated RFaci at −0.7 ± 0.5 Wm, while climate models contributing to the IPCC AR5 yield a median value of −1.4 Wm^{-2} for anthropogenic RFaci (Boucher, 2013). ERFaci is difficult to quantify since it requires distinguishing between the feedbacks arising from interactions of PM with clouds and those arising from PM interactions with radiation. IPCC AR5 estimates ERFaci at −0.45 Wm^{-2}, with a 90% confidence interval of −1.2 to 0 Wm^{-2}.

13.3.4.3 Total Radiative Forcing Due to Interactions of PM with Clouds and Radiation

Using a cloud-resolving model embedded in a global climate model, Wang et al. (2011a) calculated an ERFaci+ari of −1.05 Wm^{-2}. Murphy et al. (2009) analyzed the Earth's energy balance and derived a similar value, −1.1 Wm^{-2}, while the ACCMIP ensemble of models yields an ERFari+aci of −1.17 (−1.44 to −0.71) Wm^{-2} (Shindell et al., 2013). Broadly consistent with these estimates, the IPCC AR5 reports a best estimate of ERFaci+ari of −0.90 (−1.9 to −0.1) Wm^{-2} (Boucher, 2013). As shown in Figure 13-19, which compares the IPCC AR5 estimates of ERFari and ERFaci over the 1750−2011 timeframe with other anthropogenic forcings, most of the uncertainty in total anthropogenic forcing since 1750 arises from uncertainties in the PM forcings. Figure 13-23 (bottom panels) shows the spatial distribution of ERFari+aci, with large forcings extending over oceans, where PM can strongly influence marine cloud cover downwind of source regions (Shindell et al., 2013).

ED_002220_00002287-01813

13.3.4.4 Forcing Due to the Effects of Absorbing PM on Albedo

Recent estimates of the global mean RF from anthropogenic PM deposited on highly reflective surfaces such as snow and ice range from +0.01 to +0.04 Wm^{-2} (Bond et al., 2013; Lee et al., 2013; Skeie et al., 2011; Flanner et al., 2007). The IPCC AR5 reports a best estimate of RF from the albedo effect at the high end of this range, +0.04 Wm^{-2}, with an uncertainty range of +0.02 to +0.09 Wm^{-2} (Boucher, 2013). Table 13-1 contains a summary of these results, and Figure 13-23 (bottom right) shows the spatial distribution of this forcing from ACCMIP. As with other forcings, the uncertainty stems in part from uncertainties in emissions and in transport processes, including wet deposition (Doherty et al., 2010). The forcing is largest during March-May over the Arctic and boreal regions due to efficient winter-spring transport of pollution from Eurasia (Flanner et al., 2007).

13.3.4.5 Recent Trends in PM Forcing

In response to air quality concerns, most developed countries have made significant cuts to emissions of PM or their precursors in recent decades, and this trend is revealed in the time series of forcing estimates for the 20th century. For example, in the ACCMIP ensemble of models, trends in global mean RFari for all PM species show maximum cooling around 1980, but with a large uncertainty range, from about −0.1 to −0.5 Wm^{-2} (Shindell et al., 2013). Smith and Bond (2014) estimate that the largest total impact of absorbing and scattering aerosols on climate occurred between 1950 and 1970, with a change in total aerosol forcing over this period ranging from −0.2 to −0.8 W m^{-2}. Major sources of uncertainty in these types of estimates of trends in aerosol radiative forcing include uncertainties in the temporal changes in emissions and in the mix of scattering versus absorbing aerosols (Xing et al., 2015; Smith and Bond, 2014).

Figure 13-24 shows the time evolution of RFari for a range of species from 1850 to 2010. In Figure 13-25 (top), the spatial distribution of the 1980–2000 forcing trend from the sum of all species reveals large heterogeneity. RFari is positive over North America and Europe due to declining sulfate loading in the time period. In contrast, RFari increases significantly over India and southeast Asia, where rising concentrations of reflective sulfate outpace those of the more absorbing BC. Over China, however, the increases in sulfate and BC loadings are more balanced, leading to an RFari close to zero for this time period. The positive RFari over Africa can be traced to increases in biomass burning and the subsequent rise in BC (Figure 13-25, bottom).

The forcings depicted in Figure 13-24 and Figure 13-25 are all TOA forcings. At the TOA, the effects of absorbing and scattering particles can cancel each other out, while at the surface, the effects of both types of particles combine to yield net cooling. For example, while China shows no TOA forcing over the 1980–2000 in Figure 13-25, another study suggests that increases in BC and sulfate particles

ED_002220_00002287-01814

over this region have led to a cooling trend of −6 ± 2 Wm^{-2} per decade over the 1950−2000 time frame (Folini and Wild, 2015).

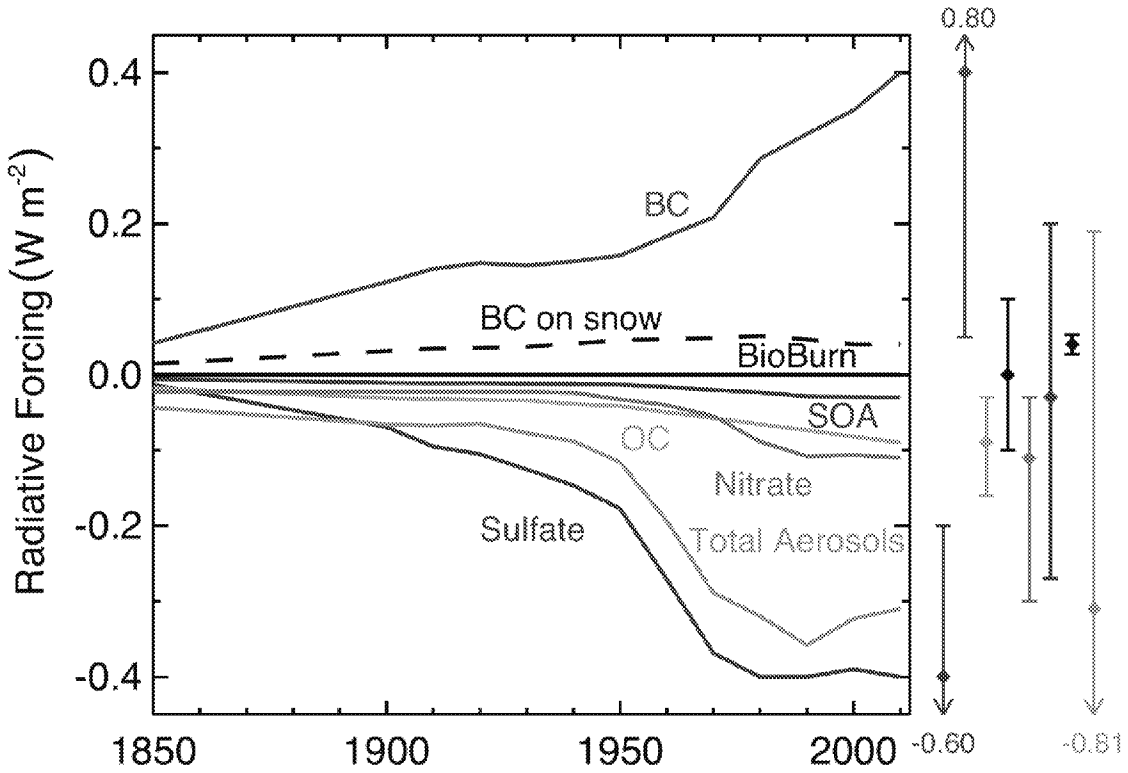

Note: The curves show the multimodel results for 1850, 1930, 1980, and 2000 from the ACCMIP ensemble for RFARI (Shindell et al., 2013) and the BC-albedo effect (Lee et al., 2013), combined with higher temporal-resolution results from two models in the ensemble. The blue curve represents the sum of all forcings shown. The 5% to 95% uncertainty ranges for 2010 are shown with vertical lines to the right of the graph. Values next to the uncertainty lines are for cases in which uncertainties go beyond the scale. All values have been scaled to the best estimates for 1750–2011 RFARI. SOA is for secondary organic particles, and "bioburn" represents the sum of RFARI of BC and primary organic particles from biomass burning. Estimates of forcings from mineral dust are not shown.

Source: Permission pending, Myhre (2013).

Figure 13-24 Time evolution of radiative forcing due to interactions of PM with radiation (RFARI) and the effects of black carbon (BC) on snow and ice albedo.

ED_002220_00002287-01815

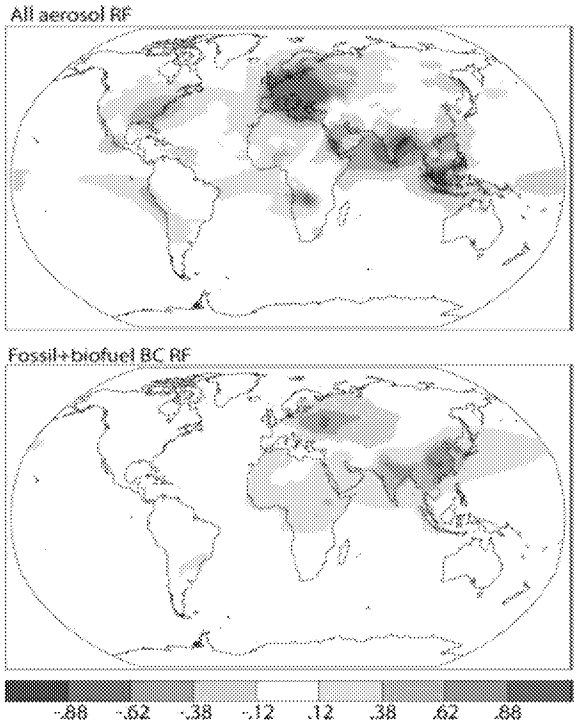

Note: The top panel shows RFari for all PM species, and the bottom panel shows RF for BC from fossil fuel and biofuel. Results are shown for only those ACCMIP models that provided results for 1980. Units are Wm^{-2}.

Source: Permission pending, Shindell et al. (2013).

Figure 13-25 Mean radiative forcings due to interactions of PM with radiation (RFARI) from a subset of the Atmospheric Chemistry and Climate Model Intercomparison Project (ACCMIP) models for the 1980 to 2000 time period.

13.3.5 Effects of PM on Climate by Species

This section describes the individual climate effects associated with the following key PM species: sulfate, nitrate, OC, BC, and dust, to the extent that quantitative estimates of the radiative forcing associated with these individual species are available in the literature. Figure 13-26 shows the AeroCom and IPCC AR5 estimates of the annual mean TOA RFari for these different PM species discussed below. Figure 13-27 shows the global spatial distributions of the forcings by species type, as calculated in the ACCMIP ensemble.

ED_002220_00002287-01816

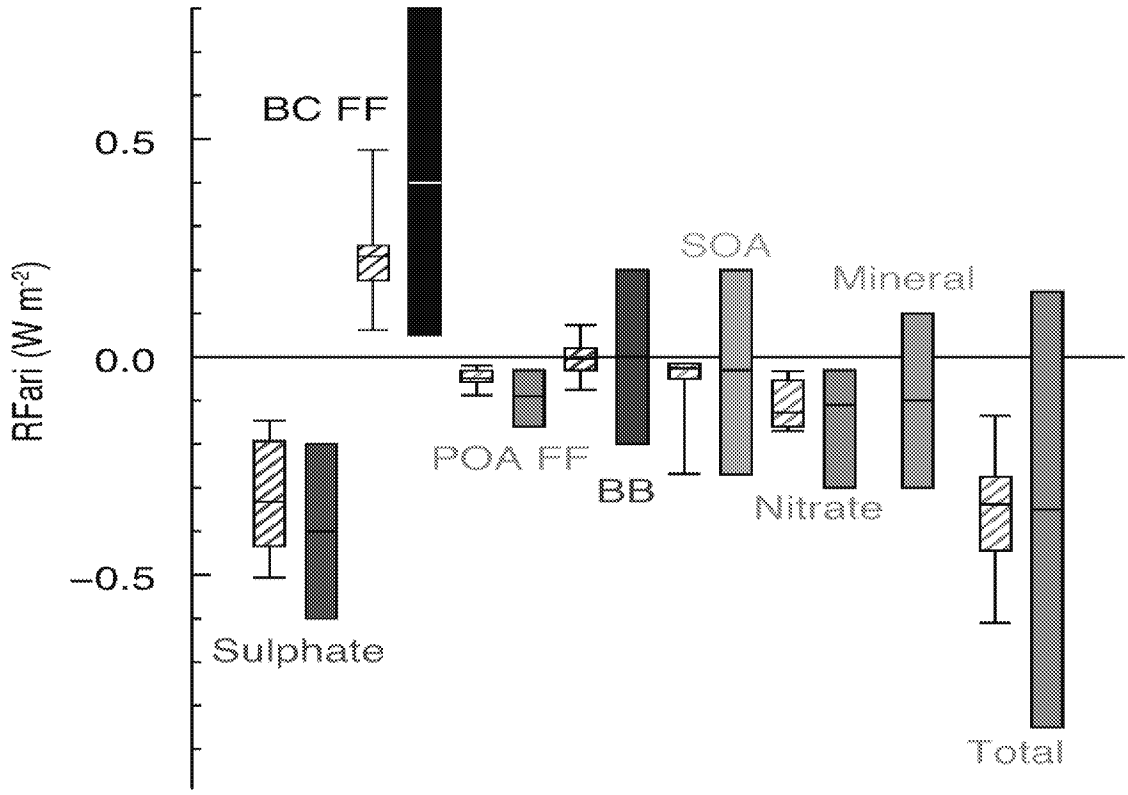

Note: These interactions are also known as aerosol-radiation interactions (RFari), and values of RFari for different PM species are shown. Units are Wm^{-2}. Hatched boxes show results from an AeroCom model study, adjusted for the 1750–2010 period, with boxes denoting the 5% to 95% uncertainty ranges and whiskers denoting the minimum and maximum values across models (Myhre et al., 2013). Solid colored boxes show the IPCC AR5 best estimates and the 5% to 95% uncertainty ranges. BC FF indicates black carbon from fossil fuel and biofuel; POA FF, primary organic PM from fossil fuel and biofuel; BB, biomass burning PM; and SOA, secondary organic PM.

Source: Permission pending, Boucher (2013).

Figure 13-26 Estimated annual mean top-of-the-atmosphere radiative forcings due to interactions of PM with radiation for the 1750–2010 period.

ED_002220_00002287-01817

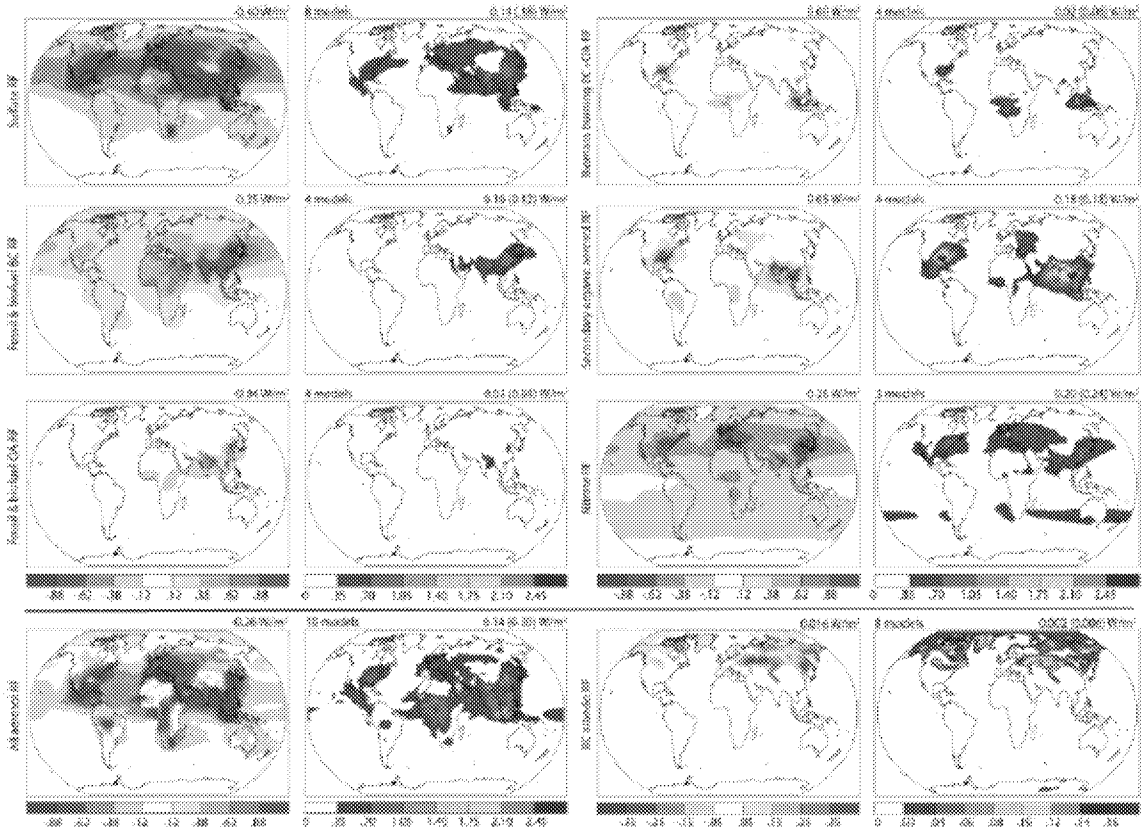

Note: The top three rows show the forcings due to PM interactions with radiation (RFari) for different PM species, the bottom left corner shows the total RFari, and the bottom right corner shows the forcing due to the effect of BC on surface albedo. Units are Wm^{-2}. Values above the RF panels represent the global mean RF. Values above the standard deviation panels show the standard deviation across the model means, with the global mean of standard deviations across gridboxes in parentheses.

Source: Permission pending, Shindell et al. (2013).

Figure 13-27 Mean radiative forcings (RF, left columns) and their standard deviations (right columns) from the ACCMIP ensemble for the 1850–2000 time period.

13.3.5.1 Sulfate

Sulfate particles form through oxidation of SO_2 by OH in the gas phase and in the aqueous phase by a number of pathways, including in particular those involving ozone and H_2O_2. The main source of anthropogenic sulfate is from coal-fired power plants, and global trends in anthropogenic SO_2 emissions are estimated to have increased dramatically during the 20th and early 21st centuries (Lamarque et al., 2013). Many developed countries have recently implemented more stringent air pollution controls that have reversed such trends (Klimont et al., 2013; Smith et al., 2011), leading to cleaner air [e.g., (Keene et al., 2014; Ruckstuhl et al., 2008)].

ED_002220_00002287-01818

Sulfate particles are highly reflective. On a global scale, the IPCC AR5 estimates that sulfate contributes more than other PM types to RF, with RFari of −0.4 (−0.6 to −0.2) Wm^{-2}, where the numbers in parentheses represent the 5% to 95% uncertainty range (Myhre, 2013). This range indicates the challenges of estimating both SO_2 sources in developing regions and the lifetime of sulfate against wet deposition. Other, more recent estimates are broadly consistent with the AR5 value. Heald et al. (2014) calculated a global RFari of −0.36 Wm^{-2}, while Zelinka et al. (2014) reported an average ERFari value of −0.52 Wm^{-2} across an ensemble of nine CMIP5 models. Sulfate is also a major contributor to the influence of PM on clouds (Takemura, 2012). In their multimodel study, Zelinka et al. (2014) estimated a total effective radiative forcing (ERFari+aci) from anthropogenic sulfate of nearly −1.0 Wm^{-2}.

13.3.5.2 Nitrate

Nitrate particles form through the oxidation of nitrogen oxides, and occur mainly in the form of ammonium nitrate. Ammonium, however, preferentially associates with sulfate rather than nitrate, leading to formation of ammonium sulfate at the expense of ammonium nitrate (Adams et al., 2001). As anthropogenic SO_2 emissions decline in response to air quality control programs, more ammonium will likely become available to react with nitrate, potentially leading to increases in this PM type (Hauglustaine et al., 2014; Shindell et al., 2013). On the other hand, a warming climate may decrease nitrate abundance, as this PM species is highly volatile at warmer temperatures (Tai et al., 2010). Like sulfate, nitrate particles are reflective. The IPCC AR5 estimates a present-day RFari of nitrate of −0.11 (−0.3 to −0.03) Wm^{-2}, approximately one-fourth of the effect of sulfate (Boucher, 2013). By the mid−21st century, however, as SO_2 emissions decline, ammonium nitrate may account for half the total PM global cooling effect (Bellouin et al., 2011).

13.3.5.3 Organic Carbon, Including Brown Carbon

Primary organic particles arise from wildfires, agricultural fires, and from biofuel or fossil fuel combustion. SOA, as mentioned above, forms when anthropogenic or biogenic nonmethane hydrocarbons are oxidized in the atmosphere, leading to less volatile products that may partition into PM [e.g., (Donahue et al., 2012; Jimenez et al., 2009)]. Organic particles are mostly reflective, but in the case of BrC, a portion is significantly absorbing at shorter wavelengths (<400 nm). BrC particles occur most frequently in smoke plumes and in urban areas in the developing world that depend on coal or biofuel for domestic heating (Liu et al., 2014; Feng et al., 2013; Arola et al., 2011).

The IPCC AR5 estimates an RFari for primary organic PM from fossil fuel combustion and biofuel use of −0.09 (−0.16 to −0.03) Wm^{-2} (Myhre, 2013). The RFari estimate for SOA from these sources is −0.03 (−0.27 to +0.20) Wm^{-2}. The wide range of both these RFari estimates, with even the sign of the forcing not consistent across models, reflects uncertainties in both the optical properties of organic

ED_002220_00002287-01819

PM and its atmospheric budgets, including the production pathways of anthropogenic SOA (Scott et al., 2014; Myhre et al., 2013; McNeill et al., 2012; Heald et al., 2010).

Trends in biogenic SOA may also have contributed to RFari. Recent work suggests that the expansion of global cropland since the preindustrial era has reduced emissions of biogenic species, resulting in a global mean warming of +0.09 Wm^{-2} due to a diminished concentration of SOA (Unger, 2014). For primary organic PM arising from biomass burning, the IPCC AR5 estimates an RFari of −0.2 Wm^{-2} (Boucher, 2013). Consideration of absorbing BrC may reduce that cooling by as much as 16−25% (Hammer et al., 2016; Lu et al., 2015). When deposited on snow or ice surfaces, BrC, like BC, may contribute to surface warming through the albedo effect, but this forcing has not been quantified.

Of the two types of organic particles—primary versus secondary—primary particles are more effective per unit mass in serving as cloud condensation nuclei (Trivitayanurak and Adams, 2014). Primary organic particles contribute both mass and number concentration in the size range needed to nucleate cloud droplets; they also contribute to the concentration of nanoparticles, which can subsequently grow to the appropriate size. Secondary organic particles (i.e., SOA) condense onto existing particles, which may fall outside the size range of cloud condensation nuclei; in addition, a large amount of SOA forms on particles that already act as cloud condensation nuclei, thereby not affecting the total number of nuclei available.

13.3.5.4 Black Carbon

BC particles occur as a result of inefficient combustion of carbon-containing fuels. Like primary organic PM, BC is emitted by biofuel and fossil fuel combustion and by biomass burning. BC is absorbing at all wavelengths and likely has a large impact on the Earth's energy budget (Bond et al., 2013). The IPCC AR5 estimates a BC RFari from anthropogenic fossil fuel and biofuel use of +0.4 (+0.05 to +0.8) Wm^{-2} (Myhre, 2013). Biomass burning contributes an additional +0.2 (+0.03 to +0.4) Wm^{-2} to BC RFari. The albedo effect of BC on snow and ice surfaces adds another +0.04 (+0.02 to +0.09) Wm^{-2} (Myhre, 2013) (see also Section 13.3.4.4 above).

BC forcing estimates are especially sensitive to the assumptions made about the mixing state of PM (Jacobson, 2012). In an external mixture, different PM types coexist, and each particle consists of a single species. In an internal mixture, each particle consists of a mixture of species. Such a mixture may be homogeneous, or it may occur as a core particle of one species coated with layers of one or more other species. Laboratory and field measurements suggest that BC particles acquire organic coatings as they age in the atmosphere, with subsequent increases in absorption of shortwave radiation (Cappa et al., 2012). These increases likely arise due to enhancement of absorption cross section as the particles grow in size. In addition, the coatings may act as a lens, focusing sunlight onto the BC core, thereby increasing absorption (Klingmueller et al., 2014). Knowledge of the photochemical aging of BC is poor.

ED_002220_00002287-01820

As implied above, a large uncertainty in BC forcing involves the magnitude of emissions from biomass burning, which includes wildfire and other forms of open burning. BC is coemitted with OC by biomass burning, and the IPCC central estimate for the total 1750–2011 forcing from biomass burning is in fact zero (+0.2 Wm^{-2} BC forcing and −0.2 Wm^{-2} OC forcing). In the AeroCom ensemble, the total forcing from biomass burning varies in both magnitude and sign across models (Myhre et al., 2013). New field research suggests that biomass burning BC can form large superaggregates in plumes downwind, and that such particles would contribute nearly double the warming per unit optical depth typically assumed for smoke PM in models (Chakrabarty et al., 2014). In one recent study, however, Sena and Artaxo (2015) used satellite data to quantify TOA forcings due to biomass burning smoke during the dry season in Amazonia. They found an overall cooling effect of -5.2 ± 2.6 Wm^{-2}, averaged over 10 seasons.

13.3.5.5 Dust

Dust, also known as mineral dust, has traditionally been classified as scattering. A recent study, however, found that observed dust may be substantially coarser (and thus more light-absorbing) than currently represented in climate models (Kok et al., 2017). Dust mobilization occurs from dry or disturbed soils, and so is linked to both meteorological conditions and human activity, with anthropogenic sources making up about 25% of the total (Ginoux et al., 2012). Through analysis of lake sediment, Neff et al. (2008) determined that the expansion of livestock grazing likely increased dust deposition in the West by a factor of five since the 19th century. Once airborne, dust can strongly attenuate incoming solar radiation (Kavouras et al., 2009; Fairlie et al., 2007). If deposited on snow, dust may accelerate snow melt since dust is darker than snow and may decrease surface albedo (Painter et al., 2012; Skiles et al., 2012). Estimates of global RF related to the change in dust presence since the preindustrial era vary widely due to lack of knowledge both of dust trends (Mahowald et al., 2010) and of dust optical properties (Li et al., 2015). The IPCC AR5 estimates RFari due to dust change since 1750 as -0.1 ± 0.2 Wm^{-2} (Boucher, 2013). The Kok et al. (2017) result, however, suggests that the anthropogenic change in dust may have led to warming, not cooling. Dust may also influence cirrus cloud cover by serving as efficient ice nuclei, although quantifying the resulting forcing is challenging (Kuebbeler et al., 2014; Nenes et al., 2014).

13.3.6 Climate Response to Changing PM, Including Feedbacks

The radiative forcing due to PM elicits a number of responses in the climate system that can lead to significant effects on weather and climate over a wide range of space and time scales, mediated by a number of feedbacks that link PM and climate. For the purposes of this ISA, we focus primarily on climate impacts in the U.S., described in the following section (Section 13.3.7). Here we briefly summarize the mechanisms of climate responses and feedbacks to PM radiative forcing.

ED_002220_00002287-01821

In contrast to long-lived greenhouse gases that are well-mixed in the atmosphere, PM has a very heterogeneous distribution across the Earth. The patterns of RFaci and RFari thus tend to correlate with PM loading, with the greatest forcings centered over continental regions (e.g., Figure 13-27). The climate response is more complicated, however, since the perturbation to one climate variable, such as temperature, cloud cover, or precipitation, typically leads to a cascade of effects on other variables. As a result, while the initial PM radiative forcing may be concentrated regionally, the eventual climate response can be spatially much broader (even, ultimately, global) or concentrated in remote regions. For example, increases in absorbing PM over Asia may induce shifts in atmospheric circulation patterns that may, in turn, affect U.S. regional climate (Teng et al., 2012). Because of the complexity of the potential climate system interactions, the spatial relationships between patterns of PM forcing and those of climate response vary greatly among models, with some studies showing relatively close correlation between forcing and surface temperature response [e.g., (Leibensperger et al., 2012a)] and other studies showing much less correlation [e.g., (Levy et al., 2013)].

These climate system responses themselves lead to feedbacks that in turn affect PM. Such PM-climate feedbacks involve a perturbation of regional climate by PM radiative forcing, which in turn leads to meteorologically driven changes in PM emissions, formation, or lifetime. A positive feedback increases PM concentration and amplifies the PM effect on climate, while a negative feedback decreases PM concentration and weakens the PM effect on climate. Examples of such feedbacks occurring on the regional scale include those involving wildfires, inversions, clouds, and convection, PM-albedo effects, and biogenic emissions.

For example, wildfires are expected to increase in a warming world [(Yue et al., 2013; Pechony and Shindell, 2010)], and agricultural fires may also increase as more land is cleared for crops and timber plantations, particularly in the tropics (Margono et al., 2012). Smoke from these fires contain a mix of absorbing (BC and BrC) and scattering particles and so may affect the climate in complex ways. In their model study, Tosca et al. (2010) found that smoke from fires reduced solar radiation at the surface by 1.3 Wm^{-2}, corresponding to a global mean temperature decrease of $-0.13 \pm 1°C$. Absorption of solar radiation by smoke particles warmed the troposphere, and that warming, together with the cooler surface temperatures, weakened the Hadley circulation and decreased precipitation over tropical forests. Such a positive feedback would further enhance fire activity in the tropics.

Another example of PM-climate feedback involves atmospheric inversions, especially over mountain basins. Such inversions limit ventilation and promote accumulation of surface PM; and the enhanced PM can further intensify the inversion. For example, over Salt Lake City in Utah, haze episodes during wintertime inversion events diminish the penetration of solar radiation and cool the surface further, strengthening the inversion and exacerbating the haze (Lareau et al., 2013). In their modeling study, Jacobson and Streets (2009) found a similar positive feedback of PM on pollution levels in Los Angeles: atmospheric stability over Los Angeles was enhanced by a combination of warming of the air by BC and

ED_002220_00002287-01822

cooling of the ground by all particle types, including BC. The resulting decrease in precipitation lengthened the lifetime of PM in that study.

Invoking similar mechanisms, Cook et al. (2009) identified atmospheric dust as a probable amplifier of the Dust Bowl drought of the 1930s. The drought, together with the agricultural practices prevalent in that era, likely resulted in the mobilization of a massive amount of dust, which would, in turn, have warmed the local atmosphere, suppressing convection and exacerbating drought conditions [see also (Xing et al., 2016)]. In contrast, Zhang et al. (2010) calculated that heating by BC particles may invigorate convection under certain conditions, thereby increasing surface ventilation and precipitation. More recently, Mashayekhi and Sloan (2014) calculated a 15% decrease in convective precipitation due to PM radiative effects in the northeastern U.S., but a 30% increase in large-scale precipitation in this region due to the influence of PM on clouds.

As described in Section 13.3.3.3, deposition of BC and other absorbing species on Arctic snow and sea ice may decrease surface albedo and accelerate warming at high latitudes (Bond et al., 2013; Lee et al., 2013; Skeie et al., 2011; Flanner et al., 2007). Model studies have suggested that this rapid warming could shift the polar jet northward, decreasing cold front frequency over mid-latitudes and lengthening stagnation episodes (Turner et al., 2013; Leibensperger et al., 2008). An increase in stagnation would likely intensify pollutant events in source regions. Transport of pollution to the Arctic could also be affected, but this feedback onto Arctic BC deposition has not been studied.

A final example involves biogenic SOA, which arises from the complex oxidation pathways of biogenic species such as isoprene and monoterpenes. As biogenic emissions are strongly temperature-dependent, SOA concentrations are expected to increase in a warming climate (Wu et al., 2012; Heald et al., 2008), even if the so-called "CO_2 inhibition effect" is taken into account (Tai et al., 2013). Such regional increases in reflective PM could significantly cool the underlying surface, thereby limiting the magnitude of SOA enhancement (Arneth et al., 2010).

13.3.7 Effect of PM on U.S. Regional Climate

The effects of PM on U.S. regional climate have been examined on several different spatial and temporal scales. Some studies have investigated the impact of PM on urban microclimates [e.g., (Jacobson et al., 2007)]. Other studies have diagnosed weekly cycles in temperature or precipitation, which taken together suggest that weekly variations in anthropogenic PM may influence regional weather patterns [e.g., (Bell et al., 2008; Forster and Solomon, 2003)]. A key question, however, is to what extent PM trends in the U.S. may have partially offset the warming effects of rising greenhouse gases over the course of the 20th century.

Over the contiguous U.S., surface temperatures warmed during the early decades of the 20th century, remained relatively flat from about 1960 to 1980, then rose rapidly by ~1°C from 1980 to 2010

ED_002220_00002287-01823

(NAS, 2014). A closer look at spatial trends in these temperatures reveals a strong cooling trend of approximately −1°C from 1930 to 1990 in the Southeast, centered over Arkansas and Oklahoma (Leibensperger et al., 2012a) (Figure 13-28). Mascioli et al. (2017) pointed out that between 1950 and 2000 the cooling extended over much of the eastern U.S. This observed cooling, which took place even as much of the globe warmed in response to greenhouse gases, is sometimes referred to as the U.S. "warming hole" (Pan, 2004). Several studies have linked the U.S. warming hole to natural variability [e.g., (Banerjee et al., 2017)], in particular to decadal variation in North Atlantic or Pacific sea surface temperatures (SSTs) (Meehl et al., 2015; Kumar et al., 2012; Meehl et al., 2012; Kunkel et al., 2006). Such variability can influence large-scale meteorological processes, which in turn may affect temperatures in continental interiors such as the central or south-central U.S. In one multimodel study, those models that best represented the Atlantic Multidecadal Oscillation also best reproduced the warming hole, although even those models showed large discrepancies with observations (Kumar et al., 2012).

ED_002220_00002287-01824

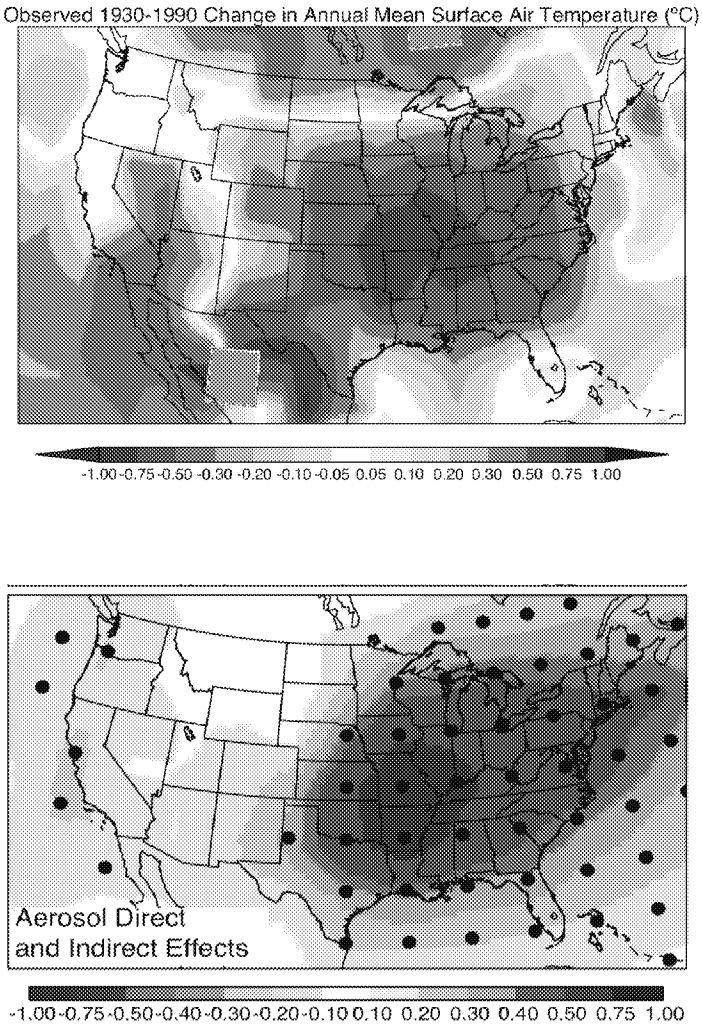

Top: Temperature change is based on a linear trend, and observations are from the NASA GISS Surface Temperature Analysis (GISTEMP, http://data.giss.nasa.gov/gistemp/).

Bottom: Units are °C. Values represent the mean difference between two sets of 5-member ensemble simulations in a climate model; one set includes U.S. anthropogenic PM sources and one does not. Interactions of PM with both radiation and clouds are considered. Dots indicate differences significant at the 95th percentile.

Source: Permission pending, Leibensperger et al. (2012a).

Figure 13-28 Top: Observed change in surface air temperatures between 1930 and 1990. Bottom: Effect of U.S. anthropogenic PM sources on surface air temperatures for the 1970–1990 period when U.S. particulate loading was at its peak.

Other studies have suggested that trends in PM loading may be partly responsible for the unusual cooling trend in the southeastern U.S. during the mid-20th century (Section 13.3.2.1). PM in the Southeast is dominated by a mix of sulfate and organic species. In recent years, PM levels in this region have declined in response to emissions controls, possibly contributing to the observed increase in solar

ED_002220_00002287-01825

radiation at the surface. For example, from 2001 to 2013, observed AOD across the Southeast decreased an average −4% per year (Figure 13-29), while surface solar radiation in the region increased by +8 Wm^{-2} (Attwood et al., 2014). Gan et al. (2014), however, reported increases in both direct and diffuse surface solar radiation, at least averaged over the whole of the eastern U.S. from 1995 to 2010. The results of Gan et al. (2014) are difficult to interpret due to the seeming discrepancy between a decrease in PM and an increase in diffuse radiation. Additionally, it is unclear why the greatest cooling occurred in the relatively rural Southeast, away from the historically large sources of anthropogenic PM such as power plants in the Ohio River Valley. As discussed above, climate responses to PM radiative forcing can be nonlocal, but it is not clear what may have caused this particular mismatch in forcing and climate response.

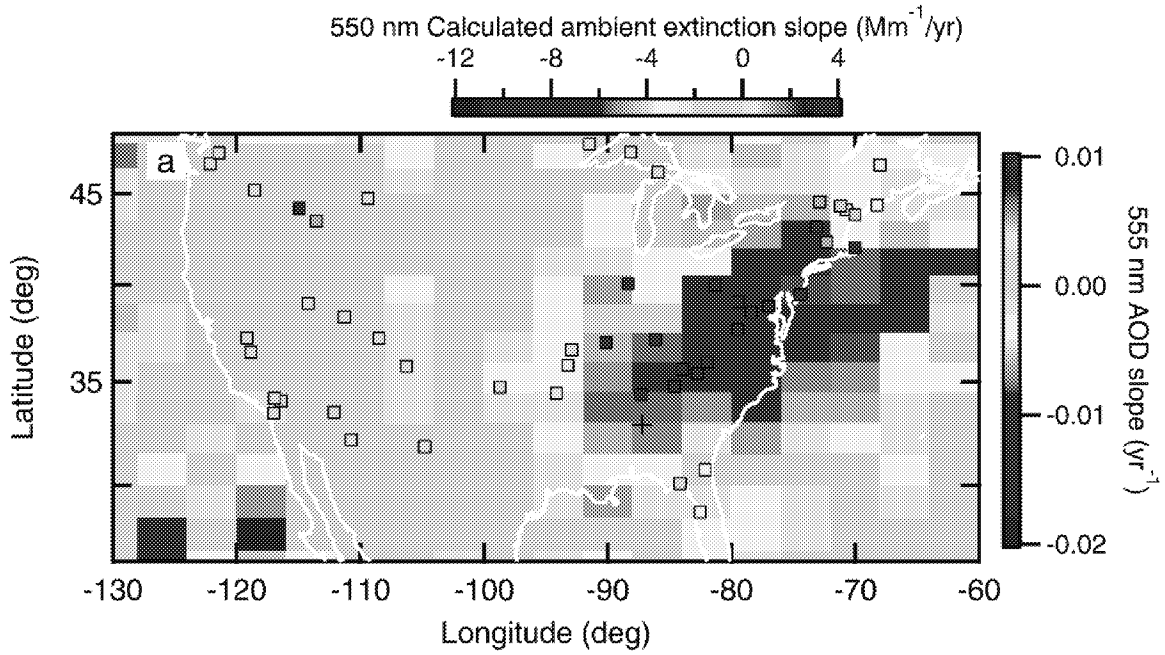

Note: The open squares denote trends in ambient extinction, a measure of how much solar radiation reaches the Earth's surface, from the IMPROVE network. The plus symbol indicates the site of the 2013 Southern Oxidant and Aerosol study, which analyzed aerosol extinction as a function of relative humidity.

Source: Permission pending, Attwood et al. (2014).

Figure 13-29 Trends in aerosol optical depth (AOD) measured by the Multi-angle Imaging SpectroRadiometer (MISR) satellite instrument over the 2001−2013 time period.

To address these issues, several model studies have tried to recreate the observed trends in AOD, surface radiation, and surface temperatures. Leibensperger et al. (2012a, 2012b) found that the regional RF from anthropogenic PM elicits a strong regional climate response, cooling the central and eastern U.S.

ED_002220_00002287-01826

by 0.5–1.0°C on average during 1970–1990, with the strongest effects on maximum daytime temperatures in summer and autumn (Figure 13-28). In this study, the spatial mismatch between maximum PM loading and maximum cooling could be partly explained by the outflow of PM cooling the North Atlantic, which then strengthens the Bermuda High in the model and increases the flow of moist air into the south-central U.S. Local feedback effects involving soil moisture and cloud cover may also amplify the surface temperature response to changing PM loading in the Southeast (Mickley et al., 2012; Liang et al., 2005; Pan, 2004).

The Leibensperger et al. (2012a, 2012b) studies suggest that the influence of PM on radiation and clouds plays a significant role in driving regional cooling in the Southeast. In contrast, a more recent model study, Yu et al. (2014) determined that the U.S. warming hole can best be explained by the PM interactions with clouds alone. Meanwhile, Attwood et al. (2014) attributed 20% of the observed increase in surface solar radiation in the Southeast to a decrease in the sulfate/organic ratio of PM. As sulfate is more hygroscopic than organic material, a decline in sulfate would decrease particle water content and thus particle extinction, leading to local brightening—i.e., more sunlight reaching the surface. In contrast to Yu et al. (2014), the Attwood et al. (2014) result implies that at least some of the warming hole can be attributed to aerosol-radiation interactions. More recently, Mascioli et al. (2017) used an ensemble of observations and IPCC model simulations to conclude that both PM and natural variability contributed to the U.S. warming hole, at least in summer.

Overall, therefore, several lines of evidence suggest an important influence of PM on observed 20th century temperature trends over the southern and eastern U.S. A number of key uncertainties, however, mean that alternative explanations cannot be ruled out at this time, and further research is needed.

13.3.8 Uncertainties in Estimates of PM Effects on Radiative Forcing and Climate: Summary

In general, uncertainties associated with clouds and aerosols continue to be the largest contributors to overall uncertainty in evaluating climate change trends and projecting future climate changes (Boucher, 2013). With respect to PM-climate uncertainties specifically, there has been significant progress since the 2009 ISA. According to the IPCC AR5, "Climate-relevant aerosol processes are better understood, and climate-relevant aerosol properties better observed, than at the time of AR4" (Boucher, 2013). Nevertheless, significant uncertainties still remain which make it difficult to precisely quantify the climate effects of PM. This is because the properties of PM, and those of the clouds with which PM interacts, vary substantially on scales much smaller than those able to be represented in even the most recent generation of climate models. In addition, as described above, the initial radiative forcing effect of PM leads to a diverse range of regionally heterogeneous climate impacts associated with changes in the hydrologic cycle and atmospheric circulation patterns, mediated by a variety of feedbacks, and interacting

ED_002220_00002287-01827

in complex ways with other forced and natural sources of climate variability and change occurring simultaneously. This makes it difficult to characterize the total net impact of PM on climate and to disentangle the unique contribution of PM to overall climate change.

As discussed throughout this section, uncertainties in estimates of PM effects on climate arise from many sources. First, there is a lack of knowledge of PM abundance. Unlike the well-mixed greenhouse gases, PM is not uniformly distributed through the atmosphere and the current spatial distribution of PM concentrations is not well quantified (Myhre, 2013). Long-term measurements of PM are rare and mainly surface-based, making it challenging to estimate trends in AOD, which are key to estimating climate impacts (Koch et al., 2011). In particular, calculation of the RF of anthropogenic PM requires precise knowledge of preindustrial particle load; this is especially true for determining RFaci (Carslaw et al., 2013). Measurements from ice cores and lake-core sediments offer the only constraints on PM of the preindustrial era; such sparse measurements cannot capture the spatial distribution of this era. Another difficulty in estimating the climate impacts of anthropogenic PM lies in quantifying the contribution of natural PM to observed trends (Heald et al., 2014). The production and loss rates of natural PM depend on meteorological variables such as temperature, and so change with changing climate. The sensitivity of these rates to meteorology is not well characterized.

Anthropogenic emissions of PM or their precursors are also not well constrained in models (Boucher, 2013), but even application of the same emission inventories to an ensemble of climate models yields a large range of PM concentrations (Shindell et al., 2013). Some of the discrepancies among models likely arise from uncertainties in the oxidation pathways leading to PM production or in PM lifetime against wet deposition (Achakulwisut et al., 2015; Wang et al., 2011b). Discrepancies in RF estimates of PM arise in part from uncertainties in the optical properties of particles. Particle size, complex refractive index, shape, and lifetime are functions of particle water content, and these properties all influence the magnitude of PM RF. Finally, the microphysics of the effects of PM on clouds are not well represented in coarse-grid climate models (Trivitayanurak and Adams, 2014; Boucher, 2013). Some processes driving the interactions between PM and clouds are relatively well understood (e.g., cloud droplet activation), while scientific knowledge of other processes is lacking (e.g., ice nucleation) (Rosenfeld et al., 2014). Both kinds of processes are challenging to translate into macroscale processes such as large-scale precipitation or radiative fluxes (Rosenfeld et al., 2014). Better knowledge of the number and size distributions of emitted particles, including nanoparticles from vehicle exhaust, is also needed to constrain PM-cloud interactions (Adams et al., 2013).

As discussed in the previous subsection, several model studies point to the possibly large influence of changing sulfate on regional surface temperatures in the southeastern U.S. However, reconciling the observed increase in diffuse radiation at some sites with decreasing PM load is challenging (Gan et al., 2014). Another uncertainty in studies of the PM effects on U.S. regional climate involves biogenic SOA. The gas/particle partitioning of organic material depends in part on ambient PM concentrations, with more SOA formed in the presence of sulfate PM (Weber et al., 2007; Donahue et al.,

ED_002220_00002287-01828

2006). Recent model studies have attempted to determine to what extent trends in anthropogenic PM in recent decades may have also influenced biogenic SOA formation (Marais et al., 2017; Carlton et al., 2010) and thus surface cooling. The uncertainties in such studies, however, are large.

More indirectly, there is a growing body of evidence that aerosol forcing may drive shifts in internal modes of long-term (e.g., multidecadal) climate variability in the North Atlantic (Zhang et al., 2013a; Booth et al., 2012; Evan et al., 2009), in turn can potentially affecting regional temperature and rainfall patterns in North America, as well as Atlantic tropical storms (Dunstone et al., 2013).

Finally, while trends in PM may affect climate at the regional scale, global climate change may, in turn, influence PM abundance. For example, climate-driven changes in monsoon strength will almost certainly affect PM abundance over Asia (Turner and Annamalai, 2012), while increasing warming surface temperatures over the western U.S. may enhance wildfire PM (Yue et al., 2014; Yue et al., 2013). Absent future changes in land use, the concentration of biogenic SOA will likely increase in response to warming temperatures and greater isoprene emissions over the 21st century (Shen et al., 2017; Tai et al., 2013), though declines in anthropogenic emissions have the potential to at least partially counteract this effect (Carlton et al., 2010). Observations also reveal a strong positive dependence of sulfate PM to temperature in the eastern U.S., which could likewise have implications in the future warmer climate (Shen et al., 2017). Disentangling these different effects on PM abundance—the influence of global climate change versus feedbacks from the regional climate response to changing PM—remains challenging and continues to be the subject of active research.

13.3.9 Summary and Causality Determination

The 2009 ISA concluded that there was sufficient evidence that a causal relationship exists between PM and climate effects—specifically on the radiative forcing of the climate system, including both direct effects of PM on radiative forcing and indirect effects involving cloud processes. Recent research reinforces and strengthens the evidence evaluated in the 2009 PM ISA. New evidence provides greater specificity about the details of these radiative forcing effects and increased understanding of additional climate impacts driven by PM radiative effects. This section describes the evaluation of evidence for climate effects, with respect to the causality determination, using the framework described in Table II of the Preamble to the ISAs (U.S. EPA, 2015).

The scientific consensus is that anthropogenic PM has generally cooled the atmosphere over the 20th and early 21st century, masking some of the effects of greenhouse gas warming (Myhre, 2013). In response to health concerns, PM concentrations have begun declining in many developed nations [e.g., (De Meij et al., 2012)], a trend that can be observed from space (Jongeward et al., 2016). Such declines likely contributed to the current trend in global "brightening," which follows a decades-long period of global "dimming" (Wild, 2009). The brightening, in turn, may have led to rapid warming in North America and Europe, as greenhouse-gas warming was unmasked (Turnock et al., 2015;

ED_002220_00002287-01829

Leibensperger et al., 2012a, b; Philipona et al., 2009; Ruckstuhl et al., 2008). In contrast, PM concentrations have increased in recent decades over developing countries in much of Asia (Jongeward et al., 2016; Shindell et al., 2013). The sign of recent RF over developing countries, however, is very uncertain due to lack of accurate information on emissions and the relative abundances of reflecting species versus absorbing species. Research since the 2009 PM ISA has also improved characterization of the key sources of uncertainty in estimating PM climate effects, particularly with respect to PM-cloud interactions. The IPCC AR5 states that "Climate-relevant aerosol processes are better understood, and climate-relevant aerosol properties better observed, than at the time of AR4" (Boucher, 2013). Substantial uncertainties, however, still remain with respect to key processes linking PM and climate, both because of the small scale of PM-relevant cloud microphysical processes compared to the resolution of state-of-the-art models, and because of the complex cascade of indirect impacts and feedbacks in the climate system that result from a given initial radiative perturbation caused by PM. These uncertainties continue to limit the precision with which these effects can be quantified. **Despite these remaining uncertainties, though, overall the evidence is sufficient to conclude that a causal relationship exists between PM and climate effects.**

13.4 Effects on Materials

13.4.1 Introduction

The 2009 PM ISA (U.S. EPA, 2009) concluded a causal relationship between PM and effects on materials, noting that building materials including metals, stone, cement, and paint undergo natural weathering processes that are enhanced by exposure to anthropogenic pollutants. Effects of PM deposition to materials include both physical damage and impaired aesthetic qualities. It was concluded that particulate deposition can result in increased cleaning frequency and reduced usefulness of soiled material, and that although attempts had been made to quantify pollutant exposure corresponding to perceived soiling and damage, insufficient data were available to improve understanding of perception thresholds with respect to pollutant concentration, particle size, and chemical composition.

The two major processes by which air pollution in general and PM in particular can bring about materials damage are soiling and corrosion. Soiling has been defined generally as "a visual nuisance resulting from the darkening of exposed surfaces by deposition of atmospheric particles" (Lombardo et al., 2005) and more precisely as "a surface degradation that can be undone by cleaning," and the physical measure of soiling has been defined as "the contrast in reflectance of particles on a substrate to the reflectance of the bare substrate," definitions that remain widely used (Watt et al., 2008; Saiz-Jimenez, 2004; Haynie, 1986a). Corrosion is a chemical attack of a material surface that degrades a material surface and decreases aesthetic value and mechanical strength (Watt et al., 2016) (Watt et al., 2008), and in ambient air it typically involves reactions of acidic PM (i.e., acidic sulfate or nitrate) with material

ED_002220_00002287-01830

surfaces, but gases like SO_2 and HNO_3 also contribute to atmospheric corrosion, and recent research on materials damage by both gaseous and particulate oxides of nitrogen and sulfur will also be considered in this section.

The increased cleaning, washing, and repainting of solid surfaces create a major economic cost and reduces the useful life of soiled material. Long-term effects of soiling are primarily from fine rather than coarse particles, as coarse particles are relatively easily removed by wind and rain (Creighton et al., 1990; Haynie and Lemmons, 1990). As reviewed in the 2009 PM ISA (U.S. EPA, 2009), soiling is dependent on atmospheric particle concentration, particle size distribution, deposition rate, and the horizontal or vertical orientation and texture of the exposed surface (Haynie, 1986b). The chemical composition and morphology of the particles and the optical properties of the surface being soiled will determine the time at which soiling is perceived by human observers (Nazaroff and Cass, 1991). Since the 2009 PM ISA (U.S. EPA, 2009), additional research has enabled further characterization of PM effects on materials, although uncertainties remain such as quantitative relationships between particle concentration and frequency of repair, deposition rates of airborne PM to surfaces, and the interaction of copollutants in regard to materials damage effects. There is new information on the soiling process, types of materials, such as glass, and dose-response and damage functions described below. Most of the recent work on this topic has been conducted outside of the U.S. on buildings and other items of cultural heritage.

13.4.2 Soiling and Corrosion

Soiling and corrosion are complex, interdependent processes, typically beginning with deposition of atmospheric PM to exposed surfaces. Constituents of deposited PM can interact directly with materials or undergo further chemical and/or physical transformation to cause soiling, corrosion, and physical damage. Weathering, including exposure to moisture, ultraviolet (UV) radiation and temperature fluctuations affects rate and degree of damage.

Deposition of SO_2 to materials such as limestone ($CaCO_3$), granite, and metal intensifies soiling. Deposited SO_2 is oxidized to sulfate, in the case of limestone ($CaCO_3$), transforming it into gypsum ($CaSO_4$). As gypsum forms, the surface becomes rougher, further increasing PM deposition (Camuffo and Bernardi, 1993). Organic and elemental carbon from deposited PM both contribute substantially to black crusts (Bonazza et al., 2005; Sabbioni et al., 2003). This not only enhances soiling because of carbonaceous PM, but the deposited PM also forms coatings, creating ideal conditions for more rapid SO_2 oxidation catalyzed by carbon and metals present in the deposited PM (McAlister et al., 2008; Grossi et al., 2007).

Research has progressed on theoretical understanding of soiling of cultural heritage since the 2009 PM ISA (U.S. EPA, 2009). Trace element concentrations were measured and heavy metals were detected in black crusts on stone monuments (Barca et al., 2010), and the nature, causes, and mitigation strategies for decay of stone-built heritage have been reviewed (Smith et al., 2008). Isotope tracers have

ED_002220_00002287-01831

also been applied to understand the origin of contaminant sources in black crusts (Kloppmann et al., 2011). Biological marker compounds indicating the presence of biogenically derived material confirmed that biological activity played a major role in producing black films on granite (de Oliveira et al., 2011). Indoor penetration and accumulation of PM and gaseous pollutants into historical buildings was also studied (Worobiec et al., 2010).

There has also been considerable progress understanding soiling of materials besides stone. Gypsum was found to be the main damage product in concrete, and organic and elemental carbon were also found in concrete damage layers (Ozga et al., 2011). Gypsum formation was also observed after exposure of rendering mortars to sulfuric acid (Lanzon and Garcia-Ruiz, 2010). A new physically based model was recently developed to predict haze[85] forming on modern glass that takes into account differences in particle size distributions observed in different locations (Alfaro et al., 2012). Results are plotted in Figure 13-30, showing good model fits under sheltered conditions from the rain and haze on the glass reaching a 50% ratio of diffuse transmitted light to direct transmitted light.

[85]In this section (13.4) haze is used as it has been defined in the scientific literature on soiling of glass, i.e., the ratio of diffuse transmitted light to direct transmitted light (Lombardo et al., 2010). This differs from the use of the word haze in Sections 13.2 and Section 13.3, where it is used as a qualitative description of the blockage of sunlight by dust, smoke, and pollution. This usage is widespread in the scientific literature on visibility and in discussion of the Regional Haze Rule. Both definitions are used in this chapter because use of the word haze in discussion of either regional haze and glass soiling is unavoidable.

ED_002220_00002287-01832

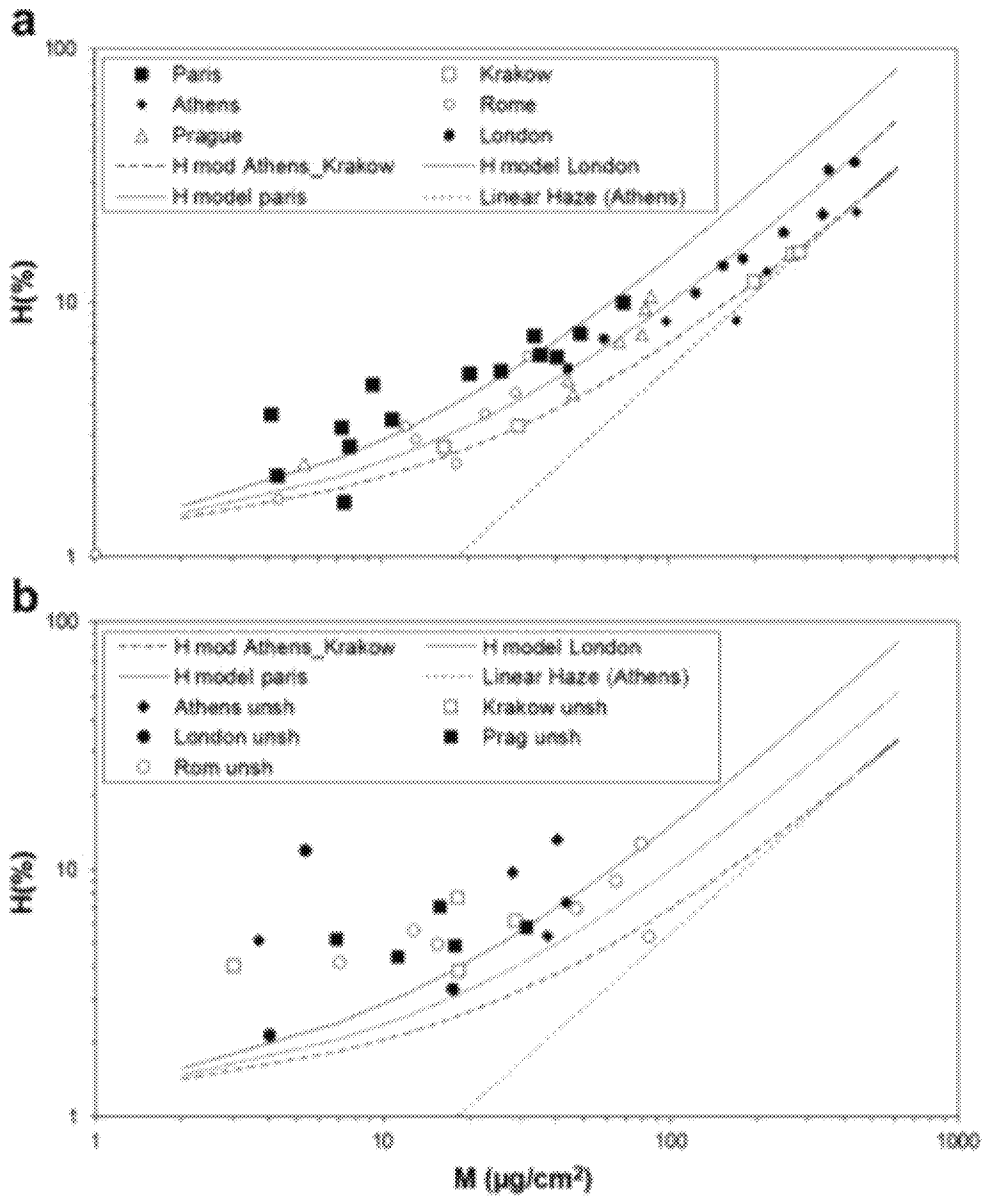

Source: Permission pending, Alfaro et al. (2012).

Figure 13-30 Increase of haze (H in %) with mass of deposit on glass (M µg/cm^2) under a) sheltered conditions and b) conditions where glass panes were exposed directly to the weather.

ED_002220_00002287-01833

Corrosion of stone has been discussed in the 2009 PM ISA, and decay of stone building materials by acid deposition and sulfate salts were described (U.S. EPA, 2009). Advances since the 2009 PM ISA include quantification of degradation rates and further characterization of factors that influence damage of stone materials. Measurable losses of surface material were used to determine decay rates of marble grave stones up to 2.5 to 3.0 mm/century in heavily polluted areas compared to natural background decay rates from a relatively pristine area of 0.25 mm/century (Mooers et al., 2016). Both time of wetness and the number of dissolution/crystallization cycles were identified as hazard indicators for stone materials, with the greatest hazard in spring and fall when both time of wetness and the number of dissolution and crystallization cycles were relatively high (Casati et al., 2015). Improvements of facilities for further research to simulate interactions between cultural heritage materials and realistic atmospheric environments that facilitate controlled experimental conditions in order to investigate various factors influencing decay are also underway (Chabas et al., 2015).

Corrosion of steel as a function of PM composition and size was also recently studied, and changes in composition of resulting rust varied with particle size (Lau et al., 2008). A multipollutant study of damage to metal materials under ambient conditions in severely polluted Hong Kong concluded that iron and steel were corroded more by air pollution than copper and copper alloys, which were in turn more corroded by air pollution than aluminum and aluminum alloys (Liu et al., 2015). SO_2, NO_2, and PM contributed to corrosion of iron and steel, while SO_2 and O_3 were mainly responsible for corrosion of copper and copper alloys, and NO_2 and PM for damage to aluminum and aluminum alloys (Liu et al., 2015).

Other atmospheric gases besides SO_2, and other components of particulate matter besides sulfate and black carbon can damage materials. Nitrates are more soluble than sulfates, and do not form stable compounds with stone building materials (Sabbioni et al., 1998). However, calcium nitrate can be formed by NO_X attack (Haneef et al., 1993). Also, NO_X can enhance sulfate attack on calcium rich building materials, and synergistic effects between NO_2 and SO_2 at high relative humidity have been reported (Johansson et al., 1988). Airborne organic compounds have also been observed on building material surfaces and can participate in damage, (Sanjurjo Sanchez et al., 2009; Sabbioni et al., 1998; Saiz-Jimenez, 1993), serving as nucleation sites for growth of gypsum crystals (Cultrone et al., 2000; Saiz-Jimenez, 1993). In some cases, soiling of limestone and building material surfaces has been attributed to biological processes (Viles and Gorbushina, 2003), and carbonaceous particles and organic compounds also enhance biological colonization (Sanjurjo-Sanchez and Alves, 2012). Black carbon has recently been observed to induce structural, composition, and functional changes in biofilms, to produce thicker and more complex biofilms, and potentially to act as a novel signal to induce biofilm formation (Hussey et al., 2017).

In addition to structural and aesthetic impacts, energy efficiency is also becoming an important consideration for impacts of air pollutants on materials. A growing area of research is the impact of air pollution on the energy yield from photovoltaic panels, especially in desert environments. Results indicate

ED_002220_00002287-01834

the type of dust deposited and glazing temperature influence light transmission (Abderrezek and Fathi, 2017). For example, on average, carbon soiling decreased solar modular efficiency by 37.6% while soil particles reduced efficiency by 68% and $CaCO_3$ by 37.6% (Radonjic et al., 2017). The relationship between the rate of degradation of photovoltaic power output due to soiling has been investigated and related to dust accumulation rate, and impacts of season and dust storms were observed (Besson et al., 2017; Boyle et al., 2017; Javed et al., 2017). In five sites in the continental U.S. (Cocoa, FL, Albuquerque, NM, and a rural, suburban, and urban location in the Front Range of Colorado) photovoltaic module power transmission was reduced by 2.8% for every g/m^2 of PM deposited on the cover plate independent of geographical location (Boyle et al., 2017). Mean deposition velocities were 1.5 cm/s. In arid environments dust fouling was observed to reduce photovoltaic module power output by 40% after 10 months without cleaning (Walwil et al., 2017). There is on-going research to reduce soiling of photovoltaic cells with transparent coatings (Quan and Zhang, 2017).

The use of materials able to reflect a large portion of solar radiation for passive cooling, such as light-colored marble panels on building exteriors, are another example of an approach to improving energy efficiency, and also to countering the urban heat island effect. Exposure to acidic pollutants in urban environments reduces solar reflectance of marble, decreasing the cooling effect of the marble envelope (Rosso et al., 2016).

13.4.3 Dose-Response Relationships

Typically, empirical models are used to estimate dose-response relationships from field measurements of data relevant to deposition and meteorological processes (Hamilton and Mansfield, 1993). There has been considerable progress since the 2009 PM ISA (U.S. EPA, 2009) in the development of dose-response relationships for soiling of building materials, although some key relationships remain poorly characterized. Dose-response estimates can be traced back to early research on surface repainting, showing a direct correlation between ambient PM concentration and the number of years between repainting (U.S. EPA, 1972). Consistent and reliable dose-response relationships for soiling of stone building materials have proved difficult to estimate, but there is a growing literature of dose-response relationships for newer building materials, such as glass, metals, and polymers.

The first general dose-response relationships for soiling of materials by particles were generated by measuring the contrast in reflectance of a soiled surface to the reflectance of the unsoiled substrate for different materials, including acrylic house paint, cedar siding, concrete, brick, limestone, asphalt shingles, and window glass in different areas with total suspended particulate (TSP) concentrations from 59 to 289 $\mu g/m^3$(Beloin and Haynie, 1975). The dose-response curve for acrylic house paint in Figure 13-31 plots change in reflectance against the square root of the dose, defined as the product of TSP and number of months exposed (Beloin and Haynie, 1975).

ED_002220_00002287-01835

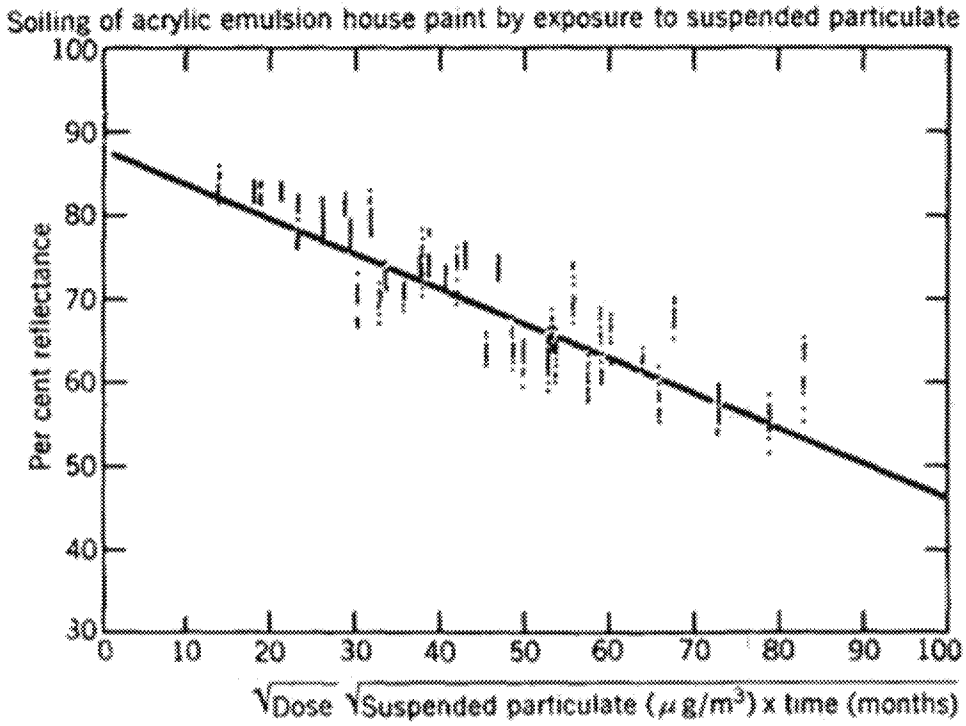

Source: Permission pending, Beloin and Haynie (1975).

Figure 13-31 Example of a dose-response curve for effects on materials, showing change in reflectance vs. square root of dose for acrylic emulsion house paint.

Efforts to develop accurate dose-response curves similar to those in Figure 13-31 have proved difficult because of multiple influences and considerable scatter in the data for most materials. Continued efforts to develop dose-response curves for soiling have led to some advancements for modern materials, but remain poorly characterized for limestone. PM_{10} measurements and collocated reflectance measurements of material surfaces for limestone, painted steel, white plastic, and polycarbonate filter material were recently used to quantify dose-response relationships between PM_{10} and soiling. In this recent case also, there was too much scatter in the data for limestone to produce a dose-response relationship (Watt et al., 2008). A dose-response relationship for silica-soda-lime window glass soiling by PM_{10}, NO_2, and SO_2 based on 31 different locations was quantified (Lombardo et al., 2010), and described by

Equation 13-8:

ED_002220_00002287-01836

$$Haze = (0.2529[SO_2] + 0.1080[NO_2] + 0.1473[PM_{10}]) \times \frac{1}{1 + \left(\frac{382}{t}\right)^{1.86}}$$

Equation 13-8

Figure 13-32 shows the raw data on which this dose-response curve was based, illustrating that long observation times of several years required as well as the challenges posed by response differences among locations.

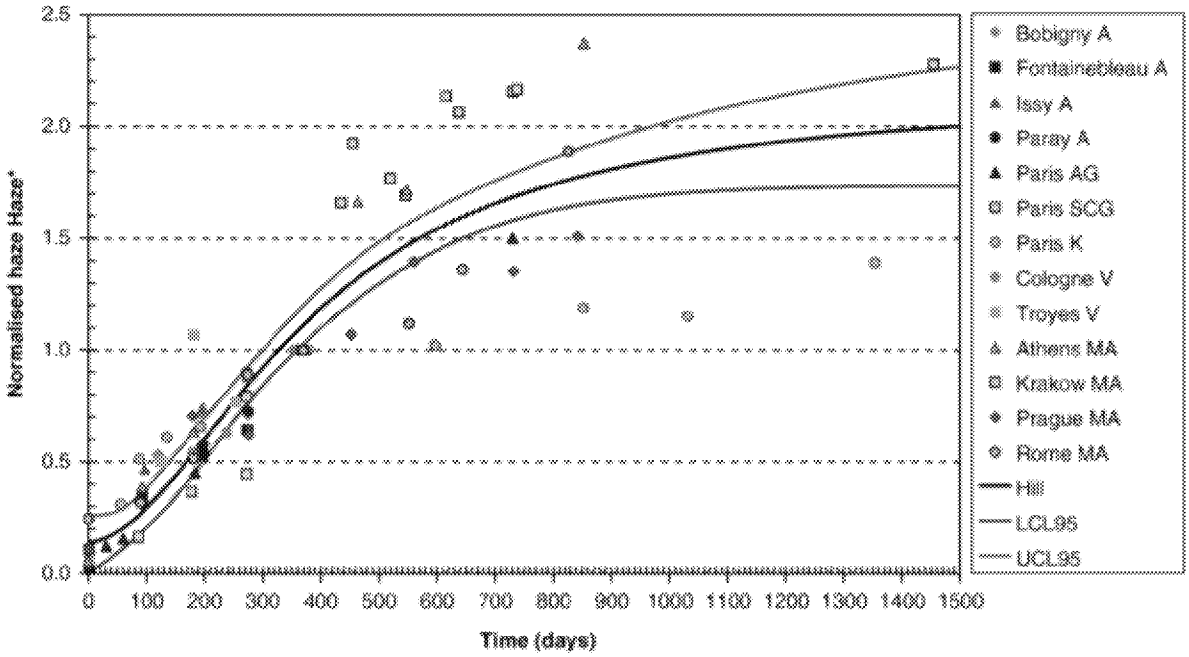

Source: Permission pending, Lombardo et al. (2010).

Figure 13-32 Temporal trend in haze values of glass at different locations. The x-axis is normalized haze values where 1-year data series were combined with longer data series and scaled by the 1-year value. Black line represents a fitted model of the data and pink and green lines represent 95% confidence.

Glass soiling was intensively studied to evaluate deposited PM composition and optical properties including reflectance, transmittance, and absorption in several European cities. After more than two years, there was no saturation phenomenon, i.e., material continued to accumulate through deposition, although

ED_002220_00002287-01837

disappearance of ammonium and possible particulate organic matter were reported. Absorption and transmittance changed "quasi-linearly" with species concentrations for elemental carbon and major ions for thin deposits, but for thicker deposits saturation was reached for absorption of 16% when elemental carbon concentrations reached 15 μg/cm^2 and for diffuse transmittance of about 30% for 65 μg/cm^2 of ions, and the overall saturation level for transmittance was dependent of composition and particle size (Favez et al., 2006).

As these studies indicate, for some materials it can sometimes take years to develop dose-response relationships that relate reflectance of materials surfaces to ambient PM concentrations. There has also been progress in developing methods to more rapidly evaluate soiling of different materials by PM mixtures. Modern buildings typically have simpler lines, more limited surface detail, and greater use of glass, tile, and metal that are easier to clean than stone. There have also been major changes in types of materials used for buildings, including a wide variety of polymers available for coatings and sealants. In addition, new economic and environmental considerations beyond aesthetic appeal and structural damage are emerging. For example, cool roofs have been designed and constructed to increase reflectance from buildings in urban areas, to decrease both air conditioning needs and urban heat island effects, and these efforts can be impeded by soiling of materials. Sleiman et al. (2014) developed a reliable and repeatable accelerated aging method for roofing products that simultaneously simulates soiling by urban PM and weathering and can be adjusted to local PM composition.

13.4.4 Damage Functions

Dose-response functions and damage functions have been used to quantify material decay as a function of pollutant type and load. The damage function approach follows a number of steps (ApSimon and Cowell, 1996). First, a dose-response function is determined with dose based on either concentration or deposition. Alternatively, damage can be determined from sample surveys or inspection of actual damage (ApSimon and Cowell, 1996). Second, a physical damage function is developed. This can then be linked to the rate of material damage to time of replacement or maintenance. Finally, a cost function links time for replacement and maintenance to a monetary cost, and an economic function links cost to dose of pollution. Figure 13-33 shows an example of how damage functions are used to assess economic damage and replacement costs (ApSimon and Cowell, 1996; Kucera et al., 1993).

ED_002220_00002287-01838

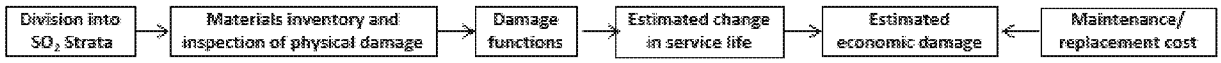

Source: Permission pending, Kucera et al. (1993) as cited by ApSimon and Cowell (1996).

Figure 13-33 Damage functions and their use to determine maintenance and replacement costs for materials damaged by SO_2.

The physical damage function is also difficult to assess because it depends on human perception of the level of soiling to be tolerated. Damage functions based on steady state loss mechanism for erosion have been calculated but did not account for effects of black crusts (Lipfert, 1989). An example of a damage function from Lipfert (1989) is given by Equation 13-9, expressing the loss of calcerous stone in mm thickness as a result of wet deposition of SO_2 in rain with pH of 3−5:

$$Loss/_{m\ rain} = 18.8 + (0.016)H^{+} + (0.18)V_d \times \frac{SO_2}{R}$$

Equation 13-9

H^+ is H^+ concentration in rain, V_d is deposition velocity of SO_2, SO_2 is SO_2 concentration in $\mu g/m^3$, and R is rain in m.

Damage functions for aluminum, zinc, copper, plastic, paint, and rubber have also been estimated and applied along with the "Lipfert function" for stone to evaluate potential damage to modern building materials expected in the 21st century. In the process, an extensive list of damage functions for a wide range of building materials from various sources was reviewed and published and used to predict potential damage to various materials under local air pollution and climate conditions, as shown in Figure 13-34 (Brimblecombe and Grossi, 2010).

ED_002220_00002287-01839

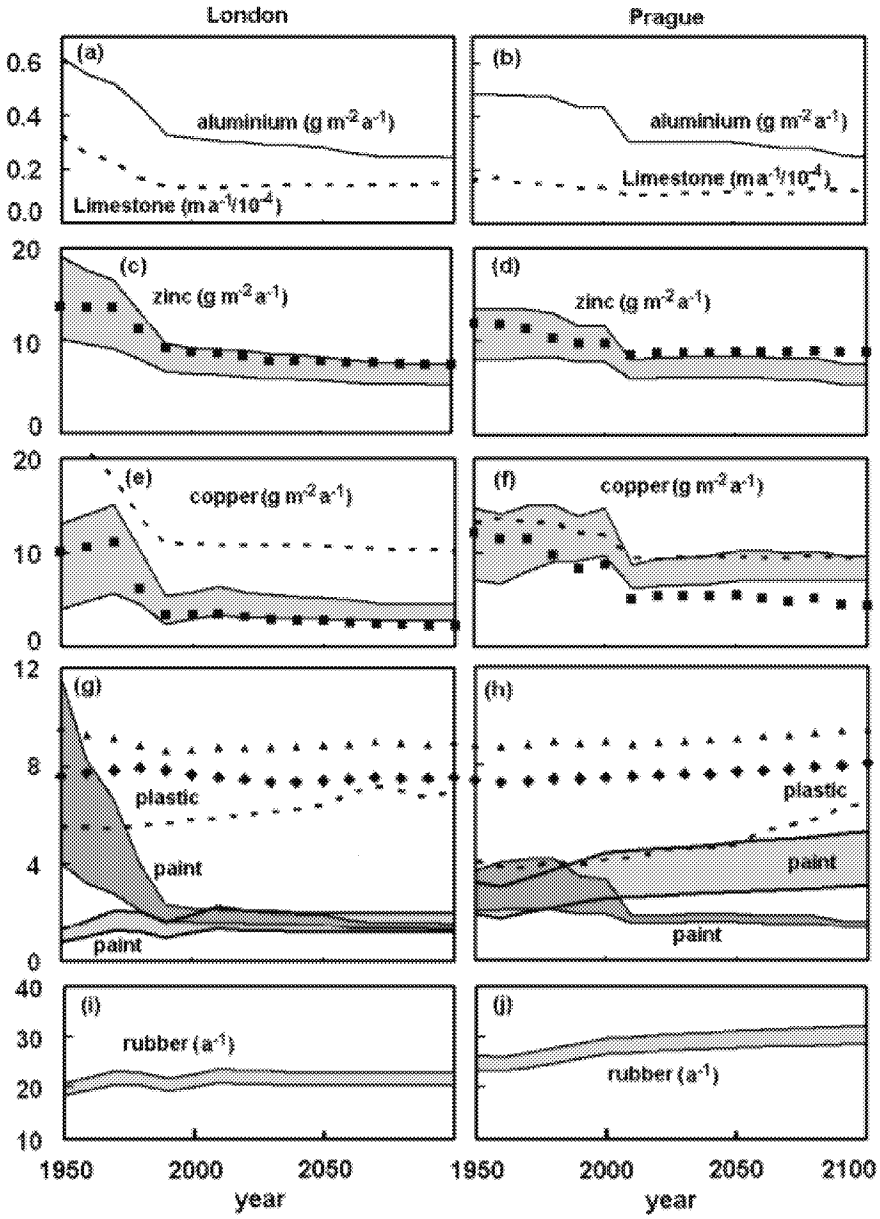

Source: Permission pending, Brimblecombe and Grossi (2010).

Figure 13-34 Predictions of materials damage to various materials based on damage functions. Rate of damage (rate of mass loss per area in the case of aluminum, limestone, zinc, copper; rate of deterioration for plastic paint and rubber) is shown on the y axis. Years are shown on the x axis.

ED_002220_00002287-01840

Damage functions were also used to estimate long-term deterioration of limestone, iron, and copper, and the blackening of stone surfaces in London between 1100–2100 using meteorological and pollution input (Brimblecombe and Grossi, 2009). Deterioration of limestone and possibly copper intensified in the 18th century, and soiling was especially rapid in the 19th century. Based on these observations it was concluded that damage to durable building material is no longer controlled by pollution as in earlier centuries, with natural weathering becoming a more important influence in modern times. However, even as damage to stone and metals from PM have decreased in modern times, potentially higher degradation rates for polymeric materials, plastic, paint, and rubber are predicted due to increased oxidant concentrations and solar radiation (Brimblecombe and Grossi, 2009).

13.4.5 Summary and Causality Determination

The conclusion in the 2009 PM ISA (U.S. EPA, 2009) that PM deposition can result in increased cleaning and maintenance costs and reduced usefulness of soiled material is supported by additional studies detailing new evidence , and there has been steady progress in understanding soiling and corrosion processes and developing approaches to quantify pollutant exposure corresponding to perceived soiling and damage, with respect to pollutant concentration, particle size, and chemical composition. The combination of this evidence further reinforces and supports the conclusion of the 2009 PM ISA of a causal relationship between PM and effects on materials. This section describes the evaluation of evidence for materials effects, with respect to the causality determination, using the framework described in Table II of the Preamble to the ISAs (U.S. EPA, 2015).

Materials damage from particulate matter and other pollutants generally involves one or both of two processes, soiling and corrosion (Section 13.4.2). Soiling is a visible darkening or decrease in reflectance of a material, and corrosion is damage to a material over time caused by chemical reactions with the material surface. Quantitative assessments of materials damage have been carried out by developing dose-response relationships (Section 13.4.3) and applying damage functions (Section 13.4.4), but much of the scientific literature on soiling, corrosion, dose-response relationships and damage functions have focused on stone used for historic monuments and buildings, and there has been a substantial gap in our understanding of processes and quantitative relationships involving other materials. It is still the case that the majority of the literature available on materials damage concerns cultural heritage and stone materials, including differences in elemental composition between crusts on building surfaces and unaffected stone surfaces, as well as documentation of an important role of microbial processes in stone decay.

Although most research on materials damage has concerned stone materials, there has been steady progress in understanding soiling and corrosion processes for glass and metals. These advances include modeling of glass soiling, identifying which pollutants are most influential in metal corrosion in a multipollutant environment, and how that varies between metals. Since the 2009 ISA characterization of

ED_002220_00002287-01841

quantitative dose-response relationships and damage functions for materials besides stone has also progressed, with a new dose-response curves published for glass, and a new summary of available materials damage functions. In addition to structural damage, aesthetic qualities, and cleaning costs that are longstanding concerns for PM and air pollution effects, a growing body of research on PM and air pollution impacts concerns energy costs. Applications from climate control and energy consumption of large buildings to efficient operation of photovoltaic systems are influenced by atmospheric soiling. **Overall, the evidence is sufficient to conclude that a causal relationship exists between PM and effects on materials.**

13.5 References

Aamaas, B; Berntsen, TK; Fuglestvedt, J, anS; Shine, KP; Bellouin, N. (2016). Regional emission metrics for short-lived climate forcers from multiple models. Atmos Chem Phys 16: 7451-7468. http://dx.doi.org/10.5194/acp-16-7451-2016

Abderrezek, M; Fathi, M. (2017). Experimental study of the dust effect on photovoltaic panels' energy yield. Solar Energy 142: 308-320. http://dx.doi.org/10.1016/j.solener.2016.12.040

Abt (Abt Associates Inc). (2001). Assessing public opinions on visibility impairment due to air pollution: Summary report. Research Triangle Park, NC: U.S. Environmental Protection Agency.

Achakulwisut, P; Mickley, LJ; Murray, LT; Tai, APK; Kaplan, JO; Alexander, B. (2015). Uncertainties in isoprene photochemistry and emissions: implications for the oxidative capacity of past and present atmospheres and for trends in climate forcing agents. Atmos Chem Phys Discuss 15: 2197-2246. http://dx.doi.org/10.5194/acpd-15-2197-2015

Achtert, P; Birmili, W; Nowak, A; Wehner, B; Wiedensohler, A; Takegawa, N; Kondo, Y; Miyazaki, Y; Hu, M; Zhu, T. (2009). Hygroscopic growth of tropospheric particle number size distributions over the North China Plain. J Geophys Res 114: D00G07. http://dx.doi.org/10.1029/2008JD010921

Adams, PJ; Donahue, NM; Pandis, SN. (2013). Atmospheric nanoparticles and climate change. AIChE J 59: 4006-4019. http://dx.doi.org/10.1002/aic.14242

Adams, PJ; Seinfeld, JH; Koch, D; Mickley, L; Jacob, D. (2001). General circulation model assessment of direct radiative forcing by the sulfate-nitrate-ammonium-water inorganic aerosol system. J Geophys Res 106: 1097-1111. http://dx.doi.org/10.1029/2000JD900512

Alfaro, SC; Chabas, A; Lombardo, T; Verney-Carron, A; Ausset, P. (2012). Predicting the soiling of modern glass in urban environments: A new physically-based model. Atmos Environ 60: 348-357. http://dx.doi.org/10.1016/j.atmosenv.2012.06.050

Allen, RJ; Norris, J. R.; Wild, M. (2013). Evaluation of multidecadal variability in CMIP5 surface solar radiation and inferred underestimation of aerosol direct effects over Europe, China, Japan, and India. J Geophys Res Atmos 118: 6311-6336. http://dx.doi.org/10.1002/jgrd.50426

Anderson, TL; Ogren, JA. (1998). Determining aerosol radiative properties using the TSI 3563 integrating nephelometer. Aerosol Sci Technol 29: 57-69. http://dx.doi.org/10.1080/02786829808965551

Andreae, MO; Gelencsér, A. (2006). Black carbon or brown carbon? The nature of light-absorbing carbonaceous aerosols. Atmos Chem Phys 6: 3131-3148.

Andreae, MO; Schmid, O; Yang, H; Chand, D; Zhen yu, J; Zeng, LM; Zhang, YH. (2008). Optical properties and chemical composition of the atmospheric aerosol in urban Guangzhou, China. Atmos Environ 42: 6335-6350. http://dx.doi.org/10.1016/j.atmosenv.2008.01.030

ApSimon, HM; Cowell, D. (1996). The benefits of reduced damage to buildings from abatement of sulphur dioxide emissions. Energy Policy 24: 651-654.

Arneth, A; Harrison, SP; Zaehle, S; Tsigaridis, K; Menon, S; Bartlein, PJ; Feichter, J; Korhola, A; Kulmala, M; O'Donnell, D; Schurgers, G; Sorvari, S; Vesala, T. (2010). Terrestrial biogeochemical feedbacks in the climate system. Nat Geosci 3: 525-532. http://dx.doi.org/10.1038/ngeo905

Arnott, WP; Hamasha, K; Moosmüller, H; Sheridan, PJ; Ogren, JA. (2005). Towards Aerosol Light-Absorption Measurements with a 7-Wavelength Aethalometer: Evaluation with a Photoacoustic Instrument and 3-Wavelength Nephelometer. Aerosol Sci Technol 39: 17-29. http://dx.doi.org/10.1080/027868290901972

Arnott, WP; Moosmuller, H; Rogers, CF; Jin, T; Bruch, R. (1999). Photoacoustic spectrometer for measuring light absorption by aerosol; instrument description. Atmos Environ 33: 2845-2852.

Arola, A; Schuster, G; Myhre, G; Kazadzis, S; Dey, S; Tripathi, SN. (2011). Inferring absorbing organic carbon content from AERONET data. Atmos Chem Phys 11: 215-225. http://dx.doi.org/10.5194/acp-11-215-2011

Atkinson, JD; Murray, BJ; Woodhouse, MT; Whale, TF; Baustian, KJ; Carslaw, KS; Dobbie, S; O'Sullivan, D; Malkin, TL. (2013). The importance of feldspar for ice nucleation by mineral dust in mixed-phase clouds (vol 498, pg 355, 2013). Nature 500: 491-491. http://dx.doi.org/10.1038/nature12384

Attwood, AR; Washenfelder, RA; Brock, CA; Hu, W; Baumann, K; Campuzano-Jost, P; Day, DA; Edgerton, ES; Murphy, DM; Palm, BB; McComiskey, A; Wagner, NL; de Sa, SS; Ortega, A; Martin, ST; Jimenez, JL; Brown, SS. (2014). Trends in sulfate and organic aerosol mass in the Southeast U.S.: Impact on aerosol optical depth and radiative forcing. Geophys Res Lett 41: 7701-7709. http://dx.doi.org/10.1002/2014GL061669

AZ-DEQ. (2003). Final ReportRecommendation for a Phoenix Area Visibility Index. Phoenix, Arizona: Arizona Department of Environmental Quality.

Baeumer, D; Vogel, B; Versick, S; Rinke, R; Moehler, O; Schnaiter, M. (2008). Relationship of visibility, aerosol optical thickness and aerosol size distribution in an ageing air mass over South-West Germany. Atmos Environ 42: 989-998. http://dx.doi.org/10.1016/j.atmosenv.2007.10.017

Ban-Weiss, GA; Jin, L; Bauer, SE; Bennartz, R; Liu, X; Zhang, K, ai; Ming, Y, i; Guo, H; Jiang, JH. (2014). Evaluating clouds, aerosols, and their interactions in three global climate models using satellite simulators and observations. J Geophys Res Atmos 119: 10876-10901. http://dx.doi.org/10.1002/2014JD021722

Banerjee, A; Polvani, LM; Fyfe, JC. (2017). The United States "warming hole": Quantifying the forced aerosol response given large internal variability. Geophys Res Lett 44: 1928-1937. http://dx.doi.org/10.1002/2016GL071567

Barca, D; Belfiore, CM; Crisci, GM; La Russa, MF; Pezzino, A; Ruffolo, SA. (2010). Application of laser ablation ICP-MS and traditional techniques to the study of black crusts on building stones: a new methodological approach. Environ Sci Pollut Res Int 17: 1433-1447. http://dx.doi.org/10.1007/s11356-010-0329-8

Bell, TL; Rosenfeld, D; Kim, KM; Yoo, JM; Lee, MI; Hahnenberger, M. (2008). Midweek increase in U.S. summer rain and storm heights suggests air pollution invigorates rainstorms. J Geophys Res 113: D02209. http://dx.doi.org/10.1029/2007JD008623

Bellouin, N; Jones, A; Haywood, J; Christopher, S. (2008). Updated estimate of aerosol direct radiative forcing from satellite observations and comparison against the Hadley Centre climate model. J Geophys Res Atmos 113: D10205. http://dx.doi.org/10.1029/2007JD009385

Bellouin, N; Rae, J; Jones, A; Johnson, C; Haywood, J; Boucher, O. (2011). Aerosol forcing in the Climate Model Intercomparison Project (CMIP5) simulations by HadGEM2-ES and the role of ammonium nitrate. J Geophys Res 116: D20206. http://dx.doi.org/10.1029/2011JD016074

Beloin, NJ; Haynie, FH. (1975). Soiling of building materials. J Air Waste Manag Assoc 25: 399-403.

Besson, P; Munoz, C; Ramirez-Sagner, G; Salgado, M; Escobar, R; Platzer, W. (2017). Long-Term Soiling Analysis for Three Photovoltaic Technologies in Santiago Region. 7: 1755-1760. http://dx.doi.org/10.1109/JPHOTOV.2017.2751752

ED_002220_00002287-01843

Bindoff, NL; Stott, PA; AchutaRao, KM; Allen, MR; Gillett, N; Gutzler, D; Hansingo, K; Hegerl, G; Hu, Y; Jain, S; Mokhov, II; Overland, J; Perlwitz, J; Sebbari, R; Zhang, X. (2013). Detection and attribution of climate change: From global to regional. In TF Stocker; D Qin; GK Plattner; MMB Tignor; SK Allen; J Boschung; A Nauels; Y Xia; V Bex; PM Midgley (Eds.), Climate change 2013: The physical science basis Contribution of Working Group I to the Fifth Assessment Report of the Intergovernmental Panel on Climate Change (pp. 867-952). Cambridge, UK: Cambridge University Press. http://www.ipcc.ch/report/ar5/wg1/

Bonazza, A; Sabbioni, C; Ghedini, N. (2005). Quantitative data on carbon fractions in interpretation of black crusts and soiling on European built heritage. Atmos Environ 39: 2607-2618. http://dx.doi.org/10.1016/j.atmosenv.2005.01.040

Bond, T; Bhardwaj, E; Dong, R; Jogani, R; Jung, S; Roden, C; Streets, D; Trautmann, N. (2007). Historical emissions of black and organic carbon aerosol from energy-related combustion, 1850-2000. Global Biogeochem Cycles 21: GB2018. http://dx.doi.org/10.1029/2006GB002840

Bond, TC; Anderson, TL; Campbell, D. (1999). Calibration and intercomparison of filter-based measurements of visible light absorption by aerosols. Aerosol Sci Technol 30: 582-600. http://dx.doi.org/10.1080/027868299304435

Bond, TC; Bergstrom, RW. (2006). Light absorption by carbonaceous particles: An investigative review. Aerosol Sci Technol 40: 27-67. http://dx.doi.org/10.1080/02786820500421521

Bond, TC; Doherty, SJ; Fahey, DW; Forster, PM; Berntsen, T; Deangelo, BJ; Flanner, MG; Ghan, S; Kärcher, B; Koch, D; Kinne, S; Kondo, Y; Quinn, PK; Sarofim, MC; Schultz, MG; Schulz, M; Venkataraman, C; Zhang, H; Zhang, S; Bellouin, N; Guttikunda, SK; Hopke, PK; Jacobson, MZ; Kaiser, JW; Klimont, Z; Lohmann, U; Schwarz, JP; Shindell, D; Storelvmo, T; Warren, SG; Zender, CS. (2013). Bounding the role of black carbon in the climate system: A scientific assessment. J Geophys Res Atmos 118: 5380-5552. http://dx.doi.org/10.1002/jgrd.50171

Booth, BB; Dunstone, NJ; Halloran, PR; Andrews, T; Bellouin, N. (2012). Aerosols implicated as a prime driver of twentieth-century North Atlantic climate variability. Nature 484: 228-232. http://dx.doi.org/10.1038/nature10946

Boucher, O. (2013). Clouds and Aerosols. In Climate Change 2013: The Physical Science Basis Contribution of Working Group I to the Fifth Assessment Report of the Intergovernmental Panel on Climate Change. Cambridge, United Kingdom and New York, NY, USA: Cambridge University Press.

Boyle, L; Burton, PD; Danner, V; Hannigan, MP; King, B. (2017). Regional and national scale spatial variability of photovoltaic cover plate soiling and subsequent solar transmission losses. 7: 1354-1361. http://dx.doi.org/10.1109/JPHOTOV.2017.2731939

Brimblecombe, P; Grossi, CM. (2009). Millennium-long damage to building materials in London. Sci Total Environ 407: 1354-1361. http://dx.doi.org/10.1016/j.scitotenv.2008.09.037

Brimblecombe, P; Grossi, CM. (2010). Potential damage to modern building materials from 21st century air pollution. ScientificWorldJournal 10: 116-125. http://dx.doi.org/10.1100/tsw.2010.17

CAA. Clean Air Act, section 302: Definitions, 42 USC 7602, 42 USC (2005). http://www.gpo.gov/fdsys/pkg/USCODE-2005-title42/pdf/USCODE-2005-title42-chap85-subchapIII-sec7602.pdf

Calvo, AI; Pont, V; Castro, A; Mallet, M; Palencia, C; Roger, JC; Dubuisson, P; Fraile, R. (2010). Radiative forcing of haze during a forest fire in Spain. J Geophys Res 115: D08206. http://dx.doi.org/10.1029/2009JD012172

Camuffo, D; Bernardi, A. (1993). Microclimatic factors affecting the trajan column. Sci Total Environ 128: 227-255.

Cappa, CD; Onasch, TB; Massoli, P; Worsnop, DR; Bates, TS; Cross, ES; Davidovits, P; Hakala, J; Hayden, KL; Jobson, B; Kolesar, KR; Lack, DA; Lerner, BM; Li, SM; Mellon, D; Nuaaman, I; Olfert, JS; Petaja, T; Quinn, PK; Song, C; Subramanian, R; Williams, EJ; Zaveri, RA. (2012). Radiative absorption enhancements due to the mixing state of atmospheric black carbon. Science 337: 1078-1081. http://dx.doi.org/10.1126/science.1223447

ED_002220_00002287-01844

Carlton, AG; Pinder, RW; Bhave, PV; Pouliot, GA. (2010). To what extent can biogenic SOA be controlled. Environ Sci Technol 44: 3376-3380. http://dx.doi.org/10.1021/es903506b

Carslaw, KS; Lee, LA; Reddington, CL; Pringle, KJ; Rap, A; Forster, PM; Mann, GW; Spracklen, DV; Woodhouse, MT; Regayre, LA; Pierce, J. R. (2013). Large contribution of natural aerosols to uncertainty in indirect forcing. Nature 503: 67-+. http://dx.doi.org/10.1038/nature12674

Casati, M; Rovelli, G; D'Angelo, L; Perrone, MG; Sangiorgi, G; Bolzacchini, E; Ferrero, L. (2015). Experimental measurements of particulate matter deliquescence and crystallization relative humidity: Application in heritage climatology. Aerosol Air Qual Res 15: 399-409. http://dx.doi.org/10.4209/aaqr.2014.11.0289

Chabas, A; Fouqueau, A; Attoui, M; Alfaro, SC; Petitmangin, A; Bouilloux, A; Saheb, M; Coman, A; Lombardo, T; Grand, N; Zapf, P; Berardo, R; Duranton, M; Durand-Jolibois, R; Jerome, M; Pangui, E; Correia, JJ; Guillot, I; Nowak, S. (2015). Characterisation of CIME, an experimental chamber for simulating interactions between materials of the cultural heritage and the environment. Environ Sci Pollut Res Int 22: 19170-19183. http://dx.doi.org/10.1007/s11356-015-5083-5

Chakrabarty, RK; Beres, ND; Moosmueller, H; China, S; Mazzoleni, C; Dubey, MK; Liu, L, i; Mishchenko, MI. (2014). Soot superaggregates from flaming wildfires and their direct radiative forcing. 4: 5508. http://dx.doi.org/10.1038/srep05508

Charlson, RJ; Porch, WM; Waggoner, AP; Ahlquist, NC. (1974). Background aerosol light-scattering characteristics - nephelometric observations at Mauna-Loa-Observatory compared with results at other remote locations. Tellus 26: 345-360.

Che, H; Xia, X; Zhu, J; Li, Z; Dubovik, O; Holben, B; Goloub, P; Chen, H; Estelles, V; Cuevas-Agullo, E; Blarel, L; Wang, H; Zhao, H; Zhang, X; Wang, Y; Sun, J; Tao, R; Zhang, X; Shi, G. (2014). Column aerosol optical properties and aerosol radiative forcing during a serious haze-fog month over North China Plain in 2013 based on ground-based sunphotometer measurements. Atmos Chem Phys 14: 2125-2138. http://dx.doi.org/10.5194/acp-14-2125-2014

Chen, J; Zhao, CS; Ma, N; Yan, P. (2014). Aerosol hygroscopicity parameter derived from the light scattering enhancement factor measurements in the North China Plain. Atmos Chem Phys 14: 8105-8118. http://dx.doi.org/10.5194/acp-14-8105-2014

Cheng, YF; Wiedensohler, A; Eichler, H; Su, H; Gnauk, T; Brueggemann, E; Herrmann, H; Heintzenberg, J; Slanina, J; Tuch, T; Hu, M; Zhang, YH. (2008). Aerosol optical properties and related chemical apportionment at Xinken in Pearl River Delta of China. Atmos Environ 42: 6351-6372. http://dx.doi.org/10.1016/j.atmosenv.2008.02.034

Cheng, Z; Jiang, J; Chen, C; Gao, J; Wang, S; Watson, JG; Wang, H; Deng, J; Wang, B; Zhou, M, in; Chow, JC; Pitchford, ML; Hao, J. (2015). Estimation of aerosol mass scattering efficiencies under high mass loading: Case study for the megacity of Shanghai, China. Environ Sci Technol 49: 831-838. http://dx.doi.org/10.1021/es504567q

Chow, JC; Lowenthal, DH; Chen, LWA; Wang, X; Watson, JG. (2015). Mass reconstruction methods for PM2.5: a review. Air Qual Atmos Health 8: 243-263. http://dx.doi.org/10.1007/s11869-015-0338-3

Chow, JC; Watson, JG; Doraiswamy, P; Chen, LW, enA; Sodeman, DA; Lowenthal, DH; Park, K; Arnott, WP; Motallebi, N. (2009). Aerosol light absorption, black carbon, and elemental carbon at the Fresno Supersite, California. Atmos Res 93: 874-887. http://dx.doi.org/10.1016/j.atmosres.2009.04.010

Claeys, M; Vermeylen, R; Yasmeen, F; Gomez-Gonzalez, Y; Chi, X; Maenhaut, W; Meszaros, T; Salma, I. (2012). Chemical characterisation of humic-like substances from urban, rural and tropical biomass burning environments using liquid chromatography with UV/vis photodiode array detection and electrospray ionisation mass spectrometry. Environ Chem 9: 273-284. http://dx.doi.org/10.1071/EN11163

Cook, BI; Miller, RL; Seager, R. (2009). Amplification of the North American "Dust Bowl" drought through human-induced land degradation. Proc Natl Acad Sci USA 106: 4997-5001. http://dx.doi.org/10.1073/pnas.0810200106

ED_002220_00002287-01845

Cook, ER; Anchukaitis, KJ; Buckley, BM; D'Arrigo, RD; Jacoby, GC; Wright, WE. (2010). Asian monsoon failure and megadrought during the last millennium. Science 328: 486-489. http://dx.doi.org/10.1126/science.1185188

Creighton, PJ; Lioy, PJ; Haynie, FH; Lemmons, TJ; Miller, JL; Gerhart, J. (1990). Soiling by atmospheric aerosols in an urban industrial area. J Air Waste Manag Assoc 40: 1285-1289.

Cultrone, G; De la Torre, MJ; Sebastian, EM; Cazalla, O; Rodriguez-Navarro, C. (2000). Behavior of brick samples in aggressive environments. Water Air Soil Pollut 119: 191-207.

De Meij, A; Pozzer, A; Lelieveld, J. (2012). Trend analysis in aerosol optical depths and pollutant emission estimates between 2000 and 2009. Atmos Environ 51: 75-85. http://dx.doi.org/10.1016/j.atmosenv.2012.01.059

de Oliveira, BP; de la Rosa, JM; Miller, AZ; Saiz-Jimenez, C; Gomez-Bolea, A; Braga, MAS; Dionisio, A. (2011). An integrated approach to assess the origins of black films on a granite monument. Environ Earth Sci 63: 1677-1690. http://dx.doi.org/10.1007/s12665-010-0773-2

Debell, L; Gebhart, K; Malm, W; Pitchford, M; Schichtel, B; White, W. (2006). Spatial and seasonal patterns and temporal variability of haze and its constituents in the United States. Report IV. Fort Collins, CO: Interagency Monitoring of Protected Visual Environments. http://vista.cira.colostate.edu/improve/publications/reports/2011/PDF/Cover_TOC.pdf

Degheidy, AR; Sallah, M; Elgarayhi, A; Shaaban, SM. (2015). Optical and radiative-transfer properties of mixed atmospheric aerosols. Adv Space Res 55: 1832-1844. http://dx.doi.org/10.1016/j.asr.2015.01.023

Deng, X; Wu, D, ui; Yu, J; Lau, AKH; Li, F, ei; Tan, H; Yuan, Z; Ng, W; Deng, T, ao; Wu, C; Zhou, X. (2013). Characterization of secondary aerosol and its extinction effects on visibility over the Pearl River Delta Region, China. J Air Waste Manag Assoc 63: 1012-1021. http://dx.doi.org/10.1080/10962247.2013.782927

Deser, C; Knutti, R; Solomon, S; Phillips, AS. (2012). Communication of the role of natural variability in future North American climate. Nat Clim Chang 2: 775-779. http://dx.doi.org/10.1038/NCLIMATE1562

Doherty, SJ; Warren, SG; Grenfell, TC; Clarke, AD; Brandt, RE. (2010). Light-absorbing impurities in Arctic snow. Atmos Chem Phys 10: 11647-11680. http://dx.doi.org/10.5194/acp-10-11647-2010

Dolgos, G; Martins, JV. (2014). Polarized Imaging Nephelometer for in situ airborne measurements of aerosol light scattering. Optics Express 22: 21972-21990. http://dx.doi.org/10.1364/OE.22.021972

Donahue, NM; Kroll, JH; Pandis, SN; Robinson, AL. (2012). A two-dimensional volatility basis set - Part 2: Diagnostics of organic-aerosol evolution. Atmos Chem Phys 12: 615-634. http://dx.doi.org/10.5194/acp-12-615-2012

Donahue, NM; Robinson, AL; Stanier, CO; Pandis, SN. (2006). Coupled partitioning, dilution, and chemical aging of semivolatile organics. Environ Sci Technol 40: 2635-2643. http://dx.doi.org/10.1021/es052297c

Du, K; Wang, K; Shi, P; Wang, Y. (2013). Quantification of atmospheric visibility with dual digital cameras during daytime and nighttime. Atmos Meas Tech 6: 2121-2130. http://dx.doi.org/10.5194/amt-6-2121-2013

Dunstone, NJ; Smith, DM; Booth, BBB; Hermanson, L; Eade, R. (2013). Anthropogenic aerosol forcing of Atlantic tropical storms. Nat Geosci 6: 534-539. http://dx.doi.org/10.1038/NGEO1854

Ely, DW; Leary, JT; Stewart, TR; Ross, DM. (1991). The establishment of the Denver Visibility Standard. Denver, Colorado: Colorado Department of Health.

Evan, AT; Vimont, DJ; Heidinger, AK; Kossin, JP; Bennartz, R. (2009). The role of aerosols in the evolution of tropical North Atlantic Ocean temperature anomalies. Science 324: 778-781. http://dx.doi.org/10.1126/science.1167404

Fairlie, TD; Jacob, DJ; Park, RJ. (2007). The impact of transpacific transport of mineral dust in the United States. Atmos Environ 41: 1251-1266. http://dx.doi.org/10.1016/j.atmosenv.2006.09.048

Fajardo, OA; Jiang, J; Hao, J. (2013). Assessing young people's preferences in urban visibility in beijing. Aerosol Air Qual Res 13: 1536-1543. http://dx.doi.org/10.4209/aaqr.2012.11.0307

ED_002220_00002287-01846

Fan, J; Rosenfeld, D; Zhang, Y; Giangrande, SE; Li, Z; Machado, LAT; Martin, ST; Yang, Y; Wang, J; Artaxo, P; Barbosa, HMJ; Braga, RC; Comstock, JM; Feng, Z; Gao, W; Gomes, HB; Mei, F; Pöhlker, C; Pöhlker, ML; Pöschl, U; de Souza, RAF. (2018). Substantial convection and precipitation enhancements by ultrafine aerosol particles. Science 359: 411-418. http://dx.doi.org/10.1126/science.aan8461

Favez, O; Cachier, H; Chabas, A; Ausset, P; Lefevre, R. (2006). Crossed optical and chemical evaluations of modern glass soiling in various European urban environments. Atmos Environ 40: 7192-7204. http://dx.doi.org/10.1016/j.atmosenv.2006.06.022

Feng, Y; Ramanathan, V; Kotamarthi, V. (2013). Brown carbon: a significant atmospheric absorber of solar radiation? Atmos Chem Phys Discuss 13: 2795-2833. http://dx.doi.org/10.5194/acp-13-8607-2013

Fialho, P; Cerqueira, M; Pio, C; Cardoso, J; Nunes, T; Custodio, D; Alves, C; Almeida, SM; Almeida-Silva, M; Reis, M; Rocha, F. (2014). The application of a multi-wavelength Aethalometer to estimate iron dust and black carbon concentrations in the marine boundary layer of Cape Verde. Atmos Environ 97: 136-143. http://dx.doi.org/10.1016/j.atmosenv.2014.08.008

Fiddler, MN; Begashaw, I; Mickens, MA; Collingwood, MS; Assefa, Z; Bililign, S. (2009). Laser spectroscopy for atmospheric and environmental sensing. Sensors 9: 10447-10512. http://dx.doi.org/10.3390/s91210447

Finlayson-Pitts, BJ; Pitts, JN, Jr. (2000). Chemistry of the upper and lower atmosphere: Theory, experiments and applications. In Chemistry of the upper and lower atmosphere: Theory, experiments and applications. San Diego, CA: Academic Press. http://www.sciencedirect.com/science/book/9780122570605

Fiore, AM; Naik, V; Leibensperger, EM. (2015). Air quality and climate connections [Review]. J Air Waste Manag Assoc 65: 645-685. http://dx.doi.org/10.1080/10962247.2015.1040526

Flanner, MG; Zender, CS; Randerson, JT; Rasch, PJ. (2007). Present-day climate forcing and response from black carbon in snow. J Geophys Res 112: D11202. http://dx.doi.org/10.1029/2006JD008003

Folini, D; Wild, M. (2015). The effect of aerosols and sea surface temperature on China's climate in the late twentieth century from ensembles of global climate simulations. J Geophys Res Atmos 120: 2261-2279. http://dx.doi.org/10.1002/2014JD022851

Forster, PM; Solomon, S. (2003). Observations of a "weekend effect" in diurnal temperature range. Proc Natl Acad Sci USA 100: 11225-11230. http://dx.doi.org/10.1073/pnas.2034034100

Freedman, MA; Hasenkopf, CA; Beaver, MR; Tolbert, MA. (2009). Optical properties of internally mixed aerosol particles composed of dicarboxylic acids and ammonium sulfate. J Phys Chem A 113: 13584-13592. http://dx.doi.org/10.1021/jp906240y

Freney, EJ; Adachi, K; Buseck, PR. (2010). Internally mixed atmospheric aerosol particles: Hygroscopic growth and light scattering. J Geophys Res 115: D19210. http://dx.doi.org/10.1029/2009JD013558

Freney, EJ; Martin, ST; Buseck, PR. (2009). Deliquescence and efflorescence of potassium salts relevant to biomass-burning aerosol particles. Aerosol Sci Technol 43: 799-807. http://dx.doi.org/10.1080/02786820902946620

Gan, CM; Pleim, J; Mathur, R; Hogrefe, C; Long, CN; Xing, J; Roselle, S; Wei, C. (2014). Assessment of the effect of air pollution controls on trends in shortwave radiation over the United States from 1995 through 2010 from multiple observation networks. Atmos Chem Phys 14: 1701-1715. http://dx.doi.org/10.5194/acp-14-1701-2014

Ginoux, P; Prospero, JM; Gill, TE; Hsu, NC; Zhao, M. (2012). Global-scale attribution of anthropogenic and natural dust sources and their emission rates based on modis deep blue aerosol products. Rev Geophys 50: RG3005. http://dx.doi.org/10.1029/2012RG000388

Goldstein, AH; Koven, CD; Heald, CL; Fung, IY. (2009). Biogenic carbon and anthropogenic pollutants combine to form a cooling haze over the southeastern United States. Proc Natl Acad Sci USA 106: 8835-8840. http://dx.doi.org/10.1073/pnas.0904128106

Griffin, D; Anchukaitis, KJ. (2014). How unusual is the 20122014 California drought? Geophys Res Lett 41: 9017-9023. http://dx.doi.org/10.1002/2014GL062433

ED_002220_00002287-01847

Grossi, CM; Brimblecombe, P; Esbert, RM; Javier Alonso, F. (2007). Color changes in architectural limestones from pollution and cleaning. Color Res Appl 32: 320-331. http://dx.doi.org/10.1002/col.20322

Hallar, AG; Lowenthal, DH; Clegg, SL; Samburova, V; Taylor, N; Mazzoleni, LR; Zielinska, BK; Kristensen, TB; Chirokova, G; Mccubbin, I, anB; Dodson, C; Collins, D, on. (2013). Chemical and hygroscopic properties of aerosol organics at Storm Peak Laboratory. J Geophys Res Atmos 118: 4767-4779. http://dx.doi.org/10.1002/jgrd.50373

Hamilton, RS; Mansfield, TA. (1993). The soiling of materials in the ambient atmosphere. Atmos Environ 27: 1369-1374.

Hammer, MS; Martin, RV; van Donkelaar, A; Buchard, V; Torres, O; Ridley, DA; Spurr, RJD. (2016). Interpreting the ultraviolet aerosol index observed with the OMI satellite instrument to understand absorption by organic aerosols: implications for atmospheric oxidation and direct radiative effects. Atmos Chem Phys 16: 2507-2523. http://dx.doi.org/10.5194/acp-16-2507-2016

Hand, J; Copeland, S; Day, D; Dillner, A; Indresand, H; Malm, W; Mcdade, C; Moore Jr, C; Pitchford, M; Schichtel, B. (2011). IMPROVE (Interagency Monitoring of Protected Visual Environments): Spatial and seasonal patterns and temporal variability of haze and its constituents in the United States. 0737-5352.

Hand, JL; Gebhart, KA; Schichtel, BA; Malm, WC. (2012a). Increasing trends in wintertime particulate sulfate and nitrate ion concentrations in the Great Plains of the United States (20002010). Atmos Environ 55: 107-110. http://dx.doi.org/10.1016/j.atmosenv.2012.03.050

Hand, JL; Malm, WC. (2007). Review of aerosol mass scattering efficiencies from ground-based measurements since 1990 [Review]. J Geophys Res 112: D16203. http://dx.doi.org/10.1029/2007JD008484

Hand, JL; Schichtel, BA; Malm, WC; Copeland, S; Molenar, JV; Frank, N; Pitchford, M. (2014a). Widespread reductions in haze across the United States from the early 1990s through 2011. Atmos Environ 94: 671-679. http://dx.doi.org/10.1016/j.atmosenv.2014.05.062

Hand, JL; Schichtel, BA; Malm, WC; Frank, NH. (2013). Spatial and Temporal Trends in PM2.5 Organic and Elemental Carbon across the United States. Adv Meterol. http://dx.doi.org/10.1155/2013/367674

Hand, JL; Schichtel, BA; Malm, WC; Pitchford, M; Frank, NH. (2014b). Spatial and seasonal patterns in urban influence on regional concentrations of speciated aerosols across the United States. J Geophys Res Atmos 119: 12832-12849. http://dx.doi.org/10.1002/2014JD022328

Hand, JL; Schichtel, BA; Malm, WC; Pitchford, ML. (2012b). Particulate sulfate ion concentration and SO2 emission trends in the United States from the early 1990s through 2010. Atmos Chem Phys 12: 10353-10365. http://dx.doi.org/10.5194/acp-12-10353-2012

Hand, JL; Schichtel, BA; Pitchford, M; Malm, WC; Frank, NH. (2012c). Seasonal composition of remote and urban fine particulate matter in the United States. J Geophys Res Atmos 117. http://dx.doi.org/10.1029/2011JD017122

Haneef, SJ; Johnson, JB; Thompson, GE; Wood, GC. (1993). The degradation of coupled stones by wet deposition processes. Corros Sci 34: 497-510. http://dx.doi.org/10.1016/0010-938X(93)90119-2

Hartmann, DL. (2013). Observations: Atmosphere and surface. In Climate Change 2013: The Physical Science Basis Contribution of Working Group I to the Fifth Assessment Report of the Intergovernmental Panel on Climate Change. Cambridge, United Kingdom and New York, NY, USA: Cambridge University Press.

Hauglustaine, DA; Balkanski, Y; Schulz, M. (2014). A global model simulation of present and future nitrate aerosols and their direct radiative forcing of climate. Atmos Chem Phys 14: 11031-11063. http://dx.doi.org/10.5194/acp-14-11031-2014

Hawkins, E; Sutton, R. (2009). The potential to narrow uncertainty in regional climate predictions. Bull Am Meteorol Soc 90: 1095-1107. http://dx.doi.org/10.1175/2009BAMS2607.1

Haynie, FH. (1986a). Theoretical model of soiling of surfaces by airborne particles.

Haynie, FH. (1986b). Environmental factors affecting corrosion of weathering steel. In R Baboian (Ed.), ACS symposium series 318 (pp. 163-171). Washington, DC: American Chemical Society.

ED_002220_00002287-01848

Haynie, FH; Lemmons, TJ. (1990). Particulate matter soiling of exterior paints at a rural site. Aerosol Sci Technol 13: 356-367. http://dx.doi.org/10.1080/02786829008959451

Heald, CL; Henze, DK; Horowitz, LW; Feddema, J; Lamarque, JF; Guenther, A; Hess, PG; Vitt, F; Seinfeld, JH; Goldstein, AH; Fung, I. (2008). Predicted change in global secondary organic aerosol concentrations in response to future climate, emissions, and land use change. J Geophys Res Atmos 113: D05211. http://dx.doi.org/10.1029/2007jd009092

Heald, CL; Ridley, DA; Kreidenweis, SM; Drury, EE. (2010). Satellite observations cap the atmospheric organic aerosol budget. Geophys Res Lett 37. http://dx.doi.org/10.1029/2010GL045095

Heald, CL; Ridley, DA; Kroll, JH; Barrett, SRH; Cady-Pereira, KE; Alvarado, MJ; Holmes, CD. (2014). Contrasting the direct radiative effect and direct radiative forcing of aerosols. Atmos Chem Phys 14: 5513-5527. http://dx.doi.org/10.5194/acp-14-5513-2014

Hegerl, GC; Hoegh-Guldberg, O; Casassa, G; Hoerling, M; Kovats, S; Parmesan, C; Pierce, D; Stott, P. (2010). Good practice guidance paper on detection and attribution related to anthropogenic climate change. In T Stocker; C Field; Q Dahe; V Barros; GK Plattner; M Tignor; P Midgley; K Ebi (Eds.), Meeting report of the Intergovernmental Panel on Climate Change Expert Meeting on detection and attribution of anthropogenic climate change. Bern, Switzerland: IPCC Working Group I Technical Support Unit, University of Bern. https://wg1.ipcc.ch/guidancepaper/IPCC_D&A_GoodPracticeGuidancePaper.pdf

Heintzenberg, J. (1978). Angular calibration of total scatter-backscatter nephelometer, consequences and applications. Staub Reinhalt Luft 38: 62-63.

Hoffer, A; Gelencser, A; Guyon, P; Kiss, G; Schmid, O; Frank, GP; Artaxo, P; Andreae, MO. (2006). Optical properties of humic-like substances (HULIS) in biomass-burning aerosols. Atmos Chem Phys 6: 3563-3570.

Hussey, SJ; Purves, J; Allcock, N; Fernandes, VE; Monks, PS; Ketley, JM; Andrew, PW; Morrissey, JA. (2017). Air pollution alters Staphylococcus aureus and Streptococcus pneumoniae biofilms, antibiotic tolerance and colonisation. Environ Microbiol 19: 1868-1880. http://dx.doi.org/10.1111/1462-2920.13686

IPCC (Intergovernmental Panel on Climate Change). (2013). Climate change 2013: The physical science basis. Contribution of working group I to the fifth assessment report of the Intergovernmental Panel on Climate Change. In TF Stocker; D Qin; G Plattner; MMB Tignor; SK Allen; J Boschung; A Mauels; Y Xia; V Bex; PM Midgley (Eds.), Climate Change 2013: The Physical Science Basis. New York, NY: Cambridge University Press. http://www.ipcc.ch/report/ar5/wg1/#.Um6aMXDkvNk

Jacobson, MZ. (2012). Investigating cloud absorption effects: Global absorption properties of black carbon, tar balls, and soil dust in clouds and aerosols. J Geophys Res 117: D06205. http://dx.doi.org/10.1029/2011JD017218

Jacobson, MZ; Kaufman, YJ; Rudich, Y. (2007). Examining feedbacks of aerosols to urban climate with a model that treats 3-D clouds with aerosol inclusions. J Geophys Res 112: D24205. http://dx.doi.org/10.1029/2007JD008922

Jacobson, MZ; Streets, DG. (2009). Influence of future anthropogenic emissions on climate, natural emissions, and air quality. J Geophys Res 114: D08118. http://dx.doi.org/10.1029/2008JD011476

Javed, W; Wubulikasimu, Y; Figgis, B; Guo, B. (2017). Characterization of dust accumulated on photovoltaic panels in Doha, Qatar. Solar Energy 142: 123-135. http://dx.doi.org/10.1016/j.solener.2016.11.053

Jimenez, JL; Canagaratna, MR; Donahue, NM; Prevot, AS; Zhang, Q; Kroll, JH; Decarlo, PF; Allan, JD; Coe, H; Ng, NL; Aiken, AC; Docherty, KS; Ulbrich, IM; Grieshop, AP; Robinson, AL; Duplissy, J; Smith, JD; Wilson, KR; Lanz, VA; Hueglin, C; Sun, YL; Tian, J; Laaksonen, A; Raatikainen, T; Rautiainen, J; Vaattovaara, P; Ehn, M; Kulmala, M; Tomlinson, JM; Collins, DR; Cubison, MJ; Dunlea, EJ; Huffman, JA; Onasch, TB; Alfarra, MR; Williams, PI; Bower, K; Kondo, Y; Schneider, J; Drewnick, F; Borrmann, S; Weimer, S; Demerjian, K; Salcedo, D; Cottrell, L; Griffin, R; Takami, A; Miyoshi, T; Hatakeyama, S; Shimono, A; Sun, JY; Zhang, YM; Dzepina, K; Kimmel, J. R.; Sueper, D; Jayne, JT; Herndon, SC; Trimborn, AM; Williams, LR; Wood, EC; Middlebrook, AM; Kolb, CE; Baltensperger, U; Worsnop, DR. (2009). Evolution of organic aerosols in the atmosphere. Science 326: 1525-1529. http://dx.doi.org/10.1126/science.1180353

ED_002220_00002287-01849

Johansson, LG; Lindqvist, O; Mangio, RE. (1988). Corrosion of calcareous stones in humid air containing SO2 and NO2. 5: 439-449.

Jones, GS; Stott, PA; Christidis, N. (2013). Attribution of observed historical near surface temperature variations to anthropogenic and natural causes using CMIP5 simulations. J Geophys Res 118: 4001-4024. http://dx.doi.org/10.1002/jgrd.50239

Jongeward, AR; Li, Z; He, H, ao; Xiong, X. (2016). Natural and anthropogenic aerosol trends from satellite and surface observations and model simulations over the North Atlantic Ocean from 2002 to 2012. J Atmos Sci 73: 4469-4485. http://dx.doi.org/10.1175/JAS-D-15-0308.1

Jung, M; Reichstein, M; Margolis, HA; Cescatti, A; Richardson, AD; Arain, MA; Arneth, A; Bernhofer, C; Bonal, D; Chen, J; Gianelle, D; Gobron, N; Kiely, G; Kutsch, W; Lasslop, G; Law, BE; Lindroth, A; Merbold, L; Montagnani, L; Moors, EJ; Papale, D; Sottocornola, M; Vaccari, F; Williams, C. (2011). Global patterns of land-atmosphere fluxes of carbon dioxide, latent heat, and sensible heat derived from eddy covariance, satellite, and meteorological observations. J Geophys Res 116. http://dx.doi.org/10.1029/2010JG001566

Kavouras, IG; Etyemezian, V; Dubois, DW; Xu, J; Pitchford, M. (2009). Source reconciliation of atmospheric dust causing visibility impairment in Class I areas of the western United States. J Geophys Res 114: D02308. http://dx.doi.org/10.1029/2008JD009923

Keene, WC; Moody, JL; Galloway, JN; Prospero, JM; Cooper, OR; Eckhardt, S; Maben, JR, JR. (2014). Long-term trends in aerosol and precipitation composition over the western North Atlantic Ocean at Bermuda. Atmos Chem Phys 14: 8119-8135. http://dx.doi.org/10.5194/acp-14-8119-2014

Kirchstetter, TW; Novakov, T; Hobbs, PV. (2004). Evidence that the spectral dependence of light absorption by aerosols is affected by organic carbon. J Geophys Res 109D21: D21208. http://dx.doi.org/10.1029/2004JD004999

Kitanovski, Z; Grgić, I; Vermeylen, R; Claeys, M; Maenhaut, W. (2012). Liquid chromatography tandem mass spectrometry method for characterization of monoaromatic nitro-compounds in atmospheric particulate matter. J Chromatogr A 1268: 35-43. http://dx.doi.org/10.1016/j.chroma.2012.10.021

Klimont, Z; Smith, S; Cofala, J. (2013). The last decade of global anthropogenic sulfur dioxide: 20002011 emissions. Environ Res Lett 8: 014003.

Klingmueller, K; Steil, B; Bruehl, C; Tost, H; Lelieveld, J. (2014). Sensitivity of aerosol radiative effects to different mixing assumptions in the AEROPT 1.0 submodel of the EMAC atmospheric-chemistry-climate model. GMD 7: 2503-2516. http://dx.doi.org/10.5194/gmd-7-2503-2014

Kloppmann, W; Bromblet, P; Vallet, JM; Verges-Belmin, V; Rolland, O; Guerrot, C; Gosselin, C. (2011). Building materials as intrinsic sources of sulphate: A hidden face of salt weathering of historical monuments investigated through multi-isotope tracing (B, O, S). Sci Total Environ 409: 1658-1669. http://dx.doi.org/10.1016/j.scitotenv.2011.01.008

Knutson, TR; Zeng, F; Wittenberg, AT. (2013). Multimodel assessment of regional surface temperature trends: CMIP3 and CMIP5 Twentieth-Century Simulations. J Clim 26: 8709-8743. http://dx.doi.org/10.1175/JCLI-D-12-00567.1

Koch, D; Bauer, SE; Del Genio, A; Faluvegi, G; Mcconnell, JR; Menon, S; Miller, RL; Rind, D; Ruedy, R; Schmidt, GA; Shindell, D. (2011). Coupled aerosol-chemistry-climate twentieth-century transient model investigation: Trends in short-lived species and climate responses. J Clim 24: 2693-2714. http://dx.doi.org/10.1175/2011JCLI3582.1

Koch, D; Del Genio, AD. (2010). Black carbon semi-direct effects on cloud cover: Review and synthesis. Atmos Chem Phys 10: 7685-7696. http://dx.doi.org/10.5194/acp-10-7685-2010

Kok, JF; Ridley, DA; Zhou, Q; Miller, R, onL; Zhao, C; Heald, CL; Ward, DS; Albani, S; Haustein, K. (2017). Smaller desert dust cooling effect estimated from analysis of dust size and abundance. Nat Geosci 10: 274-278. http://dx.doi.org/10.1038/NGEO2912

Koschmieder, H. (1924). Theorie der horizontalen Sichtweite. 12: 33-55.

ED_002220_00002287-01850

Kristensen, TB; Wex, H; Nekat, B; Nojgaard, JK; Pinxteren, D; Lowenthal, DH; Mazzoleni, LR; Dieckmann, K; Koch, CB; Mentel, TF; Herrmann, H; Hallar, AG; Stratmann, F; Bilde, M. (2012). Hygroscopic growth and CCN activity of HULIS from different environments: American Geophysical Union. http://dx.doi.org/10.1029/2012JD018249

Kucera, V; Henriksen, J; Knotkova, D; Sjostrom, C. (1993). Model for calculations of corrosion cost caused by air pollution and its application in three cities.

Kuebbeler, M; Lohmann, U; Hendricks, J; Kaercher, B. (2014). Dust ice nuclei effects on cirrus clouds. Atmos Chem Phys 14: 3027-3046. http://dx.doi.org/10.5194/acp-14-3027-2014

Kumar, S; Kinter, J; Dirmeyer, PA; Pan, Z; Adams, J. (2012). Multidecadal Climate Variability and the Warming Hole in North America: Results from CMIP5 Twentieth- and Twenty-First-Century Climate Simulations*. J Clim 26: 3511-3527. http://dx.doi.org/10.1175/JCLI-D-12-00535.1

Kunkel, KE; Liang, XZ; Zhu, J; Lin, Y. (2006). Can CGCMs Simulate the Twentieth-Century Warming Hole in the Central United States? J Clim 19: 4137-4153. http://dx.doi.org/10.1175/JCLI3848.1

Lack, DA; Bahreni, R; Langridge, JM; Gilman, JB; Middlebrook, AM. (2013). Brown carbon absorption linked to organic mass tracers in biomass burning particles. Atmos Chem Phys 13: 2415-2422. http://dx.doi.org/10.5194/acp-13-2415-2013

Lamarque, JF; Shindell, DT; Josse, B; Young, PJ; Cionni, I; Eyring, V; Bergmann, D; Cameron-Smith, P; Collins, WJ; Doherty, R; Dalsoren, S; Faluvegi, G; Folberth, G; Ghan, SJ; Horowitz, LW; Lee, YH; Mackenzie, IA; Nagashima, T; Naik, V; Plummer, D; Righi, M; Rumbold, ST; Schulz, M; Skeie, RB; Stevenson, DS; Strode, S; Sudo, K; Szopa, S; Voulgarakis, A; Zeng, G. (2013). The Atmospheric Chemistry and Climate Model Intercomparison Project (ACCMIP): overview and description of models, simulations and climate diagnostics. GMD 6: 179-206. http://dx.doi.org/10.5194/gmd-6-179-2013

Lanzon, M; Garcia-Ruiz, PA. (2010). Deterioration and damage evaluation of rendering mortars exposed to sulphuric acid. Mater Struct 43: 417-427. http://dx.doi.org/10.1617/s11527-009-9500-4

Lareau, NP; Crosman, E; Whiteman, CD; Horel, JD; Hoch, SW; Brown, WOJ; Horst, TW. (2013). The persistent cold-air pool study. Bull Am Meteorol Soc 94: 51-63. http://dx.doi.org/10.1175/BAMS-D-11-00255.1

Lau, NT; Chan, CK; Chan, L; Fang, M. (2008). A microscopic study of the effects of particle size and composition of atmospheric aerosols on the corrosion of mild steel. Corros Sci 50: 2927-2933. http://dx.doi.org/10.1016/j.corsci.2008.07.009

Lawrimore, JH; Menne, MJ; Gleason, BE; Williams, CN; Wuertz, DB; Vose, RS; Rennie, J. (2011). An overview of the Global Historical Climatology Network monthly mean temperature data set, version 3. J Geophys Res 116: D19121. http://dx.doi.org/10.1029/2011JD016187

Lee, YH; Adams, PJ. (2012). A fast and efficient version of the TwO-Moment Aerosol Sectional (TOMAS) global aerosol microphysics model. Aerosol Sci Technol 46: 678-689. http://dx.doi.org/10.1080/02786826.2011.643259

Lee, YH; Lamarque, JF; Flanner, MG; Jiao, C; Shindell, DT; Berntsen, T; Bisiaux, MM; Cao, J; Collins, WJ; Curran, M; Edwards, R; Faluvegi, G; Ghan, S; Horowitz, LW; Mcconnell, J. R.; Ming, J; Myhre, G; Nagashima, T; Naik, V; Rumbold, ST; Skeie, RB; Sudo, K; Takemura, T; Thevenon, F; Xu, B; Yoon, JH. (2013). Evaluation of preindustrial to present-day black carbon and its albedo forcing from Atmospheric Chemistry and Climate Model Intercomparison Project (ACCMIP). Atmos Chem Phys 13: 2607-2634. http://dx.doi.org/10.5194/acp-13-2607-2013

Leibensperger, EM; Mickley, LJ; Jacob, DJ. (2008). Sensitivity of US air quality to mid-latitude cyclone frequency and implications of 1980-2006 climate change. Atmos Chem Phys 8: 7075-7086. http://dx.doi.org/10.5194/acp-8-7075-2008

Leibensperger, EM; Mickley, LJ; Jacob, DJ; Chen, WT; Seinfeld, JH; Nenes, A; Adams, PJ; Streets, DG; Kumar, N; Rind, D. (2012a). Climatic effects of 1950-2050 changes in US anthropogenic aerosols - Part 2: Climate response. Atmos Chem Phys 12: 3349-3362. http://dx.doi.org/10.5194/acp-12-3349-2012

ED_002220_00002287-01851

Leibensperger, EM; Mickley, LJ; Jacob, DJ; Chen, WT; Seinfeld, JH; Nenes, A; Adams, PJ; Streets, DG; Kumar, N; Rind, D. (2012b). Climatic effects of 1950–2050 changes in US anthropogenic aerosols – Part 1: Aerosol trends and radiative forcing. Atmos Chem Phys 12: 3333-3348. http://dx.doi.org/10.5194/acp-12-3333-2012

Levy, H; Horowitz, LW; Schwarzkopf, MD; Ming, Y, i; Golaz, JC; Naik, V; Ramaswamy, V. (2013). The roles of aerosol direct and indirect effects in past and future climate change. J Geophys Res Atmos 118: 4521-4532. http://dx.doi.org/10.1002/jgrd.50192

Li, J; Min, Q; Peng, Y; Sun, Z; Zhao, JQ, i. (2015). Accounting for dust aerosol size distribution in radiative transfer. J Geophys Res Atmos 120: 6537-6550. http://dx.doi.org/10.1002/2015JD023078

Li, W; Shao, L; Shi, Z; Chen, J; Yang, L; Yuan, Q, i; Yan, C; Zhang, X; Wang, Y; Sun, J; Zhang, Y; Shen, X; Wang, Z; Wang, W. (2014). Mixing state and hygroscopicity of dust and haze particles before leaving Asian continent. J Geophys Res Atmos 119: 1044-1059. http://dx.doi.org/10.1002/2013JD021003

Liang, XZ; Pan, JP; Zhu, JH; Kunkel, KE; Wang, JXL; Dai, A. (2005). Regional climate model downscaling of US summer climate and future change. J Geophys Res 111.

Lipfert, FW. (1989). Atmospheric damage to calcareous stones - Comparison and reconciliation of recent experimental findings. Atmos Environ 23: 415-429.

Liu, B; Wang, DW; Guo, H; Ling, ZH; Cheung, K. (2015). Metallic corrosion in the polluted urban atmosphere of Hong Kong. Environ Monit Assess 187: 4112. http://dx.doi.org/10.1007/s10661-014-4112-z

Liu, J; Scheuer, E; Dibb, J; Ziemba, LD; Thornhill, KL; Anderson, BE; Wisthaler, A; Mikoviny, T; Devi, JJ, ai; Bergin, M; Weber, RJ. (2014). Brown carbon in the continental troposphere. Geophys Res Lett 41: 2191-2195. http://dx.doi.org/10.1002/2013GL058976

Liu, X; Gu, J; Li, Y; Cheng, Y; Qu, Y, u; Han, T; Wang, J; Tian, H; Chen, J; Zhang, Y. (2013). Increase of aerosol scattering by hygroscopic growth: Observation, modeling, and implications on visibility. Atmos Res 132: 91-101. http://dx.doi.org/10.1016/j.atmosres.2013.04.007

Liu, X; Zhang, Y; Cheng, Y; Hu, M, in; Han, T. (2012). Aerosol hygroscopicity and its impact on atmospheric visibility and radiative forcing in Guangzhou during the 2006 PRIDE-PRD campaign. Atmos Environ 60: 59-67. http://dx.doi.org/10.1016/j.atmosenv.2012.06.016

Lombardo, T; Ionescu, A; Chabas, A; Lefevre, RA; Ausset, P; Candau, Y. (2010). Dose-response function for the soiling of silica-soda-lime glass due to dry deposition. Sci Total Environ 408: 976-984. http://dx.doi.org/10.1016/j.scitotenv.2009.10.040

Lombardo, T; Ionescu, A; Lefevre, RA; Chabas, A; Ausset, P; Cachier, H. (2005). Soiling of silica-soda-lime float glass in urban environment: Measurements and modelling. Atmos Environ 39: 989-997. http://dx.doi.org/10.1016/j.atmosenv.2004.10.030

Lowenthal, D; Zielinska, B; Mason, B; Samy, S; Samburova, V; Collins, D, on; Spencer, C; Taylor, N; Allen, J; Kumar, N. (2009). Aerosol characterization studies at Great Smoky Mountains National Park, summer 2006. J Geophys Res Atmos 114. http://dx.doi.org/10.1029/2008JD011274

Lowenthal, D; Zielinska, B; Samburova, V; Collins, D; Taylor, N; Kumar, N. (2015). Evaluation of assumptions for estimating chemical light extinction at U.S. national parks. J Air Waste Manag Assoc 65: 249-260. http://dx.doi.org/10.1080/10962247.2014.986307

Lowenthal, DH; Kumar, N. (2004). Variation of mass scattering efficiencies in IMPROVE. J Air Waste Manag Assoc 54: 926-934.

Lowenthal, DH; Kumar, N. (2016). Evaluation of the IMPROVE Equation for estimating aerosol light extinction. 66: 726-737. http://dx.doi.org/10.1080/10962247.2016.1178187

Lu, Z; Streets, DG; Winijkul, E; Yan, F; Chen, Y; Bond, TC; Feng, Y; Dubey, MK; Liu, S; Pinto, JP; Carmichael, GR. (2015). Light absorption properties and radiative effects of primary organic aerosol emissions. Environ Sci Technol 49: 4868-4877. http://dx.doi.org/10.1021/acs.est.5b00211

ED_002220_00002287-01852

Mahowald, NM; Kloster, S; Engelstaedter, S; Moore, JK; Mukhopadhyay, S; Mcconnell, J. R.; Albani, S; Doney, SC; Bhattacharya, A; Curran, MAJ; Flanner, MG; Hoffman, FM; Lawrence, DM; Lindsay, K; Mayewski, PA; Neff, J; Rothenberg, D; Thomas, E; Thornton, PE; Zender, CS. (2010). Observed 20th century desert dust variability: impact on climate and biogeochemistry. Atmos Chem Phys 10: 10875-10893. http://dx.doi.org/10.5194/acp-10-10875-2010

Malm, W; Cismoski, S; Schichtel, B. (2015). Use of webcam images for quantitative characterization of haze. In Air & Waste Management Association Annual Meeting. Raleigh, NC.

Malm, WC. (2016). Visibility: The seeing of near and distant landscape features (First ed.). Amsterdam, the Netherlands: Elsevier. http://store.elsevier.com/Visibility/William-Malm/isbn-9780128044506/

Malm, WC; Day, DE; Kreidenweis, SM; Collett, JL; Lee, T. (2003). Humidity dependent optical properties of fine particle during the Big Bend Regional Aerosol and Visibility Observational Study (BRAVO). J Geophys Res Atmos 108: 4279. http://dx.doi.org/10.1029/2002JD002998

Malm, WC; Hand, JL. (2007). An examination of the physical and optical properties of aerosols collected in the IMPROVE program. Atmos Environ 41: 3407-3427. http://dx.doi.org/10.1016/j.atmosenv.2006.12.012

Malm, WC; McMeeklng, GR; Kreidenwals, SM; Levin, E; Carrico, CM; Day, DE; Collett Jr, JL; Lee, T; Sullivan, AP; Raja, S. (2009). Using high time resolution aerosol and number size distribution measurements to estimate atmospheric extinction. J Air Waste Manag Assoc 59: 1049-1060. http://dx.doi.org/10.3155/1047-3289.59.9.1049

Malm, WC; Schichtel, BA; Pitchford, ML. (2011). Uncertainties in PM2.5 gravimetric and speciation measurements and what we can learn from them. J Air Waste Manag Assoc 61: 1131-1149. http://dx.doi.org/10.1080/10473289.2011.603998

Malm, WC; Sisler, JF; Huffman, D; Eldred, RA; Cahill, TA. (1994). Spatial and seasonal trends in particle concentration and optical extinction in the United States. J Geophys Res 99: 1347-1370. http://dx.doi.org/10.1029/93JD02916

Marais, EA; Jacob, DJ; Turner, J, ayR; Mickley, LJ. (2017). Evidence of 1991-2013 decrease of biogenic secondary organic aerosol in response to SO2 emission controls. Environ Res Lett 12. http://dx.doi.org/10.1088/1748-9326/aa69c8

Margono, BA; Turubanova, S; Zhuravleva, I; Potapov, P; Tyukavina, A; Baccini, A; Goetz, S; Hansen, MC. (2012). Mapping and monitoring deforestation and forest degradation in Sumatra (Indonesia) using Landsat time series data sets from 1990 to 2010. Environ Res Lett 7. http://dx.doi.org/10.1088/1748-9326/7/3/034010

Mascioli, NR; Previdi, M; Fiore, AM; Ting, M. (2017). Timing and seasonality of the United States warming hole. Environ Res Lett 12: 034008.

Mashayekhi, R; Sloan, JJ. (2014). Effects of aerosols on precipitation in north-eastern North America. Atmos Chem Phys 14: 5111-5125. http://dx.doi.org/10.5194/acp-14-5111-2014

Massoli, P; Murphy, DM; Lack, DA; Baynard, T; Brock, CA; Lovejoy, ER. (2009). Uncertainty in light scattering measurements by TSI nephelometer: results from laboratory studies and implications for ambient measurements. Aerosol Sci Technol 43: 1064-1074. http://dx.doi.org/10.1080/02786820903156542

McAlister, J; Smith, BJ; Torok, A. (2008). Transition metals and water-soluble ions in deposits on a building and their potential catalysis of stone decay. Atmos Environ 42: 7657-7668. http://dx.doi.org/10.1016/j.atmosenv.2008.05.067

McCrowey, CJ; Tinilau, SS; Calderon, G; Koo, J; Curtis, DB. (2013). A portable high-resolution polar nephelometer for measurement of the angular scattering properties of atmospheric aerosol: Design and validation. Aerosol Sci Technol 47: 592-605. http://dx.doi.org/10.1080/02786826.2013.775400

McNeill, VF; Woo, JL; Kim, DD; Schwier, AN; Wannell, NJ; Sumner, AJ; Barakat, JM. (2012). Aqueous-phase secondary organic aerosol and organosulfate formation in atmospheric aerosols: a modeling study. Environ Sci Technol 46: 8075-8081. http://dx.doi.org/10.1021/es3002986

ED_002220_00002287-01853

McRoberts, DB; Nielsen-Gammon, JW. (2011). A new homogenized climate division precipitation dataset for analysis of climate variability and climate change. J Appl Meteor Climatol 50: 1187-1199. http://dx.doi.org/10.1175/2010JAMC2626.1

Meehl, GA; Arblaster, JM; Branstator, G. (2012). Mechanisms Contributing to the Warming Hole and the Consequent U.S. EastWest Differential of Heat Extremes. J Clim 25: 6394-6408. http://dx.doi.org/10.1175/JCLI-D-11-00655.1

Meehl, GA; Arblaster, JM; Chung, CTY. (2015). Disappearance of the southeast US "warming hole" with the late 1990s transition of the Interdecadal Pacific Oscillation. Geophys Res Lett 42: 5564-5570. http://dx.doi.org/10.1002/2015GL064586

Meehl, GA; Tebaldi, C; Adams-Smith, D. (2016). US daily temperature records past, present, and future. Proc Natl Acad Sci USA 113: 13977-13982. http://dx.doi.org/10.1073/pnas.1606117113

Meehl, GA; Tebaldi, C; Walton, G; Easterling, D; McDaniel, L. (2009). Relative increase of record high maximum temperatures compared to record low minimum temperatures in the U.S. Geophys Res Lett 36: L23701. http://dx.doi.org/10.1029/2009GL040736

Melillo, JM; Richmond, T; Yohe, GW. (2014). Climate change impacts in the United States: The third National Climate Assessment. In JM Melillo; T Richmond; GW Yohe (Eds.), Climate change impacts in the United States: The third National Climate Assessment. Washington, D.C.: U.S. Government Printing Office. http://nca2014.globalchange.gov/report

Mickley, L; Fiore, A; Henze, D. (2014). Interactions between Climate Change and US Air Quality.

Mickley, LJ; Leibensperger, EM; Jacob, DJ; Rind, D. (2012). Regional warming from aerosol removal over the United States: Results from a transient 20102050 climate simulation. Atmos Environ 46: 545-553. http://dx.doi.org/http://dx.doi.org/10.1016/j.atmosenv.2011.07.030

Middleton, W. (1968). Vision through the atmosphere. Toronto, Canada: University of Toronto Press; Corrected edition.

Mie, G. (1908). Beitrage zur Optik truber Medien, speziell kolloidaler Metallosungen [Optics of cloudy media, especially colloidal metal solutions]. Ann Phys 25: 377-445.

Mooers, HD; Cota-Guertin, AR; Regal, RR; Sames, AR; Dekan, AJ; Henkels, LM. (2016). A 120-year record of the spatial and temporal distribution of gravestone decay and acid deposition. Atmos Environ 127: 139-154. http://dx.doi.org/10.1016/j.atmosenv.2015.12.023

Moosmueller, H; Engelbrecht, JP; Skiba, M; Frey, G; Chakrabarty, RK; Arnott, WP. (2012). Single scattering albedo of fine mineral dust aerosols controlled by iron concentration. J Geophys Res 117: D11210. http://dx.doi.org/10.1029/2011JD016909

Moosmüller, H; Chakrabarty, RK; Arnott, WP. (2009). Aerosol light absorption and its measurement: A review. J Quant Spectrosc Radiat Transf 110: 844-878. http://dx.doi.org/10.1016/j.jqsrt.2009.02.035

Moosmuller, H; Varma, R; Arnott, WP. (2005). Cavity ring-down and cavity-enhanced detection techniques for the measurement of aerosol extinction. Aerosol Sci Technol 39: 30-39. http://dx.doi.org/10.1080/027868290903880

Mueller, T; Henzing, JS; de Leeuw, G; Wiedensohler, A; Alastuey, A; Angelov, H; Bizjak, M; Coen, MC; Engstrom, JE; Gruening, C; Hillamo, R; Hoffer, A; Imre, K; Ivanow, P; Jennings, G; Sun, JY; Kalivitis, N; Karlsson, H; Komppula, M; Laj, P; Li, SM; Lunder, C; Marinoni, A; dos Santos, SM; Moerman, M; Nowak, A; Ogren, JA; Petzold, A; Pichon, JM; Rodriquez, S; Sharma, S; Sheridan, PJ; Teinila, K; Tuch, T; Viana, M; Virkkula, A; Weingartner, E; Wilhelm, R; Wang, YQ. (2011a). Characterization and intercomparison of aerosol absorption photometers: result of two intercomparison workshops. Atmos Meas Tech 4: 245-268. http://dx.doi.org/10.5194/amt-4-245-2011

Mueller, T; Laborde, M; Kassell, G; Wiedensohler, A. (2011b). Design and performance of a three-wavelength LED-based total scatter and backscatter integrating nephelometer. Atmos Meas Tech 4: 1291-1303. http://dx.doi.org/10.5194/amt-4-1291-2011

ED_002220_00002287-01854

Mueller, T; Nowak, A; Wiedensohler, A; Sheridan, P; Laborde, M; Covert, DS; Marinoni, A; Imre, K; Henzing, B, as; Roger, JC; dos Santos, SM; Wilhelm, R; Wang, Y, aQ; de Leeuw, G. (2009). Angular Illumination and Truncation of Three Different Integrating Nephelometers: Implications for Empirical, Size-Based Corrections. Aerosol Sci Technol 43: 581-586. http://dx.doi.org/10.1080/02786820902798484

Murphy, DM; Chow, JC; Leibensperger, EM; Malm, WC; Pitchford, M; Schichtel, BA; Watson, JG; White, WH. (2011). Decreases in elemental carbon and fine particle mass in the United States. Atmos Chem Phys 11: 4679-4686. http://dx.doi.org/10.5194/acp-11-4679-2011

Murphy, DM; Solomon, S; Portmann, RW; Rosenlof, KH; Forster, PM; Wong, T. (2009). An observationally based energy balance for the Earth since 1950. J Geophys Res 114: D17107. http://dx.doi.org/10.1029/2009JD012105

Myhre, G. (2009). Consistency between satellite-derived and modeled estimates of the direct aerosol effect. Science 325: 187-190. http://dx.doi.org/10.1126/science.1174461

Myhre, G. (2013). Anthropogenic and Natural Radiative Forcing. In Climate Change 2013: The Physical Science Basis Contribution of Working Group I to the Fifth Assessment Report of the Intergovernmental Panel on Climate Change. Cambridge, United Kingdom and New York, NY, USA: Cambridge University Press.

Myhre, G; Samset, BH; Schulz, M; Balkanski, Y; Bauer, S; Berntsen, TK; Bian, H; Bellouin, N; Chin, M; Diehl, T; Easter, RC; Feichter, J; Ghan, SJ; Hauglustaine, D; Iversen, T; Kinne, S; Kirkevag, A; Lamarque, JF; Lin, G; Liu, X; Lund, MT; Luo, G; Ma, X; van Noije, T; Penner, JE; Rasch, PJ; Ruiz, A; Seland, O; Skeie, RB; Stier, P; Takemura, T; Tsigaridis, K; Wang, P; Wang, Z; Xu, L; Yu, H; Yu, F; Yoon, JH; Zhang, K; Zhang, H; Zhou, C. (2013). Radiative forcing of the direct aerosol effect from AeroCom Phase II simulations. Atmos Chem Phys 13: 1853-1877. http://dx.doi.org/10.5194/acp-13-1853-2013

NAS (National Academy of Sciences). (2014). Climate change: Evidence and causes. Washington, DC.

Nazaroff, WW; Cass, GR. (1991). Protecting museum collections from soiling due to the deposition of airborne particles. Atmos Environ 25: 841-852. http://dx.doi.org/10.1016/0960-1686(91)90127-S

Neff, JC; Ballantyne, AP; Farmer, GL; Mahowald, NM; Conroy, JL; Landry, CC; Overpeck, JT; Painter, TH; Lawrence, CR; Reynolds, RL. (2008). Increasing eolian dust deposition in the western United States linked to human activity. Nat Geosci 1: 189-195. http://dx.doi.org/10.1038/ngeo133

Nenes, A; Murray, B; Bougiatioti, A. (2014). Mineral dust and its microphysical interactions with clouds. In Mineral Dust. Netherlands: Springer. http://dx.doi.org/10.1007/978-94-017-8978-3_12

NOAA (National Oceanic and Atmospheric Administration). (1998). Automated surface observing system: ASOS user's guide. Washington, D.C.: U.S. Dept. of Commerce, National Oceanic and Atmospheric Administration : Federal Aviation Administration : U.S. Navy.

NOAA NCEI (NOAA National Centers for Environmental Information). (2017). State of the climate: Global climate report for annual 2016. Available online at https://www.ncdc.noaa.gov/sotc/global/201613

Northrop, PJ; Chandler, RE. (2014). Quantifying sources of uncertainty in projections of future climate. J Clim 27: 8793-8808. http://dx.doi.org/10.1175/JCLI-D-14-00265.1

Ouimette, JR; Flagan, RC. (1982). The extinction coefficient of multicomponent aerosols. Atmos Environ 16: 2405-2420. http://dx.doi.org/10.1016/0004-6981(82)90131-7

Ozga, I; Bonazza, A; Bernardi, E; Tittarelli, F; Favoni, O; Ghedini, N; Morselli, L; Sabbioni, C. (2011). Diagnosis of surface damage induced by air pollution on 20th-century concrete buildings. Atmos Environ 45: 4986-4995. http://dx.doi.org/10.1016/j.atmosenv.2011.05.072

Painter, TH; Skiles, SM; Deems, JS; Brandt, WT; Dozier, J. (2018). Variation in rising limb of Colorado River snowmelt runoff hydrograph controlled by dust radiative forcing in snow. Geophys Res Lett 45: 797-808. http://dx.doi.org/10.1002/2017GL075826

Painter, TH; Skiles, SM; Deems, JS; Bryant, A, nnC; Landry, CC. (2012). Dust radiative forcing in snow of the Upper Colorado River Basin: 1. A 6 year record of energy balance, radiation, and dust concentrations. Water Resour Res 48. http://dx.doi.org/10.1029/2012WR011985

ED_002220_00002287-01855

Pan, Z. (2004). Altered hydrologic feedback in a warming climate introduces a warming hole. Geophys Res Lett 31: L17109. http://dx.doi.org/10.1029/2004GL020528

Pandolfi, M; Ripoll, A; Querol, X; Alastuey, A. (2014). Climatology of aerosol optical properties and black carbon mass absorption cross section at a remote high-altitude site in the western Mediterranean Basin. Atmos Chem Phys 14: 6443-6460. http://dx.doi.org/10.5194/acp-14-6443-2014

Pechony, O; Shindell, DT. (2010). Driving forces of global wildfires over the past millennium and the forthcoming century. Proc Natl Acad Sci USA 107: 19167-19170. http://dx.doi.org/10.1073/pnas.1003669107

Peckhaus, A; Grass, S; Treuel, L; Zellner, R. (2012). Deliquescence and efflorescence behavior of ternary inorganic/organic/water aerosol particles. J Phys Chem A 116: 6199-6210. http://dx.doi.org/10.1021/jp211522t

Petzold, A; Ogren, JA; Fiebig, M; Laj, P; Li, SM; Baltensperger, U; Holzer-Popp, T; Kinne, S; Pappalardo, G; Sugimoto, N; Wehrli, C; Wiedensohler, A; Zhang, XY. (2013). Recommendations for reporting "black carbon" measurements. Atmos Chem Phys 13: 8365-8379. http://dx.doi.org/10.5194/acp-13-8365-2013

Philipona, R; Behrens, K; Ruckstuhl, C. (2009). How declining aerosols and rising greenhouse gases forced rapid warming in Europe since the 1980s. Geophys Res Lett 36: L02806. http://dx.doi.org/10.1029/2008GL036350

Pierce, JR; Adams, PJ. (2007). Efficiency of cloud condensation nuclei formation from ultrafine particles. Atmos Chem Phys 7: 1367-1379. http://dx.doi.org/10.5194/acp-7-1367-2007

Pitchford, M; Maim, W; Schichtel, B; Kumar, N; Lowenthal, D; Hand, J. (2007). Revised algorithm for estimating light extinction from IMPROVE particle speciation data. J Air Waste Manag Assoc 57: 1326-1336.

Pitchford, ML; Malm, WC. (1994). Development and applications of a standard visual index. Atmos Environ 28: 1049-1054. http://dx.doi.org/10.1016/1352-2310(94)90264-X

Pope, FD; Tong, HJ; Dennis-Smither, BJ; Griffiths, PT; Clegg, SL; Reid, JP; Cox, RA. (2010). Studies of single aerosol particles containing malonic acid, glutaric acid, and their mixtures with sodium chloride. II. Liquid-state vapor pressures of the acids. J Phys Chem A 114: 10156-10165. http://dx.doi.org/10.1021/jp1052979

Prenni, AJ; Day, DE; Evanoski-Cole, AR; Sive, BC; Hecobian, A; Zhou, Y; Gebhart, KA; Hand, JL; Sullivan, AP; Li, Y; Schurman, MI; Desyaterik, Y; Malm, WC; Schichtel, BA; Collett, JL. (2015). Oil and gas impacts on air quality in federal lands in the Bakken region: an overview of the Bakken Air Quality Study and first results. Atmos Chem Phys Discuss 15: 28749-28792. http://dx.doi.org/10.5194/acpd-15-28749-2015

Pryor, SC. (1996). Assessing public perception of visibility for standard setting exercises. Atmos Environ 30: 2705-2716. http://dx.doi.org/10.1016/1352-2310(95)00365-7

Quaas, J; Boucher, O; Bellouin, N; Kinne, S. (2008). Satellite- based estimate of the direct and indirect aerosol climate forcing. J Geophys Res 113: D05204. http://dx.doi.org/10.1029/2007JD008962

Quaas, J; Ming, Y; Menon, S; Takemura, T; Wang, M; Penner, JE; Gettelman, A; Lohmann, U; Bellouin, N; Boucher, O; Sayer, AM; Thomas, GE; Mccomiskey, A; Feingold, G; Hoose, C; Kristjansson, JE; Liu, X; Balkanski, Y; Donner, LJ; Ginoux, PA; Stier, P; Grandey, B; Feichter, J; Sednev, I; Bauer, SE; Koch, D; Grainger, RG; Kirkevag, A; Iversen, T; Seland, O; Easter, R; Ghan, SJ; Rasch, PJ; Morrison, H; Lamarque, JF; Iacono, MJ; Kinne, S; Schulz, M. (2009). Aerosol indirect effects - general circulation model intercomparison and evaluation with satellite data. Atmos Chem Phys 9: 8697-8717.

Quan, Y; Zhang, L. (2017). Experimental investigation of the anti-dust effect of transparent hydrophobic coatings applied for solar cell covering glass. Sol Energy Mater Sol Cells 160: 382-389. http://dx.doi.org/10.1016/j.solmat.2016.10.043

Quirantes, A; Olmo, FJ; Lyamani, H; Alados-Arboledas, L. (2008). Correction factors for a total scatter/backscatter nephelometer. J Quant Spectrosc Radiat Transf 109: 1496-1503. http://dx.doi.org/10.1016/j.jqsrt.2007.12.014

Radonjic, IS; Pavlovic, TM; Mirjanic, DL, j; Radovic, MK; Milosavljevic, DD; Pantic, LS. (2017). Investigation of the impact of atmospheric pollutants on solar module energy efficiency. Thermal Science 21: 2021-2030. http://dx.doi.org/10.2298/TSCI160408176R

ED_002220_00002287-01856

Raes, F; Van Dingenen, R; Vignati, E; Wilson, J; Putaud, JP; Seinfeld, JH; Adams, P. (2000). Formation and cycling of aerosols in the global troposphere. Atmos Environ 34: 4215-4240.

Reid, JS; Eck, TF; Christopher, SA; Koppman, R; Dubovik, O; Eleuterio, DP; Holben, BN; Reid, EA; Zhang, J. (2005). A review of biomass burning emissions part III: intensive optical properties of biomass burning particles. Atmos Chem Phys 5: 827-849.

Richards, LW; Dye, TS; Arthur, M; Byars, MS. (1996). Analysis of ASOS data for visibility purposes, final report. (STI-996231-1610-FR). San Rafael, CA: Systems Applications International, Inc.

Rosenfeld, D; Andreae, MO; Asmi, A, ri; Chin, M; de Leeuw, G; Donovan, DP; Kahn, R; Kinne, S; Kivekas, N; Kulmala, M; Lau, W; Schmidt, KS; Suni, T; Wagner, T; Wild, M; Quaas, J. (2014). Global observations of aerosol-cloud-precipitation-climate interactions. Rev Geophys 52: 750-808. http://dx.doi.org/10.1002/2013RG000441

Rosso, F; Pisello, AL; Jin, WH; Ghandehari, M; Cotana, F; Ferrero, M. (2016). Cool marble building envelopes: The effect of aging on energy performance and aesthetics. Sustainability 8: Article #753. http://dx.doi.org/10.3390/su8080753

Ruckstuhl, C; Philipona, R; Behrens, K; Coen, MC; Dürr, B; Heimo, A; Mätzler, C; Nyeki, S; Ohmura, A; Vuilleumier, L; Weller, M; Wehrli, C; Zelenka, A. (2008). Aerosol and cloud effects on solar brightening and recent rapid warming. Geophys Res Lett 35: L12708. http://dx.doi.org/10.1029/2008GL034228

Ryan, PA; Lowenthal, D; Kumar, N. (2005). Improved light extinction reconstruction in interagency monitoring of protected visual environments. J Air Waste Manag Assoc 55: 1751-1759.

Sabbioni, C; Ghedini, N; Bonazza, A. (2003). Organic anions in damage layers on monuments and buildings. Atmos Environ 37: 1261-1269. http://dx.doi.org/10.1016/S1352-2310(02)01025-7

Sabbioni, C; Zappia, G; Ghedini, N; Gobbi, G; Favoni, O. (1998). Black crusts on ancient mortars. Atmos Environ 32: 215-223.

Saiz-Jimenez, C. (1993). Deposition of airborne organic pollutants on historic buildings. Atmos Environ 27: 77-85.

Saiz-Jimenez, C. (2004). Air pollution and cultural heritage. In C Saiz-Jimenez (Ed.), Air pollution and cultural heritage : proceedings of the International Workshop on Air Pollution and Cultural Heritage. London, England: CRC Press.

Sanjurjo-Sanchez, J; Alves, C. (2012). Decay effects of pollutants on stony materials in the built environment. Environ Chem Lett 10: 131-143. http://dx.doi.org/10.1007/s10311-011-0346-y

Sanjurjo Sanchez, J; Alves, CAS; Vidal Romani, JR, JR; Fernandez Mosquera, D. (2009). Origin of gypsum-rich coatings on historic buildings. Water Air Soil Pollut 204: 53-68. http://dx.doi.org/10.1007/s11270-009-0025-9

Schmidt, A; Carslaw, KS; Mann, GW; Rap, A; Pringle, KJ; Spracklen, DV; Wilson, M; Forster, PM. (2012). Importance of tropospheric volcanic aerosol for indirect radiative forcing of climate. Atmos Chem Phys 12: 7321-7339. http://dx.doi.org/10.5194/acp-12-7321-2012

Scott, CE; Rap, A; Spracklen, DV; Forster, PM; Carslaw, KS; Mann, GW; Pringle, KJ; Kivekas, N; Kulmala, M; Lihavainen, H; Tunved, P. (2014). The direct and indirect radiative effects of biogenic secondary organic aerosol. Atmos Chem Phys 14: 447-470. http://dx.doi.org/10.5194/acp-14-447-2014

Sena, ET; Artaxo, P. (2015). A novel methodology for large-scale daily assessment of the direct radiative forcing of smoke aerosols. Atmos Chem Phys 15: 5471-5483. http://dx.doi.org/10.5194/acp-15-5471-2015

Shahzad, MI; Nichol, JE; Wang, J; Campbell, JR; Chan, PW. (2013). Estimating surface visibility at Hong Kong from ground-based LIDAR, sun photometer and operational MODIS products. J Air Waste Manag Assoc 63: 1098-1110. http://dx.doi.org/10.1080/10962247.2013.801372

Sharma, N; Arnold, IJ; Moosmueller, H; Arnott, WP; Mazzoleni, C. (2013). Photoacoustic and nephelometric spectroscopy of aerosol optical properties with a supercontinuum light source. Atmos Meas Tech 6: 3501-3513. http://dx.doi.org/10.5194/amt-6-3501-2013

ED_002220_00002287-01857

Shen, L, u; Mickley, LJ; Murray, L, eeT. (2017). Influence of 2000-2050 climate change on particulate matter in the United States: results from a new statistical model. Atmos Chem Phys 17: 4355-4367. http://dx.doi.org/10.5194/acp-17-4355-2017

Shindell, D; Faluvegi, G. (2009). Climate response to regional radiative forcing during the twentieth century. Nat Geosci 2: 294-300. http://dx.doi.org/10.1038/ngeo473

Shindell, DT. (2012). Evaluation of the absolute regional temperature potential. Atmos Chem Phys 12: 7955-7960. http://dx.doi.org/10.5194/acp-12-7955-2012

Shindell, DT; Lamarque, JF; Schulz, M; Flanner, M; Jiao, C; Chin, M; Young, PJ; Lee, YH; Rotstayn, L; Mahowald, N; Milly, G; Faluvegi, G; Balkanski, Y; Collins, WJ; Conley, AJ; Dalsoren, S; Easter, R; Ghan, S; Horowitz, L; Liu, X; Myhre, G; Nagashima, T; Naik, V; Rumbold, ST; Skeie, R; Sudo, K; Szopa, S; Takemura, T; Voulgarakis, A; Yoon, JH; Lo, F. (2013). Radiative forcing in the ACCMIP historical and future climate simulations. Atmos Chem Phys 13: 2939-2974. http://dx.doi.org/10.5194/acp-13-2939-2013

Shindell, DT; Voulgarakis, A; Faluvegi, G; Milly, G. (2012). Precipitation response to regional radiative forcing. Atmos Chem Phys 12: 6969-6982. http://dx.doi.org/10.5194/acp-12-6969-2012

Sickles, JE; Shadwick, DS. (2008). Comparison of particulate sulfate and nitrate at collocated CASTNET and IMPROVE sites in the eastern US. Atmos Environ 42: 2062-2073. http://dx.doi.org/10.1016/j.atmosenv.2007.11.051

Singh, S; Fiddler, MN; Smith, D; Bililign, S. (2014). Error analysis and uncertainty in the determination of aerosol optical properties using cavity ring-down spectroscopy, integrating nephelometry, and the extinction-minus-scattering method. Aerosol Sci Technol 48: 1345-1359. http://dx.doi.org/10.1080/02786826.2014.984062

Skeie, RB; Berntsen, TK; Myhre, G; Tanaka, K; Kvalevåg, MM; Hoyle, CR. (2011). Anthropogenic radiative forcing time series from pre-industrial times until 2010. Atmos Chem Phys 11: 11827-11857. http://dx.doi.org/10.5194/acp-11-11827-2011

Skiles, SM; Painter, TH; Deems, JS; Bryant, A, nnC; Landry, CC. (2012). Dust radiative forcing in snow of the Upper Colorado River Basin: 2. Interannual variability in radiative forcing and snowmelt rates. Water Resour Res 48. http://dx.doi.org/10.1029/2012WR011986

Sleiman, M; Kirchstetter, TW; Berdahl, P; Gilbert, HE; Quelen, S; Marlot, L; Preble, CV; Chen, S; Montalbano, A; Rosseler, O; Akbari, H; Levinson, R; Destaillats, H. (2014). Soiling of building envelope surfaces and its effect on solar reflectance - Part II: Development of an accelerated aging method for roofing materials. Sol Energy Mater Sol Cells 122: 271-281. http://dx.doi.org/10.1016/j.solmat.2013.11.028

Smith, AE. (2013). An evaluation of the robustness of the visual air quality "preference study" method. J Air Waste Manag Assoc 63: 405-417. http://dx.doi.org/10.1080/10962247.2012.759165

Smith, BJ; Gomez-Heras, M; Mccabe, S. (2008). Understanding the decay of stone-built cultural heritage. Progr Phys Geogr 32: 439-461. http://dx.doi.org/10.1177/0309133308098119

Smith, ML; Bertram, AK; Martin, ST. (2012). Deliquescence, efflorescence, and phase miscibility of mixed particles of ammonium sulfate and isoprene-derived secondary organic material. Atmos Chem Phys 12: 9613-9628. http://dx.doi.org/10.5194/acp-12-9613-2012

Smith, SJ; Bond, TC. (2014). Two hundred fifty years of aerosols and climate: the end of the age of aerosols. Atmos Chem Phys 14: 537-549. http://dx.doi.org/10.5194/acp-14-537-2014

Smith, SJ; Van Aardenne, J; Klimont, Z; Andres, RJ; Volke, A; Delgado arias, S. (2011). Anthropogenic sulfur dioxide emissions: 18502005. Atmos Chem Phys 11: 1101-1116. http://dx.doi.org/10.5194/acp-11-1101-2011

So, R; Vingarzan, R; Jones, K; Pitchford, M. (2015). Modeling of time-resolved light extinction and its applications to visibility management in the Lower Fraser Valley of British Columbia, Canada. J Air Waste Manag Assoc 65: 707-720. http://dx.doi.org/10.1080/10962247.2015.1010750

Soden, BJ; Vecchi, GA. (2011). The vertical distribution of cloud feedback in coupled ocean-atmosphere models. Geophys Res Lett 38. http://dx.doi.org/10.1029/2011GL047632

ED_002220_00002287-01858

Spence, JW; Haynie, FH. (1972). Paint technology and air pollution: a survey and economic assessment. Spence, JW; Haynie, FH.

Stephens, GL; Li, J; Wild, M; Clayson, CA; Loeb, N; Kato, S; L'Ecuyer, T; Stackhouse, PW, Jr; Lebsock, M; Andrews, T. (2012). An update on Earth's energy balance in light of the latest global observations. Nat Geosci 5: 691-696. http://dx.doi.org/10.1038/NGEO1580

Stock, M; Cheng, YF; Birmili, W; Massling, A; Wehner, B; Mueller, T; Leinert, S; Kalivitis, N; Mihalopoulos, N; Wiedensohler, A. (2011). Hygroscopic properties of atmospheric aerosol particles over the Eastern Mediterranean: implications for regional direct radiative forcing under clean and polluted conditions. Atmos Chem Phys 11: 4251-4271. http://dx.doi.org/10.5194/acp-11-4251-2011

Stocker, TF. (2013). Technical summary. In Climate Change 2013: The Physical Science Basis Contribution of Working Group I to the Fifth Assessment Report of the Intergovernmental Panel on Climate Change. Cambridge, United Kingdom and New York, NY, USA: Cambridge University Press.

Tai, APK; Mickley, LJ; Heald, CL; Wu, S. (2013). Effect of CO2 inhibition on biogenic isoprene emission: Implications for air quality under 2000 to 2050 changes in climate, vegetation, and land use. Geophys Res Lett 40: 3479-3483. http://dx.doi.org/10.1002/grl.50650

Tai, APK; Mickley, LJ; Jacob, DJ. (2010). Correlations between fine particulate matter (PM2.5) and meteorological variables in the United States: Implications for the sensitivity of PM2.5 to climate change. Atmos Environ 44: 3976-3984. http://dx.doi.org/10.1016/j.atmosenv.2010.06.060

Takemura, T. (2012). Distributions and climate effects of atmospheric aerosols from the preindustrial era to 2100 along Representative Concentration Pathways (RCPs) simulated using the global aerosol model SPRINTARS. Atmos Chem Phys 12: 11555-11572. http://dx.doi.org/10.5194/acp-12-11555-2012

Tao, J, un; Zhang, L; Ho, K; Zhang, R; Lin, Z; Zhang, Z; Lin, M; Cao, J; Liu, S; Wang, G. (2014). Impact of PM2.5 chemical compositions on aerosol light scattering in Guangzhou - the largest megacity in South China. Atmos Res 135: 48-58. http://dx.doi.org/10.1016/j.atmosres.2013.08.015

Teng, H; Washington, WM; Branstator, G; Meehl, GA; Lamarque, JF. (2012). Potential impacts of Asian carbon aerosols on future US warming. Geophys Res Lett 39: n/a-n/a. http://dx.doi.org/10.1029/2012GL051723

Tian, S; Pan, Y; Liu, Z; Wen, T; Wang, Y. (2014). Size-resolved aerosol chemical analysis of extreme haze pollution events during early 2013 in urban Beijing, China. J Hazard Mater 279: 452-460. http://dx.doi.org/10.1016/j.jhazmat.2014.07.023

Titos, G; Foyo-Moreno, I; Lyamani, H; Querol, X; Alastuey, A; Alados-Arboledas, L. (2012). Optical properties and chemical composition of aerosol particles at an urban location: An estimation of the aerosol mass scattering and absorption efficiencies. J Geophys Res Atmos 117. http://dx.doi.org/10.1029/2011JD016671

Tosca, MG; Randerson, JT; Zender, CS; Flanner, MG; Rasch, PJ. (2010). Do biomass burning aerosols intensify drought in equatorial Asia during El Nino? Atmos Chem Phys 10: 3515-3528.

Trenberth, KE; Fasullo, JT; Kiehl, J. (2009). Earth's global energy budget. Bull Am Meteorol Soc 90: 311-+. http://dx.doi.org/10.1175/2008BAMS2634.1

Trivitayanurak, W; Adams, PJ. (2014). Does the POA-SOA split matter for global CCN formation? Atmos Chem Phys 14: 995-1010. http://dx.doi.org/10.5194/acp-14-995-2014

Turner, AG; Annamalai, H. (2012). Climate change and the South Asian summer monsoon. 2: 587-595. http://dx.doi.org/10.1038/NCLIMATE1495

Turner, AJ; Fiore, AM; Horowitz, LW; Bauer, M. (2013). Summertime cyclones over the Great Lakes Storm Track from 1860-2100: variability, trends, and association with ozone pollution. Atmos Chem Phys 13: 565-578. http://dx.doi.org/10.5194/acp-13-565-2013

Turnock, ST; Spracklen, DV; Carslaw, KS; Mann, GW; Woodhouse, MT; Forster, PM; Haywood, J; Johnson, CE; Dalvi, M; Bellouin, N; Sanchez-Lorenzo, A. (2015). Modelled and observed changes in aerosols and surface solar radiation over Europe between 1960 and 2009. Atmos Chem Phys 15: 9477-9500. http://dx.doi.org/10.5194/acp-15-9477-2015

ED_002220_00002287-01859

Twomey, S. (1977). The influence of pollution on the shortwave albedo of clouds. J Atmos Sci 34: 1149-1152. http://dx.doi.org/10.1175/1520-0469(1977)034<1149:TIOPOT>2.0.CO;2

U.S. EPA (U.S. Environmental Protection Agency). (1972). Paint technology and air pollution: a survey and economic assessment.

U.S. EPA (U.S. Environmental Protection Agency). (2001). Interpolating relative humidity weighting factors to calculate visibility impairment and the effects of IMPROVE monitor outliers. 68-D-98-113/WA 3-39.

U.S. EPA (U.S. Environmental Protection Agency). (2003). Guidance for tracking progress under the Regional Haze Rule. EPA-454/B-03-004.

U.S. EPA (U.S. Environmental Protection Agency). (2004). Air quality criteria for particulate matter [EPA Report]. (EPA/600/P-99/002aF-bF). Research Triangle Park, NC: U.S. Environmental Protection Agency, Office of Research and Development, National Center for Environemntal Assessment- RTP Office. http://cfpub.epa.gov/ncea/cfm/recordisplay.cfm?deid=87903

U.S. EPA (U.S. Environmental Protection Agency). (2009). Integrated science assessment for particulate matter [EPA Report]. (EPA/600/R-08/139F). Research Triangle Park, NC: U.S. Environmental Protection Agency, Office of Research and Development, National Center for Environmental Assessment- RTP Division. http://cfpub.epa.gov/ncea/cfm/recordisplay.cfm?deid=216546

U.S. EPA (U.S. Environmental Protection Agency). (2012). Report to Congress on black carbon [EPA Report]. (EPA-450/R-12-001). http://www.epa.gov/blackcarbon/2012report/fullreport.pdf

U.S. EPA (U.S. Environmental Protection Agency). (2015). Preamble to the integrated science assessments [EPA Report]. (EPA/600/R-15/067). Research Triangle Park, NC: U.S. Environmental Protection Agency, Office of Research and Development, National Center for Environmental Assessment, RTP Division. https://cfpub.epa.gov/ncea/isa/recordisplay.cfm?deid=310244

U.S. EPA (U.S. Environmental Protection Agency). (2018). Integrated science assessment for oxides of nitrogen, oxides of sulfur and particulate matter -Ecological criteria (2nd external review draft). (EPA/600/R-18/097). Research Triangle Park, NC: U.S. Environmental Protection Agency, Office of Research and Development, National Center for Environmental Assessment. http://cfint.rtpnc.epa.gov/ncea/prod/recordisplay.cfm?deid=340671

Unger, N. (2014). Human land-use-driven reduction of forest volatiles cools global climate. Nat Clim Chang 4: 907-910. http://dx.doi.org/10.1038/nclimate2347

Van de Hulst, H. (1981). Light scattering by small particles. New York: Dover.

Vecchi, R; Bernardoni, V; Paganelli, C; Valli, G. (2014). A filter-based light-absorption measurement with polar photometer: Effects of sampling artefacts from organic carbon. J Aerosol Sci 70: 15-25. http://dx.doi.org/10.1016/j.jaerosci.2013.12.012

Viles, HA; Gorbushina, AA. (2003). Soiling and microbial colonisation on urban roadside limestone: A three year study in Oxford, England. Build Environ 38: 1217-1224.

Vose, RS; Applequist, S; Menne, MJ; Williams, CN; Thorne, P. (2012). An intercomparison of temperature trends in the U.S. Historical Climatology Network and recent atmospheric reanalyses. Geophys Res Lett 39: n/a-n/a. http://dx.doi.org/10.1029/2012GL051387

Wagner, F; Bortoli, D; Pereira, S; Costa, MJ; Silva, A, naM; Weinzierl, B; Esselborn, M; Petzold, A; Rasp, K; Heinold, B; Tegen, I, na. (2009). Properties of dust aerosol particles transported to Portugal from the Sahara desert. Tellus B Chem Phys Meteorol 61: 297-306. http://dx.doi.org/10.1111/j.1600-0889.2008.00393.x

Walwil, HM; Mukhaimer, A; Al-Sulaiman, FA; Said, SAM. (2017). Comparative studies of encapsulation and glass surface modification impacts on PV performance in a desert climate. Solar Energy 142: 288-298. http://dx.doi.org/10.1016/j.solener.2016.12.020

Wang, M; Ghan, S; Ovchinnikov, M; Liu, X; Easter, R; Kassianov, E; Qian, Y; Morrison, H. (2011a). Aerosol indirect effects in a multi-scale aerosol-climate model PNNL-MMF. Atmos Chem Phys 11: 5431-5455. http://dx.doi.org/10.5194/acp-11-5431-2011

ED_002220_00002287-01860

Wang, M; Xu, B; Cao, J; Tie, X; Wang, H; Zhang, R; Qian, Y; Rasch, PJ; Zhao, S; Wu, G; Zhao, H; Joswiak, DR; Li, J; Xie, Y. (2015). Carbonaceous aerosols recorded in a southeastern Tibetan glacier: analysis of temporal variations and model estimates of sources and radiative forcing. Atmos Chem Phys 15: 1191-1204. http://dx.doi.org/10.5194/acp-15-1191-2015

Wang, Q; Jacob, DJ; Fisher, JA; Mao, J; Leibensperger, EM; Carouge, CC; Le Sager, P; Kondo, Y; Jimenez, JL; Cubison, MJ; Doherty, SJ. (2011b). Sources of carbonaceous aerosols and deposited black carbon in the Arctic in winter-spring: implications for radiative forcing. Atmos Chem Phys 11: 12453-12473. http://dx.doi.org/10.5194/acp-11-12453-2011

Wang, X; Chen, J; Cheng, T; Zhang, R; Wang, X. (2014a). Particle number concentration, size distribution and chemical composition during haze and photochemical smog episodes in Shanghai. J Environ Sci 26: 1894-1902. http://dx.doi.org/10.1016/j.jes.2014.07.003

Wang, X; Wang, W; Yang, L; Gao, X; Nie, W, ei; Yu, Y; Xu, P, en; Zhou, Y; Wang, Z, he. (2012). The secondary formation of inorganic aerosols in the droplet mode through heterogeneous aqueous reactions under haze conditions. Atmos Environ 63: 68-76. http://dx.doi.org/10.1016/j.atmosenv.2012.09.029

Wang, Y; Li, A; Xie, PH; Wagner, T; Chen, H; Liu, WQ; Liu, JG. (2014b). A rapid method to derive horizontal distributions of trace gases and aerosols near the surface using multi-axis differential optical absorption spectroscopy. Atmos Meas Tech 7: 1663-1680. http://dx.doi.org/10.5194/amt-7-1663-2014

Watson, JG; Chow, JC; Chen, LWA. (2005). Summary of organic and elemental carbon/black carbon analysis methods and intercomparisons. Aerosol Air Qual Res 5: 69102.

Watt, J; Jarrett, D; Hamilton, R. (2008). Dose-response functions for the soiling of heritage materials due to air pollution exposure. Sci Total Environ 400: 415-424. http://dx.doi.org/10.1016/j.scitotenv.2008.07.024

Watt, J; Kucera, V; Tidblad, J; Hamilton, R. (2016). The effects of air pollution on cultural heritage. In J Watt; V Kucera; J Tidblad; R Hamilton (Eds.), The Effects of Air Pollution on Cultural Heritage. London, England: Springer US. http://dx.doi.org/10.1007/978-0-387-84893-8

Weber, RJ; Sullivan, A; Peltier, RE; Russell, A; Yan, B, o; Zheng, M, ei; de Gouw, J; Warneke, C; Brock, C; Holloway, JS; Atlas, EL; Edgerton, E. (2007). A study of secondary organic aerosol formation in the anthropogenic-influenced southeastern United States. J Geophys Res Atmos 112. http://dx.doi.org/10.1029/2007JD008408

Wheeler, MD; Newman, SM; Orr-Ewing, AJ; Ashfold, MNR. (1998). Cavity ring-down spectroscopy. J Chem Soc Faraday Trans 94: 337-351.

White, WH. (2008). Chemical markers for sea salt in IMPROVE aerosol data. Atmos Environ 42: 261-274. http://dx.doi.org/10.1016/j.atmosenv.2007.09.040

Wild, M. (2009). Global dimming and brightening: A review. J Geophys Res 114: D00D16. http://dx.doi.org/10.1029/2008JD011470

Worobiec, A; Samek, L; Krata, A; Van Meel, K; Krupinska, B; Stefaniak, EA; Karaszkiewicz, P; Van Grieken, R. (2010). Transport and deposition of airborne pollutants in exhibition areas located in historical buildings - study in Wawel Castle Museum in Cracow, Poland. J Cult Herit 11: 354-359. http://dx.doi.org/10.1016/j.culher.2009.11.009

Wu, S; Mickley, LJ; Kaplan, JO; Jacob, DJ. (2012). Impacts of changes in land use and land cover on atmospheric chemistry and air quality over the 21st century. Atmos Chem Phys 12: 1597-1609. http://dx.doi.org/10.5194/acp-12-1597-2012

Wu, ZJ; Nowak, A; Poulain, L; Herrmann, H; Wiedensohler, A. (2011). Hygroscopic behavior of atmospherically relevant water-soluble carboxylic salts and their influence on the water uptake of ammonium sulfate. Atmos Chem Phys 11: 12617-12626. http://dx.doi.org/10.5194/acp-11-12617-2011

Xing, J; Mathur, R; Pleim, J; Hogrefe, C; Gan, CM; Wong, DC; Wei, C. (2015). Can a coupled meteorology-chemistry model reproduce the historical trend in aerosol direct radiative effects over the Northern Hemisphere? Atmos Chem Phys 15: 9997-10018. http://dx.doi.org/10.5194/acp-15-9997-2015

ED_002220_00002287-01861

Xing, J; Wang, J; Mathur, R; Pleim, J; Wang, S; Hogrefe, C; Gan, CM; Wong, DC; Hao, J. (2016). Unexpected benefits of reducing aerosol cooling effects. Environ Sci Technol 50: 7527-7534. http://dx.doi.org/10.1021/acs.est.6b00767

Xu, L; Guo, H; Boyd, CM; Klein, M; Bougiatioti, A; Cerully, KM; Hite, J. R.; Isaacman-Vanwertz, G; Kreisberg, NM; Knote, C; Olson, K; Koss, A; Goldstein, AH; Hering, SV; de Gouw, J; Baumann, K; Lee, SH; Nenes, A; Weber, RJ; Ng, NL. (2015). Effects of anthropogenic emissions on aerosol formation from isoprene and monoterpenes in the southeastern United States. Proc Natl Acad Sci USA 112: 37-42. http://dx.doi.org/10.1073/pnas.1417609112

Yang, F; Chen, H; Du, J; Yang, X; Gao, S; Chen, J; Geng, F. (2012). Evolution of the mixing state of fine aerosols during haze events in Shanghai. Atmos Res 104-105: 193-201. http://dx.doi.org/10.1016/j.atmosres.2011.10.005

Yang, M; Howell, SG; Zhuang, J; Huebert, BJ. (2009). Attribution of aerosol light absorption to black carbon, brown carbon, and dust in China -- interpretations of atmospheric measurements during EAST-AIRE. Atmos Chem Phys 9: 2035-2050. http://dx.doi.org/10.5194/acp-9-2035-2009

Yu, S; Alapaty, K; Mathur, R; Pleim, J; Zhang, Y; Nolte, C; Eder, B; Foley, K; Nagashima, T. (2014). Attribution of the United States "warming hole": Aerosol indirect effect and precipitable water vapor. 4: 6929. http://dx.doi.org/10.1038/srep06929

Yue, D; Hu, M; Wu, Z; Wang, Z; Guo, S; Wehner, B; Nowak, A; Achtert, P; Wiedensohler, A; Jung, J; Kim, YJ; Liu, S. (2009). Characteristics of aerosol size distributions and new particle formation in the summer in Beijing. J Geophys Res 114: D00G12. http://dx.doi.org/10.1029/2008JD010894

Yue, X; Mickley, LJ; Logan, JA; Kaplan, JO. (2013). Ensemble projections of wildfire activity and carbonaceous aerosol concentrations over the western United States in the mid-21st century. Atmos Environ 77: 767-780. http://dx.doi.org/10.1016/j.atmosenv.2013.06.003

Yue, X, u; Mickley, LJ; Logan, JA. (2014). Projection of wildfire activity in southern California in the mid-twenty-first century. Clim Dynam 43: 1973-1991. http://dx.doi.org/10.1007/s00382-013-2022-3

Zelinka, MD; Andrews, T; Forster, PM; Taylor, KE. (2014). Quantifying components of aerosol-cloud-radiation interactions in climate models. J Geophys Res Atmos 119: 7599-7615. http://dx.doi.org/10.1002/2014JD021710

Zhang, R; Delworth, TL; Sutton, R; Hodson, DLR; Dixon, KW; Held, IM; Kushnir, Y; Marshall, J; Ming, Y, i; Msadek, R, ym; Robson, J, on; Rosati, AJ; Ting, M; Vecchi, GA. (2013a). Have Aerosols Caused the Observed Atlantic Multidecadal Variability? J Atmos Sci 70: 1135-1144. http://dx.doi.org/10.1175/JAS-D-12-0331.1

Zhang, R, ui; Bian, Q; Fung, JCH; Lau, AKH. (2013b). Mathematical modeling of seasonal variations in visibility in Hong Kong and the Pearl River Delta region. Atmos Environ 77: 803-816. http://dx.doi.org/10.1016/j.atmosenv.2013.05.048

Zhang, Y; Easter, RC; Ghan, SJ; Abdul-Razzak, H. (2002). Impact of aerosol size representation on modeling aerosol-cloud interactions. J Geophys Res 107: 4558. http://dx.doi.org/10.1029/2001JD001549

Zhang, Y; Wen, XY; Jang, CJ. (2010). Simulating chemistryaerosolcloudradiationclimate feedbacks over the continental U.S. using the online-coupled Weather Research Forecasting Model with chemistry (WRF/Chem). Atmos Environ 44: 3568-3582. http://dx.doi.org/10.1016/j.atmosenv.2010.05.056

Zhao, M; Golaz, JC; Held, IM; Ramaswamy, V; Lin, SJ; Ming, Y; Ginoux, P; Wyman, B; Donner, LJ; Paynter, D; Guo, H. (2016). Uncertainty in model climate sensitivity traced to representations of cumulus precipitation microphysics. J Clim 29: 543-560. http://dx.doi.org/10.1175/JCLI-D-15-0191.1

ED_002220_00002287-01862

APPENDIX 1 EVALUATION OF STUDIES ON HEALTH EFFECTS OF PARTICULATE MATTER

This appendix describes the approach used in the Integrated Science Assessment (ISA) for Particulate Matter (PM) to evaluate study quality in the available health effects literature. As described in the Preamble to the ISA (U.S. EPA, 2015), causality determinations were informed by the integration of evidence across scientific disciplines (e.g., exposure, animal toxicology, epidemiology) and related outcomes and by judgments of the strength of inference in individual studies. Table A-1 describes aspects considered in evaluating study quality of controlled human exposure, animal toxicological, and epidemiologic studies. The aspects found in Table A-1 are consistent with current best practices for reporting or evaluating health science data.[86] Additionally, the aspects are compatible with published U.S. EPA guidelines related to cancer, neurotoxicity, reproductive toxicity, and developmental toxicity (U.S. EPA, 2005, 1998, 1996, 1991).

These aspects were not used as a checklist, and judgments were made without considering the results of a study. The presence or absence of particular features in a study did not necessarily lead to the conclusion that a study was less informative or to exclude it from consideration in the ISA. Further, these aspects were not used as criteria for determining causality in the five-level hierarchy. As described in the Preamble, causality determinations were based on judgments of the overall strengths and limitations of the collective body of available studies and the coherence of evidence across scientific disciplines and related outcomes. Table A-1 is not intended to be a complete list of aspects that define a study's ability to inform the relationship between PM and health effects, but it describes the major aspects considered in this ISA to evaluate studies. Where possible, study elements, such as exposure assessment and confounding (i.e., bias due to a relationship with the outcome and correlation with exposures to PM), are considered specifically for PM. Thus, judgments on the ability of a study to inform the relationship between an air pollutant and health can vary depending on the specific pollutant being assessed.

[86]For example, NTP OHAT approach (Rooney et al., 2014), IRIS Preamble (U.S. EPA, 2013), ToxRTool (Klimisch et al., 1997), STROBE guidelines (von Elm et al., 2007), and ARRIVE guidelines (Kilkenny et al., 2010).

ED_002220_00002287-01863

Table A-1 Scientific considerations for evaluating the strength of inference from studies on the health effects of particulate matter.

Study Design
Controlled Human Exposure
Studies should clearly describe the primary and any secondary objectives of the study, or specific hypotheses being tested. Study subjects should be randomly exposed without knowledge of the exposure condition. Preference is given to balanced crossover (repeated measures) or parallel design studies which include control exposures (e.g., to clean filtered air). In crossover studies, a sufficient and specified time between exposure days should be provided to avoid carry over effects from prior exposure days. In parallel design studies, all arms should be matched for individual characteristics such as age, sex, race, anthropometric properties, and health status. In studies evaluating effects of disease, appropriately matched healthy controls are desired for interpretative purposes.
Animal Toxicology
Studies should clearly describe the primary and any secondary objectives of the study, or specific hypotheses being tested. Studies should include appropriately matched control exposures (e.g., to clean filtered air, time matched). Studies should use methods to limit differences in baseline characteristics of control and exposure groups. Studies should randomize assignment to exposure groups and where possible conceal allocation to research personnel. Groups should be subjected to identical experimental procedures and conditions; animal care including housing, husbandry, etc. should be identical between groups. Blinding of research personnel to study group may not be possible due to animal welfare and experimental considerations; however, differences in the monitoring or handling of animals in all groups by research personnel should be minimized.
Epidemiology
Inference is stronger for studies that clearly describe the primary and any secondary aims of the study, or specific hypotheses being tested. For short-term exposure, time-series, case crossover, and panel studies are emphasized over cross-sectional studies because they examine temporal correlations and are less prone to confounding by factors that differ between individuals (e.g., SES, age). Panel studies with scripted exposures, in particular, can contribute to inference because they have consistent, well-defined exposure durations across subjects, measure personal ambient pollutant exposures, and measure outcomes at consistent, well-defined lags after exposures. Studies with large sample sizes and conducted over multiple years are considered to produce more reliable results. Additionally, multi-city studies are preferred over single-city studies because they examine associations large diverse geographic areas using a consistent statistical methodology, avoiding the publication bias often associated with single-city studies[a]. If other quality parameters are equal, multicity studies carry more weight than single-city studies because they tend to have larger sample sizes and lower potential for publication bias. For long-term exposure, inference is considered to be stronger for prospective cohort studies and case-control studies nested within a cohort (e.g., for rare diseases) than cross-sectional, other case-control, or ecologic studies. Cohort studies can better inform the temporality of exposure and effect. Other designs can have uncertainty related to the appropriateness of the control group or validity of inference about individuals from group-level data. Study design limitations can bias health effect associations in either direction.

ED_002220_00002287-01864

Table A-1 (Continued): Scientific considerations for evaluating the strength of inference from studies on the health effects of particulate matter.

Study Population/Test Model
Controlled Human Exposure
In general, the subjects recruited into study groups should be similarly matched for age, sex, race, anthropometric properties, and health status. In studies evaluating effects of specific subject characteristics (e.g., disease, genetic polymorphism, etc.), appropriately matched healthy controls are preferred. Relevant characteristics and health status should be reported for each experimental group. Criteria for including and excluding subjects should be clearly indicated. For the examination of populations with an underlying health condition (e.g., asthma), independent, clinical assessment of the health condition is ideal, but self-report of physician diagnosis generally is considered to be reliable for respiratory and cardiovascular disease outcomes[b]. The loss or withdrawal of recruited subjects during the course of a study should be reported. Specific rationale for excluding subject(s) from any portion of a protocol should be explained.
Animal Toxicology
Ideally, studies should report species, strain, substrain, genetic background, age, sex, and weight. Unless data indicate otherwise, all animal species and strains are considered appropriate for evaluating effects of PM exposure. It is preferred that the authors test for effects in both sexes and multiple lifestages, and report the result for each group separately. All animals used in a study should be accounted for, and rationale for exclusion of animals or data should be specified.
Epidemiology
There is greater confidence in results for study populations that are recruited from and representative of the target population. Studies with high participation and low drop-out over time that is not dependent on exposure or health status are considered to have low potential for selection bias. Clearly specified criteria for including and excluding subjects can aid assessment of selection bias. For populations with an underlying health condition, independent, clinical assessment of the health condition is valuable, but self-report of physician diagnosis generally is considered to be reliable for respiratory and cardiovascular diseases[b]. Comparisons of groups with and without an underlying health condition are more informative if groups are from the same source population. Selection bias can influence results in either direction or may not affect the validity of results but rather reduce the generalizability of findings to the target population.
Pollutant
Controlled Human Exposure
Studies should: (1) include a composite measure of PM (i.e., $PM_{2.5}$, $PM_{10-2.5}$, or ultrafine particles [UFP][c]) or (2) apply some approach (e.g., particle trap or filter) to assess the effects of PM in a complex air pollution mixture (i.e., diesel exhaust, gasoline exhaust, wood smoke).
Animal Toxicology
Studies should: (1) include a composite measure of PM (i.e., $PM_{2.5}$, $PM_{10-2.5}$, or ultrafine particles [UFP][c]) or (2) apply some approach (e.g., particle trap or filter) to assess the effects of PM in a complex air pollution mixture (i.e., diesel exhaust, gasoline exhaust, wood smoke).
Epidemiology
Health effects are evaluated primarily using a composite measure of PM (i.e., $PM_{2.5}$, $PM_{10-2.5}$, or ultrafine particles [UFP][c]) from studies using ambient measurements, model predictions, or a combination of measured and modeled data. Studies of PM components must also include a composite measure of PM. Studies of source-related indicators are also evaluated where the indicator is derived using ambient PM concentrations.

ED_002220_00002287-01865

Table A-1 (Continued): Scientific considerations for evaluating the strength of inference from studies on the health effects of particulate matter.

Exposure Assessment or Assignment
Controlled Human Exposure
For this assessment, the focus is on studies that utilize PM concentrations <2 mg/m^3. Studies that use higher exposure concentrations may provide information relevant to biological plausibility, dosimetry, or inter-species variation. Studies should have well-characterized pollutant concentration, temperature, and relative humidity and/or have measures in place to adequately control the exposure conditions. Preference is given to balanced crossover or parallel design studies which include control exposures (e.g., to clean filtered air). Study subjects should be randomly exposed without knowledge of the exposure condition. Method of exposure (e.g., chamber, facemask, etc.) should be specified and activity level of subjects during exposures should be well characterized.
Animal Toxicology
For this assessment, the focus is on studies that utilize PM concentrations <2 mg/m^3. Studies that use higher exposure concentrations may provide information relevant to biological plausibility, dosimetry, or inter-species variation. Studies should characterize pollutant concentration, temperature, and relative humidity and/or have measures in place to adequately control the exposure conditions. The focus is on inhalation exposure. Non-inhalation exposure experiments (i.e., intratracheal instillation [IT]) are informative for size fractions (e.g., $PM_{10-2.5}$) that cannot penetrate the airway of a study animal and may provide information relevant to biological plausibility and dosimetry. In vitro studies may be included if they provide mechanistic insight or examine similar effects as in vivo studies, but are generally not included. All studies should include exposure control groups (e.g., clean filtered air).

ED_002220_00002287-01866

Table A-1 (Continued): Scientific considerations for evaluating the strength of inference from studies on the health effects of particulate matter.

Epidemiology
Of primary relevance are relationships of health effects with the ambient component of PM exposure. However, information about ambient exposure rarely is available for individual subjects; most often, inference is based on ambient concentrations. Studies that compare exposure assessment methods are considered to be particularly informative. Inference is stronger when the duration or lag of the exposure metric corresponds with the time course for physiological changes in the outcome (e.g., up to a few days for symptoms) or latency of disease (e.g., several years for cancer). Given that the spatial variability of PM composite measures varies among size fractions, with more homogeneity for $PM_{2.5}$ than either $PM_{10-2.5}$ or UFP, the need for capturing spatial contrasts is stronger for $PM_{10-2.5}$ or UFP compared with $PM_{2.5}$. Validated measurements, whether averaged across multiple monitors or assigned from the nearest or single available monitor, adequately capture temporal or spatial variation in exposure to $PM_{2.5}$ due to the high correlation between personal exposure and ambient concentration. However, for more spatially heterogeneous $PM_{10-2.5}$ and UFP, the spatial correlation between personal exposure and ambient concentrations is lower. Similarly, PM components show increased spatial variability relative to $PM_{2.5}$. In this case, validated methods that capture the extent of variability for the particular study design (temporal vs. spatial contrasts) and location carry greater weight. Inference based on central site measurements can be adequate if correlated with personal exposures, closely located to study subjects, highly correlated across monitors within a location, used in locations with well-distributed sources, or combined with time-activity information. In studies of short-term exposure, temporal variability of the exposure metric is of primary interest. For all PM size fractions, studies that incorporate time-activity data with personal or microenvironmental monitoring or modeling data may carry greater weight because residential, in-vehicle, and workplace PM exposures may differ in their temporal variability. Results for total personal and indoor PM exposure are other lines of evidence that may inform judgments about causality of PM because inference is based on an individual's microenvironmental exposures and the potential for copollutant confounding may be reduced compared to ambient exposures. Results for total personal exposure can inform understanding of the effects of ambient exposure when well correlated with ambient concentrations. For long-term exposures, methods that well represent within-community spatial variation in individual exposure may be given more weight for spatially-variable ambient $PM_{10-2.5}$ or ultrafine particles. For $PM_{2.5}$, within-community variation in exposure is less important given that $PM_{2.5}$ tends to be more homogeneous. Exposure measurement error often attenuates health effect estimates or increases the imprecision of the association (i.e., width of 95% CIs), particularly associations based on temporal variation in short-term exposure. However, exposure measurement error can bias estimates away from the null in some epidemiologic studies of long-term exposures where the PM size fraction is more spatially heterogeneous (i.e., $PM_{10-2.5}$ or UFP), depending on the locations of the monitor and sources with respect to the study population. To streamline the health effects discussion on studies that are most policy-relevant, for those health categories where the 2009 PM ISA concluded a "causal relationship" the focus is on studies with mean $PM_{2.5}$ concentrations <20 μg/m^3. However, studies that examine a previously identified uncertainty or limitation in the evidence are evaluated even if mean $PM_{2.5}$ concentrations are >20 μg/m^3.
Outcome Assessment/Evaluation
Controlled Human Exposure
Endpoints should be assessed in the same manner for control and exposure groups (e.g., time after exposure, methods, endpoint evaluator) using valid, reliable methods. Blinding of endpoint evaluators is ideal, especially for qualitative endpoints (e.g., histopathology). For each experiment and each experimental group, including controls, precise details of all procedures carried out should be provided including how, when, and where. Time of the endpoint evaluations is a key consideration that will vary depending on endpoint evaluated. Endpoints should be assessed at time points that are appropriate for the research questions.

ED_002220_00002287-01867

Table A-1 (Continued): Scientific considerations for evaluating the strength of inference from studies on the health effects of particulate matter.

Animal Toxicology
Endpoints should be assessed in the same manner for control and exposure groups (e.g., time after exposure, methods, endpoint evaluator) using valid, reliable methods. Blinding of endpoint evaluators is ideal, especially for qualitative endpoints (e.g., histopathology). For each experiment and each experimental group, including controls, precise details of all procedures carried out should be provided including how, when, and where. Time of the endpoint evaluations is a key consideration that will vary depending on endpoint evaluated. Endpoints should be assessed at time points that are appropriate for the research questions.
Epidemiology
Inference is stronger when outcomes are assessed or reported without knowledge of exposure status. Knowledge of exposure status could produce artefactual associations. Confidence is greater when outcomes assessed by interview, self-report, clinical examination, or analysis of biological indicators are defined by consistent criteria and collected by validated, reliable methods. Independent, clinical assessment is valuable for outcomes such as lung function or incidence of disease, but report of physician diagnosis has shown good reliability[b]. When examining short-term exposures, evaluation of the evidence focuses on specific lags based on the evidence presented in individual studies. Specifically, the following hierarchy is used in the process of selecting results from individual studies to assess in the context of results across all studies for a specific health effect or outcome: • Distributed lag models; • Average of multiple days (e.g., 0–2); • If a priori lag days were used by the study authors these are the effect estimates presented; or • If a study focuses on only a series of individual lag days, expert judgment is applied to select the appropriate result to focus on considering the time course for physiologic changes for the health effect or outcome being evaluated. When health effects of long-term exposure are assessed by acute events such as symptoms or hospital admissions, inference is strengthened when results are adjusted for short-term exposure. Validated questionnaires for subjective outcomes such as symptoms are regarded to be reliable[c], particularly when collected frequently and not subject to long recall. For biological samples, the stability of the compound of interest and the sensitivity and precision of the analytical method is considered. If not based on knowledge of exposure status, errors in outcome assessment tend to bias results toward the null.
Potential Copollutant Confounding
Controlled Human Exposure
Exposure should be well characterized to evaluate independent effects of PM of various size fractions. Studies should apply some approach (e.g., particle trap or filter) to assess the effects of PM when examining exposures to complex air pollution mixtures (i.e., diesel exhaust, gasoline exhaust, wood smoke).
Animal Toxicology
Exposure should be well characterized to evaluate independent effects of PM of various size fractions. Studies should apply some approach (e.g., particle trap or filter) to assess the effects of PM when examining exposures to complex air pollution mixtures (i.e., diesel exhaust, gasoline exhaust, wood smoke).

ED_002220_00002287-01868

Table A-1 (Continued): Scientific considerations for evaluating the strength of inference from studies on the health effects of particulate matter.

Epidemiology
Not accounting for potential copollutant confounding can produce artefactual associations; thus, studies that examine copollutant confounding carry greater weight. The predominant method is copollutant modeling (i.e., two-pollutant models), which is especially informative when correlations are not high. However, when correlations are high ($r > 0.7$), such as those often encountered for UFP and other traffic-related copollutants, copollutant modeling is less informative. Although the use of single-pollutant models to examine the association between PM and a health effect or outcome are informative, ideally studies should also include copollutant analyses. Copollutant confounding is evaluated on an individual study basis considering the extent of correlations observed between the copollutant and PM, and relationships observed with PM and health effects in copollutant models.
Other Potential Confounding Factors[d]
Controlled Human Exposure
Preference is given to studies utilizing experimental and control groups that are matched for individual level characteristics (e.g., race/ethnicity, sex, body weight, smoking history, age) and time varying factors (e.g., seasonal and diurnal patterns).
Animal Toxicology
Preference is given to studies utilizing experimental and control groups that are matched for individual level characteristics (e.g., strain, sex, body weight, litter size, food and water consumption) and time varying factors (e.g., seasonal and diurnal patterns).
Epidemiology
Factors are considered to be potential confounders if demonstrated in the scientific literature to be related to health effects and correlated with PM. Not accounting for confounders can produce artefactual associations; thus, studies that statistically adjust for multiple factors or control for them in the study design are emphasized. Less weight is placed on studies that adjust for factors that mediate the relationship between PM and health effects, which can bias results toward the null. Confounders vary according to study design, exposure duration, and health effect and may include, but are not limited to the following: Short-term exposure studies: Meteorology, day of week, season, medication use, allergen exposure, and long-term temporal trends. Long-term exposure studies: Socioeconomic status, race, age, medication use, smoking status, stress, noise, and occupational exposures.
Statistical Methodology
Controlled Human Exposure
Statistical methods should be clearly described and appropriate for the study design and research question (e.g., correction for multiple comparisons). Generally, statistical significance is used to evaluate the findings of controlled human exposure studies. However, consistent trends are also informative. Detection of statistical significance is influenced by a variety of factors including, but not limited to, the size of the study, exposure and outcome measurement error, and statistical model specifications. Sample size is not a criterion for exclusion; ideally, the sample size should provide adequate power to detect hypothesized effects (e.g., sample sizes less than 3 are considered less informative). Because statistical tests have limitations, consideration is given to both trends in data and reproducibility of results.

ED_002220_00002287-01869

Table A-1 (Continued): Scientific considerations for evaluating the strength of inference from studies on the health effects of particulate matter.

Animal Toxicology
Statistical methods should be clearly described and appropriate for the study design and research question (e.g., correction for multiple comparisons). Generally, statistical significance is used to evaluate the findings of animal toxicology studies. However, consistent trends are also informative. Detection of statistical significance is influenced by a variety of factors including, but not limited to, the size of the study, exposure and outcome measurement error, and statistical model specifications. Sample size is not a criterion for exclusion; ideally, the sample size should provide adequate power to detect hypothesized effects (e.g., sample sizes less than 3 are considered less informative). Because statistical tests have limitations, consideration is given to both trends in data and reproducibility of results.
Epidemiology
Multivariable regression models that include potential confounding factors are emphasized. However, multipollutant models (more than two pollutants) are considered to produce too much uncertainty due to copollutant collinearity to be informative. Models with interaction terms aid in the evaluation of potential confounding as well as effect modification. Sensitivity analyses with alternate specifications for potential confounding inform the stability of findings and aid in judgments of the strength of inference from results. In the case of multiple comparisons, consistency in the pattern of association can increase confidence that associations were not found by chance alone. Statistical methods that are appropriate for the power of the study carry greater weight. For example, categorical analyses with small sample sizes can be prone to bias results toward or away from the null. Statistical tests such as *t*-tests and Chi-squared tests are not considered sensitive enough for adequate inferences regarding PM-health effect associations. For all methods, the effect estimate and precision of the estimate (i.e., width of 95% CI) are important considerations rather than statistical significance.

[a](U.S. EPA, 2008).

[b]Murgia et al. (2014); Weakley et al. (2013); Yang et al. (2011); Heckbert et al. (2004); Barr et al. (2002); Muhajarine et al. (1997); Toren et al. (1993); Burney et al. (1989).

[c]UFPs are defined as particles <100 nm in size, but studies often include size fractions larger than 100 nm in the assessment of the relationship between UFP exposure and health effects.

[d]Many factors evaluated as potential confounders can be effect measure modifiers (e.g., season, comorbid health condition) or mediators of health effects related to PM (comorbid health condition).

the relationship between an air pollutant and health can vary depending on the specific pollutant being assessed.

ED_002220_00002287-01870

1.1 References

Barr, RG; Herbstman, J; Speizer, FE; Camargo, CA, Jr. (2002). Validation of self-reported chronic obstructive pulmonary disease in a cohort study of nurses. Am J Epidemiol 155: 965-971. http://dx.doi.org/10.1093/aje/155.10.965

Burney, PG; Laitinen, LA; Perdrizet, S; Huckauf, H; Tattersfield, AE; Chinn, S; Poisson, N; Heeren, A; Britton, JR; Jones, T. (1989). Validity and repeatability of the IUATLD (1984) Bronchial Symptoms Questionnaire: an international comparison. Eur Respir J 2: 940-945.

Heckbert, SR; Kooperberg, C; Safford, MM; Psaty, BM; Hsia, J; McTiernan, A; Gaziano, JM; Frishman, WH; Curb, JD. (2004). Comparison of self-report, hospital discharge codes, and adjudication of cardiovascular events in the Women's Health Initiative. Am J Epidemiol 160: 1152-1158. http://dx.doi.org/10.1093/aje/kwh314

Kilkenny, C; Browne, WJ; Cuthill, IC; Emerson, M; Altman, DG. (2010). Improving bioscience research reporting: The ARRIVE guidelines for reporting animal research [Review]. PLoS Biol 8: e1000412. http://dx.doi.org/10.1371/journal.pbio.1000412

Klimisch, HJ; Andreae, M; Tillmann, U. (1997). A systematic approach for evaluating the quality of experimental toxicological and ecotoxicological data. Regul Toxicol Pharmacol 25: 1-5. http://dx.doi.org/10.1006/rtph.1996.1076

Muhajarine, N; Mustard, C; Roos, LL; Young, TK; Gelskey, DE. (1997). Comparison of survey and physician claims data for detecting hypertension. J Clin Epidemiol 50: 711-718. http://dx.doi.org/10.1016/S0895-4356(97)00019-X

Murgia, N; Brisman, J; Claesson, A; Muzi, G; Olin, AC; Torén, K. (2014). Validity of a questionnaire-based diagnosis of chronic obstructive pulmonary disease in a general population-based study. BMC Pulm Med 14: 49. http://dx.doi.org/10.1186/1471-2466-14-49

Rooney, AA; Boyles, AL; Wolfe, MS; Bucher, JR; Thayer, KA. (2014). Systematic review and evidence integration for literature-based environmental health science assessments. Environ Health Perspect 122: 711-718. http://dx.doi.org/10.1289/ehp.1307972

Toren, K; Brisman, J; Jarvholm, B. (1993). Asthma and asthma-like symptoms in adults assessed by questionnaires: A literature review [Review]. Chest 104: 600-608. http://dx.doi.org/10.1378/chest.104.2.600

U.S. EPA (U.S. Environmental Protection Agency). (1991). Guidelines for developmental toxicity risk assessment (pp. 1-71). (EPA/600/FR-91/001). Washington, DC: U.S. Environmental Protection Agency, Risk Assessment Forum. http://cfpub.epa.gov/ncea/cfm/recordisplay.cfm?deid=23162

U.S. EPA (U.S. Environmental Protection Agency). (1996). Guidelines for reproductive toxicity risk assessment (pp. 1-143). (EPA/630/R-96/009). Washington, DC: U.S. Environmental Protection Agency, Risk Assessment Forum.

U.S. EPA (U.S. Environmental Protection Agency). (1998). Guidelines for neurotoxicity risk assessment [EPA Report] (pp. 1-89). (EPA/630/R-95/001F). Washington, DC: U.S. Environmental Protection Agency, Risk Assessment Forum. http://www.epa.gov/risk/guidelines-neurotoxicity-risk-assessment

U.S. EPA (U.S. Environmental Protection Agency). (2005). Guidelines for carcinogen risk assessment [EPA Report] (pp. 1-166). (EPA/630/P-03/001F). Washington, DC: U.S. Environmental Protection Agency, Risk Assessment Forum. http://www2.epa.gov/osa/guidelines-carcinogen-risk-assessment

U.S. EPA (U.S. Environmental Protection Agency). (2008). Integrated science assessment for sulfur oxides: Health criteria [EPA Report]. (EPA/600/R-08/047F). Research Triangle Park, NC: U.S. Environmental Protection Agency, Office of Research and Development, National Center for Environmental Assessment- RTP. http://cfpub.epa.gov/ncea/cfm/recordisplay.cfm?deid=198843

U.S. EPA (U.S. Environmental Protection Agency). (2013). Toxicological review of trimethylbenzenes (CASRN 25551-13-7, 95-63-6, 526-73-8, and 108-67-8) in support of summary information on the Integrated Risk Information System (IRIS): revised external review draft [EPA Report]. (EPA/635/R13/171a). Washington, D.C.: U.S. Environmental Protection Agency, National Center for Environmental Assessment. http://yosemite.epa.gov/sab/SABPRODUCT.NSF/b5d8a1ce9b0729348525737500701 2b7/ee1e280e77586de985257b65005d37e7!OpenDocument

U.S. EPA (U.S. Environmental Protection Agency). (2015). Preamble to the integrated science assessments [EPA Report]. (EPA/600/R-15/067). Research Triangle Park, NC: U.S. Environmental Protection Agency, Office of Research and Development, National Center for Environmental Assessment, RTP Division. https://cfpub.epa.gov/ncea/isa/recordisplay.cfm?deid=310244

von Elm, E; Altman, DG; Egger, M; Pocock, SJ; Gotzsche, PC; Vandenbroucke, JP. (2007). The Strengthening the Reporting of Observational Studies in Epidemiology (STROBE) statement: Guidelines for reporting observational studies [Review]. PLoS Med 4: e296. http://dx.doi.org/10.1371/journal.pmed.0040296

Weakley, J; Webber, MP; Ye, F; Zeig-Owens, R; Cohen, HW; Hall, CB; Kelly, K; Prezant, DJ. (2013). Agreement between obstructive airways disease diagnoses from self-report questionnaires and medical records. Prev Med 57: 38-42. http://dx.doi.org/10.1016/j.ypmed.2013.04.001

Yang, CL; To, T; Foty, RG; Stieb, DM; Dell, SD. (2011). Verifying a questionnaire diagnosis of asthma in children using health claims data. BMC Pulm Med 11. http://dx.doi.org/10.1186/1471-2466-11-52

ED_002220_00002287-01872